Assessing the impact of plastic waste accumulation on flood events with citizen observations

A case study in Kumasi, Ghana

J.A.L. Tjia

Technische Universiteit Delft

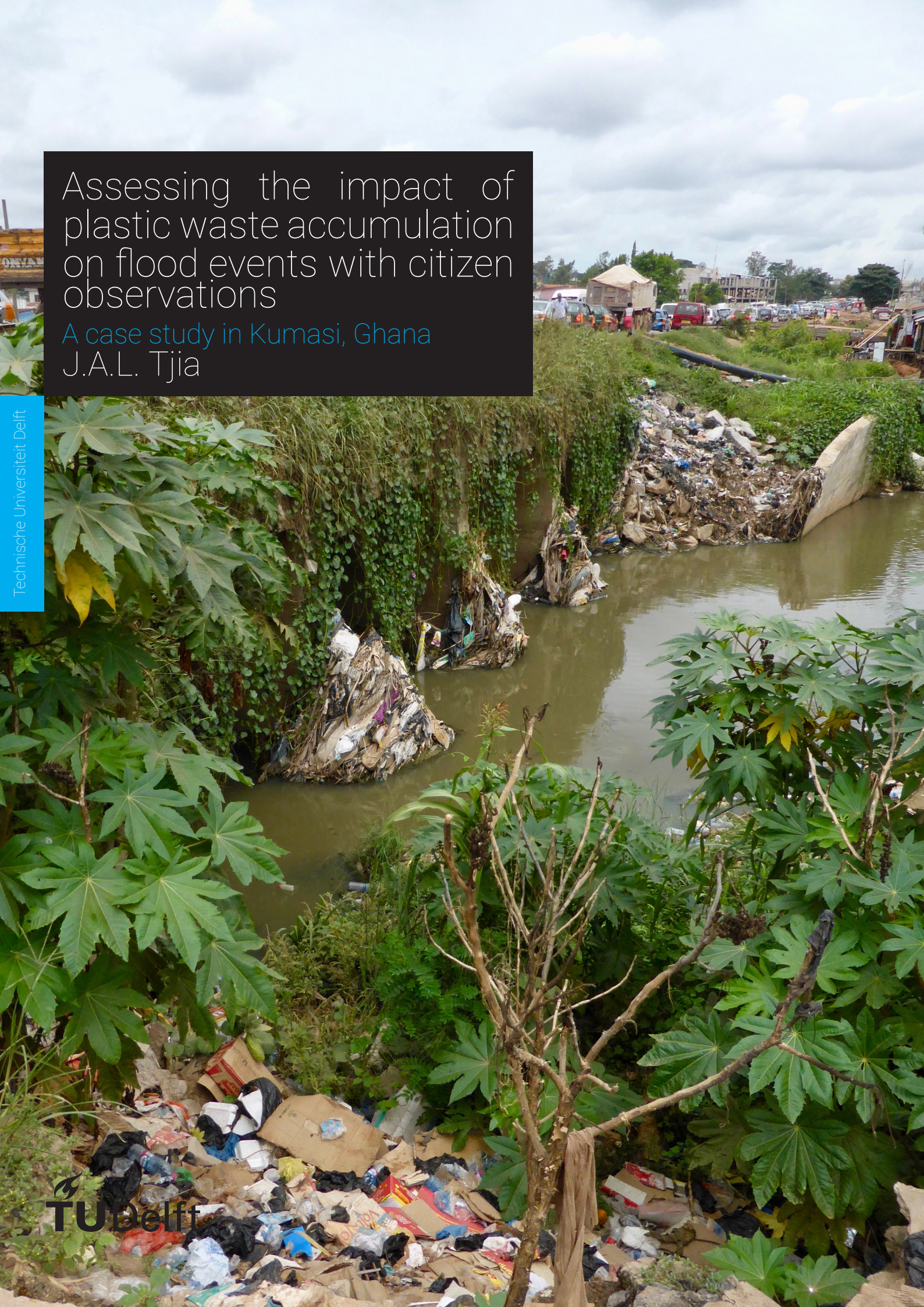

TU Delft

Assessing the impact of plastic waste accumulation on flood events with citizen observations

A case study in Kumasi, Ghana

by

J.A.L. Tjia

to obtain the degree of Master of Science
at the Delft University of Technology,
to be defended publicly on Tuesday April 28, 2020 at 15:30 PM.

Student number:	4244990	
Project duration:	March 9, 2019 – April 28, 2020	
Thesis committee:	Dr. ir. M.C. ten Veldhuis,	TU Delft, chair
	Prof. dr. ir. N. van de Giesen,	TU Delft
	Dr. ir. H. Winsemius,	TU Delft
	Prof. dr. ir. W. S. J. Uijttewaal,	TU Delft

This thesis is confidential and cannot be made public until April 28, 2020.

TU Delft

Acknowledgements

This thesis is the finishing piece to complete my masters degree in Environmental Science at Delft University of Technology. As this period has learnt me many lessons, I am forever grateful to have had the opportunity to work on such a challenging project. Plastic pollution is very real and made me realise we are just at the beginning of a serious global problem. However, as we are facing another global problem at the moment, I feel extremely fortunate to be able to finish my studies in the safety and comfort of my own home.

First of all, I would like to thank Marie-Claire ten Veldhuis for introducing me to this project and most of all to a new adventure in Kumasi, Ghana. Her enthusiasm for the topic and always providing time, guidance and feedback when necessary was greatly appreciated during the entire process, even in Ghana and working from home. Furthermore, I would like to thank Hessel Winsemius, Nick van de Giesen and Wim Uijttewaal for their guidance and feedback during this process as well.

During my time in Kumasi, I was immediately part of a family whom I cannot thank enough for all their help, making me feel at home and all the lovely memories we shared together. Thank you Deborah, Elizabeth and Lydia for taking me in as your own sister and showing me the Ghanaian lifestyle. I feel blessed to know how to make a proper jollof rice whenever I miss Kumasi. Furthermore, all of this was not possible without the help of Frank Annor, who connected me to you and many others in Kumasi in the first place.

Furthermore, the fieldwork would not have been a success without the amazing team of the Kumasi Business Incubator at KNUST. Thank you Sam and Isaac for making the fieldwork possible and arranging support. But most of all, thank you Evans and Lael for assisting me in the field daily during hot weather, heavy downpour and sometimes the unpleasant task of sorting waste. Without you this research would really have not been possible, or at least not as much fun.

Looking back at my time at TU Delft, I was very lucky to meet a lot of amazing people who became very close friends. Your company and support during my entire studies have made it an unforgettable time. A special thanks to Fiona, who was so kind to thrust me with her heavy windows laptop. Without her, flood modelling in HEC-RAS would have become very complicated on my own Macbook from 2010. Another special thanks to Pim, whom I shared all great moments together with the past 10 years; from living together in Delft and Mozambique, graduating high school and now virtually in the same month as #teamciviel.

Lastly, I would like to thank my parents, partner and family for their unconditional support and patience during my entire studies. I am very lucky to have such a loving family, who are always open minded and supportive of my new adventures. Let's see where the next adventure will bring me.

J.A.L. Tjia
The Hague, April 2020

Summary

This research assesses the impact of plastic waste accumulation on flood events with citizen observations in Kumasi, Ghana. In Kumasi, the fastest growing city in Ghana, flooding events have become more intense due to rapid urbanisation and land use intensification. Additionally, rapid population growth, urbanisation and lack of organised waste collection, brings along tonnes of solid (plastic) waste on the streets, riverbeds and -ways. Plastic waste creates blockages in drains and rivers, which causes flooding of open areas, streets and houses. To what degree plastic waste accumulation aggrevates flooding in Kumasi remains poorly understood. Therefore, this study investigates to what extent plastic accumulation impacts flood severity, in response to rainfall events in the city of Kumasi, Ghana. This is done by modelling different rainfall scenarios in a 1D-2D model developed with the software HEC-RAS. This model was forced with static and dynamic data available from open source databases and collected during fieldwork. Data collection took place during six consecutive weeks in May-June 2019 and consists of bathymetry and discharge measurements, a flood- and plastic waste survey performed together with citizens. The impact can be determined using different model scenarios varying in rainfall magnitude and in obstruction of riverways, serving as plastic accumulation. Flood severity was analysed in terms of extent, depth, velocity, local hydraulic impact and flow distribution. The model has been validated with two events, one during which velocity and stage was measured, which results in the same order of magnitude, modelled slightly lower than measured in the field. The second event was a historic rainfall event, which could be validated with community reported flood depths. From this validation it became clear the flood extent of the event was underestimated and depths close to the streams were overestimated. The results show that the selected rainfall events without blockage cover the studied area between 11-25% with water depths higher than 10 cm. The inundated areas are adjacent to the river streams and inundate flat and low lying areas. Comparing this to the scenarios where bridges where obstructed to 33% and 67% individually, the total inundated area remains more or less the same, varying between 0-3% in inundated area compared to the scenario without blockage. However, in terms of flood distribution, areas around the blocked bridge are impacted more, thus inundation areas shift within the observed study area. Comparing this to the rest of the area, upstream or downstream less flooded areas arise, making the change in total flood extent only change slightly. Furthermore, the two bridges that are obstructed have different impact on the flow in the study area, as the scenarios of obstructing the second bridge with 33% produce a numerical instability and therefore incorrect results. From the plastic waste survey it followed that plastic waste is very much abundant in the study area, thus the occurrence of plastic accumulation at the bottleneck locations seem inevitable. The results of this research have shown the main contribution to flooding is flow from upstream areas exceeding river capacity, while local blockages mainly aggravate flooding around the blocked locations.

Contents

1 Introduction

1.1. Problem statement

Flood disasters remain a severe challenge in developing countries. Rivers and floodplains are threatened by anthropogenic pressures and are one of the most degraded ecosystems in urban areas in many developing countries [44]. Due to climate change and rapid urbanisation, many cities in developing countries face serious threats of increased floods. In Kumasi, the fastest growing city in Ghana, flooding events have become more intense due to rapid urbanisation. Due to this rapid urbanisation and population pressure, land use in the city has intensified. Land use has expanded to the city's public parks and natural vegetation of open spaces, riparian lands and wetlands. This expansion creates a lot of large areas with impervious surfaces, which leads to increased volumes of runoff from precipitation [33]. Additionally, rapid population growth, urbanisation and lack of organised waste collection, brings along tonnes of solid (plastic) waste on the streets, riverbeds and -ways. Plastic waste creates blockages in drains and rivers, which causes flooding of open areas, streets and houses.

Previous research has concluded floods now occur at least 4 times per year in Kumasi, and are becoming increasingly severe [34] [18]. The floods occur more regularly after moderate to heavy rainfall events as a consequence of uncontrolled occupation of inland water areas, especially rivers and floodplains by urban developments [34]. As human settlements are getting increasingly close to floodplains of river channels due to rapid and uncontrolled urbanisation, communities are becoming more vulnerable to these floods [18]. Additionally, previous research has explored if floods have been increasing due to the effects of climate change. The studies of Owusu-Ansah (2016) [33] and Campion and Venzke (2013) [18] have analysed historical rainfall data from the Ghana Meteorological Agency going back to 1961 and concluded the amount of precipitation has declined slightly over the years [33] or found no significant rainfall trends [18]. Based on the available data, it appears that the total rainfall and shifts in seasonality are not significant contributors to flooding in Kumasi [33] and could therefore not be attributable to changes in climate [18].

However, it is clear the city's sewerage system and river network does not have sufficient capacity to drain or runoff the current water volumes. The city's sewerage infrastructure is only limited to a few suburbs, leaving the rest to be drained by streams which are often filled with large quantities of uncollected municipal waste and eroded materials. Hence it is not surprising that many drains and streams overflow their banks after heavy rain showers [33]. The research of Amoateng et al. (2018) [34] observed that the few existing rivers have small and separated channels which cannot support smooth flow of runoff, while physical structures constructed in waterways have resulted in obstruction and/or loss of pathways of the runoff. Currently, any excessive runoff on rainy days overflows the river banks, and flows through any available land, as well as inundating houses [34].

Additionally, the growth of the population in Kumasi, has resulted in a lot of solid (plastic) waste generation. The Kumasi metropolitan area recorded the highest waste generation rate of 0.75 kg/person/day which was slightly above that of the capital city Accra, 0.74 kg/person/day [47]. As waste management is barely existing in Kumasi, a lot of plastic waste is left at streets, riverbanks, waterbodies and other places in urban areas. This plastic waste causes clogged drains and blocked riverways, resulting in more floods. As streams and floodplains are already under threat of urban developments, the existing ones are also affected by solid (plastic) waste. Not only is there opportunity to reduce flooding events by cleaning the environment of plastic waste, there is also

the opportunity to recycle these plastics [28].

1.2. Research context

This thesis is part of a larger project: TWIGA, which is funded by the European Union's Horizon 2020 Research and Innovation Programme. TWIGA's goal is to provide currently unavailable geo-information on weather, water, and climate for sub-Saharan Africa by enhancing satellite-based geo-data with innovative in-situ sensors and developing related information services [45]. There are few places on Earth that are served worse with geo-information than Africa while at the same time, the potential value of geo-information services in Africa is extremely large. This ambitious goal can be achieved thanks to recent advances in sensor and communication technology, as well as new sensing platforms such as UAVs and citizens' observations. Their concept is to provide a systematic feedback loop to collectively validate in situ measurements and satellite data in one integrated model [45].

A number of (potential) geo-services have been identified in the work plan setup of TWIGA, of which mapping of floods and solid (plastic) waste disposal are two of the topics. This can be supported with citizen science, where data collection is performed by citizens on local level. Community mapped data can support planning and management by using smartphones with accurate GPS sensors and internet access. In 2018 several steps have already been made in the work plan, where conducting a UAV flight to produce a high resolution image of the study area was one of these actions. Now, this can serve as input for the next steps in the work plan, where *producing a integrated flood model of satellite data and in situ measurements will be explored.*

1.2.1. Research scope

The objective of this research is *to determine the impact of plastic accumulation on flood severity*. More specifically, the attribution of solid waste on severeness of flood impacts is investigated. This will be done in urban area, on neighbourhood scale in the city of Kumasi, Ghana. As to what degree plastic waste accumulation aggrevates flooding in Kumasi remains poorly understood, the impact will quantitatively be investigated. Model scenarios varying the probability of rainfall events and solid waste blockages, will give insight in the severity of flooding. Through fieldwork it will be observed how and where plastic waste is distributed and located. With citizen observations it will be explored if data on plastic can collaboratively be collected. Furthermore, it will be investigated if currently available satellite data and TAHMO precipitation data can provide a basis for a trustworthy flood model. This model will be developed using HEC-RAS, a free software for this application. Additionally it is investigated how citizen's observations and in situ measurements can validate and support development of scenarios of this flood model. The model output will be validated with discharge measurements taken during an observed rainfall event and the local community's reports on flood depth from a historical flood event. The latter will be collected in a flood extent survey. From modelling scenarios, the impact of solid waste on flooding will be investigated, by adding data on solid waste blockages to the model.

1.2.2. Research questions

The main research question of this master thesis will be:

To what extent does plastic accumulation impact flood severity, in response to rainfall events in the city of Kumasi, Ghana?

Which can be divided into the following sub questions:

- What is the impact of moderate and heavy rainfall events on flood distribution in the study area?
- How does the occurrence of plastic accumulation impact the magnitude of flood events in terms of flood extent, depth and distribution?

These questions will be researched with means of literature study, fieldwork and modelling.

1.3. Report structure

The next chapter 2 'Background', introduces background theory for this research by reviewing literature and concepts that are relevant for flood risk and urbanisation, plastic waste and flood modelling. Chapter 5.5.2 'Study area' introduces the case study area of a neighbourhood in Kumasi. Chapter 4 'Methods' presents a framework of analysis and all data sets that constitute the flood model, which is presented in chapter 5 "Model Development". Chapter 6 'Results and Discussion' presents the results of the performed surveys and most importantly the model simulations, together with relevant discussion points. Chapter 7 concludes the thesis with the conclusion and recommendations to continue future research in this field.

2
Background

This chapter introduces the theoretical background for this research by performing a literature review to support the research regarding flood risk, urbanisation, plastic waste as cause of floods and the concepts used for flood modelling in HEC-RAS. Firstly, the phenomena of flooding and urbanisation in Ghana and more specifically Kumasi are elaborated on with relevant studies performed in this field. Then, the problem of plastic waste and its management in the study area is described. Last, the hydrologic principles and hydraulic theories that are applied in the flood model are discussed.

2.1. Flooding and urbanisation in Ghana

2.1.1. Flood risk and climate change

Flooding is an inevitable phenomenon but in recent years, flooding of major Ghanaian cities has been the cause of disasters on an unprecedented scale [5]. The World Bank [10] has described flooding in Ghana largely as an urban phenomenon mainly due to rapid urbanisation and poor urban planning, often creating urban configurations that are rapidly coming up in floodplains. Ghanaian cities are highly prone to flooding and areas include: the Accra plains along the coast; Pra River and Ankobra River basins in the Western Region; White Volta basin in the Northern region; Black Volta basin in the Upper West Region; and Afram basin in the Eastern and Ashanti regions [8] [26]. Between 1990 and 2008 Ghana experienced six major floods with devastating results in 1991 (2 million people affected), 1995 (700,000), 1999 (325,000), 2001 (144,000), 2007 (325,000), and 2008 (58,000) [26]. More recently in 2019 there were 4 extreme flood events throughout the country. These flood events revealed weaknesses in the disaster preparedness and emergency response system, and exposed vulnerabilities of people, land use and infrastructure systems [7]. Campion and Venzke (2013) [18] investigated the main causes of floods in Kumasi and concluded that there are two types of floods that affect the suburbs studied in their research: flash floods and effluent stream floods. The flash floods arise from overland flow due to heavy rainfall events. Effluent stream floods arise due to a rise in the water table during the peak rainy season of June–July causing relatively long-term surface inundation [18].

Increasing urbanisation and remarkable growth of human settlements is beginning to have very serious repercussions towards the impact of floods in Ghana, which is typical for many developing countries south of the Sahara [5]. Cases and risks of flooding in cities worldwide are reported to be on the rise, with aspects of flooding linked to climate change and urbanisation ([21]; [24]). For instance, rapid urbanisation coupled with changing climate is often reported as forcing rural communities to migrate to cities and settle in areas that are highly prone to flooding in developing countries [10]. However, in Ghanaian cities such as Kumasi and Accra, climate change is not an aspect that can directly be linked to increase in flood risk, concluding from previous research. Ahadzie and Proverbs (2010) [6] analyzed 167 newspapers between 2000-2010 that suggest floods have become an ongoing phenomenon in Ghana and indicate that their impacts generally are becoming more severe, in terms of lives lost, lives affected and destructions of infrastructure and properties. They investigated the average annual rainfall of Greater Accra between 1995-2010, and found it was declining. However, this is not very informative as high rainfall intensities determine flooding and not average annual rainfall. Furthermore, they argued that in Ghanaian cities flooding can no more be attributed to natural causes of rainfall but rather is exacerbated by uncontrolled and unregulated growth in human activities and settlements [6]. Moreover, several researches about Kumasi conclude that rainfall levels are declining or not significantly changing [18] [33] but it can be concluded that the impact in terms of death tolls is rising [6].

2.1.2. Rapid urbanisation consequences

According to Cobbinah et al. (2015) [20], urbanisation refers to demographic patterns, ecological characteristics, sociological factors and economic phenomena that concentrate population in urban areas. It has the potential to either stimulate or interfere growth and development of these areas across the world [27]. Although urbanisation is a relatively recent phenomenon in Ghana, over half of the total population is now concentrated in urban areas [39]. The World Bank [10] summarised Ghana's urban transformation with the following numbers: urban population was increased 3.5 times between 1984-2014; agricultural employment share was decreased with 21 percentage point between 1992-2019 and an annual GDP growth of 5.7% between 1984-2013.

In Kumasi specifically, urbanisation contributed to rapid expansion of the built-up area to almost three times between 1986 and 2015. In 1986, the total undeveloped land was 64% of the total land area. By 2015 the undeveloped land has decreased to 19% of the total land area, which is expected to decrease even further. [27] The situation in Kumasi is common across all major cities in Ghana. Converting undeveloped land to built-up area has consequence on flooding, because land use changes can increase the risk of flooding. Converting undeveloped land to built-up area reduces the absorption capacity of soils and infiltration while increasing surface runoff [27].

The unsystematic physical development across Ghanaian cities is often reported as the main cause of flooding ([18]; [26]; [33]; [27]). Thus, it is not unexpected that in the past decade flooding has become an annual occurrence in several Ghanaian cities. Aside the loss of human lives, important infrastructure such as roads and utility services are often destroyed [27]. Additionally, recent rapid urbanisation can be described as a socio-economic risk in several African countries, including Ghana. Cobinnah et al. (2015) [20] believe that the relationship between urbanisation and improved livelihoods is inverse and not benificial, as several African cities increasingly find it difficult to manage rapid, unplanned and unsustainable urbanisation. Eventually this is eradicating the benefits associated with urbanisation [20]. They state that the growing evidence of urban poverty, flooding and unsustainable exploitation of resources in African cities is associated with rapid urbanisation [20]. In such situations, African urbanisation is described as demographically driven and is occurring without socio-economic and environmental benefits [20];[27].

2.1.3. Vulnerability of communities

Due to unorganised building and expansion of urban areas to riverbeds and floodplains, communities become more exposed to floods. However, there is no other choice due to lack of building codes, lack of social safety nets, land scarcity and economic means. Building close to or even on riverbeds and floodplains is done because this land is often more affordable [47]. Furthermore, decades ago when the floods were not yet occurring frequently, people were already living near rivers. As time passed, the riverbeds expanded and became increasingly closer to the settlements. When floods started to occur people were not able to move due to economic factors. Lack of affordable ground, housing and means to move, results in communities living on floodplains and riverbeds. According to the government, awareness of not building on the riverbeds is lacking among communities [47].

When disasters happen, the rapid response to issue relief items is crucial and much needed. In order to develop an effective response strategy, the understanding of flooding and its prediction is very crucial. Currently, very little or no risk management strategy is in place to predict and warn victims of a potential flooding. The lack of awareness amongst communities on evacuation and safety awareness is potentially dangerous and could increase the effects of floods. Innovative strategies should be put in place to develop a robust and well-packaged education of the general public on evacuation and safety awareness programmes in the event of floods. [6]

2.2. Plastic waste as cause of flooding

With the rise of a growing middle class, globalisation and demand for consumer goods in urban areas like Kumasi, the use of plastics has been in increasing. Lacking a proper waste management strategy and system, plastics end up on streets or open landfills. Additionally, attitude of people and lack in education seem to hinder the proper waste disposal. Eventually, plastics clog drains and rivers resulting in a obstruction of runoff and riverways, resulting in floods. This poses a serious threat on the health and safety of communities in Kumasi.

2.2.1. The plastic problem

Plastics are a unique sort of material which belong to the chemical family of high polymers and are unimaginable in our daily lives almost all over the world. They are essentially made up of a long chain of molecules containing repeated units of carbon atoms. Due to this internal molecular stability, plastics do not easily break down into smaller components [28]. A scary thought considering that in the 1960s, less than 1% of our waste was plastic. The increased use has resulted in concern with (1) the consumption of natural resources such as oil, (2) the toxicity associated with their manufacture and use, and (3) the environmental impact arising from discarded plastics [11]. The most substantial use of plastics today, accounting for well over a third of production, is for disposable items of packaging, most of which are discarded within a year of manufacturing [42]. Well over a billion single use plastic bags are given out for free every day. The durability and increasing usage of plastics create a major waste management problem with plastic accounting for approximately 10% of the waste we generate. Some of this is recycled, but a substantial part is disposed of to landfill. Two of plastics advantages; their light weight and durability, make plastic items a significant environmental hazard once in water. Close to half of plastics are buoyant and remain so until they become waterlogged or assemble too much epibiota to float [48]. Furthermore, plastics do not biodegrade. Through photodegradation and abrasion plastics only break into smaller and smaller pieces so 'that they can be consumed by the smallest marine life at the base of the food web' according to the United Nations Environment Programme [37].

In Ghana, per capita generation of plastic waste stand at 0.016-0.035 kg/person/day and plastics make up between 8 to 9% of the component materials in the waste stream. Currently, most products are packaged in polyethylene which forms about 70% of the plastic waste in the municipal waste stream. Additionally, over 10,000 metric tonnes of finished plastic products are imported each year into the country. Available records from the city authority, Accra Metropolitan Assembly indicate that out of the over 2,500 tonnes of waste generated daily, only approximately 45% is collected. The remaining 55%, of mainly plastics remain in the system. [28]

In a number of African countries, plastic pollution is causing severe environmental and health damage that manifests itself in a number of ways. Plastic bags can block storm drains and sewage systems, leading to flooding and increased spread of disease. Trapped water, for example in plastic bags, also provide an ideal breeding ground for mosquitos, furthermore raising the risk of malaria transmission. Since most landfills are not routinely covered with soil in Africa, the plastic waste is easily transported around the countryside where wildlife and livestock consume these materials. The increasing urbanisation of Africa also increases the stress on its limited waste management systems which otherwise could better contain the plastic problem [11].

2.2.2. Waste management in Kumasi

Solid waste management is an important aspect of flood risk management. Poor waste management has consequences on urban flooding by blocking drains, increasing debris and harbouring disease vectors. Poor disposal of solid waste leads to blockages in watercourses and drainage systems, which reduces the capacity of storage and water flowing to areas with lower water levels leading to flooding [47]. The research of Vafa et al. (2019) [47] and Asase et al. (2009) [9] investigated the waste management system in Kumasi. Both researches concluded that the strategy for solid waste management is poorly defined, with no specific targets [47] [9]. The Kumasi Metropolitan Assembly produced a strategic sanitation plan for Kumasi for the period 1990-2000 which was later reviewed and extended until 2005. The component of solid waste management within the plan seeks to develop a landfill for the city and to engage the private sector in waste management services, which have been achieved in the city. However, no specific plan exists for waste management in the city specifically, with for example targets to meet and indicators to measure the progress. In Ghana, no distinct law has been identified for the management of solid waste. However, a key policy documents exist. The Kumasi Metropolitan Assembly has bye-laws related to the handling of wastes, which are presumed to be outdated particularly in terms of penalties. [9] The enforcement of these by-laws has also been weak, as it has currently been observed that there are less penalties given than compared to the past [47].

The collection of municipal waste in Kumasi is operated with two types of methods. These are the house-to-house (curbside) solid waste collection which are collected with compactor trucks and communal solid waste collection. The communal collection system involves the location of metal containers at designated sites known as transfer stations, which are shared by a number of houses within that community. When the containers are full, they are transported and emptied at a final disposal site by container loading trucks. Collection of waste from institutional and industrial premises also relies on container services. Approximately

85% of the waste generated is collected in the municipality of Kumasi. The waste collection service in the city is carried out by the private sector under various agreements with the metropolitan assembly. [9]

All waste collected in Kumasi is disposed of at two sites with a capacity of $4,6km^3$; a sanitary landfill site and an open dump. The sanitary landfill is constructed on a 100 acre land and treats both solid waste and sewage. The sanitary landfill is managed by a private contractor on behalf of the city authority. Processing waste through recycling and reuse is carried out on an informal basis, which is not widely recognised as contributing to waste management in the city. [9]

2.3. Flood modelling of urban areas in HEC-RAS

Hydraulic models can be used to predict the consequences of flooding events. These models are used as a tool to gain an in-depth perspective of hydraulic systems, so that more effective mitigation measures can be developed, such as inundation maps and flood hazard zones or even planning for levees and dams [43]. Hydraulic modelling involves the use of mathematical equations representing the fundamental physics of how water moves, in order to gain understanding of the system's behaviour. Models take into account time, land cover, conveyance area, basic physics of water behaviour and water volume to portray the effects a river can have on the surrounding area and community [43]. The most significant challenge in developing a flood model for the neighbourhood in Kumasi, is that many of the city's or even country's rivers are not gauged and hydrologic or hydraulic data are not widely collected for research purposes.

This research develops a physically-based model, which consists of finite elements that represent physical entities of the modelled area in 1D and 2D. This means that the one-dimensional part of the model simulate flows that are assumed to flow in a longitudinal direction, such as rivers and channels. One-dimensional models are computationally efficient but are subjected to modelling limitations, such as the inability to simulate flood wave lateral diffusion, the subjectivity of cross section location and orientation, and the discretisation of topography as cross sections rather than as a continuous surface [41]. In this case, the two dimensional part of the model is used to simulate the floodplain flow, in order to visualise the extent of floods which only a 1D model cannot provide. Two-dimensional models simulate floods with the assumption that the water depth in a vertical direction can be neglected, in comparison to the other two dimensions [29].

2.3.1. Components of a flood model

The word 'model' is used in a lot of different ways, but in this research it is referred to a mathematical, computer-based model. More specifically, it is a physically-based model of flow which represents the inputs (discharge) and convert them into the information that is needed: flow rate and depth within the system and its outlets. The model carries out this conversion by representing (mathematically) the main physical processes that take place. However, these 'models' are simply tools that simulate a flow in a particular catchment [50].

- Rainfall: The model will be used to find the response of the catchment to particular rainfall events. Rainfall with a particular storm profile, thus whose rain intensity varies with time. Actual rain gauge records are used as rainfall input to the model.
- Rainfall to runoff: The conversion of rainfall into runoff, water destined to find its way into the sewer system, is a complex process. There are many reasons for rainwater not to become stormwater in the sewer. It may, for example, infiltrate into the ground, form puddles and later evaporate, or be caught in the leaves of a tree. However, infiltration and evaporation are not taken into account, as HEC-RAS does not have an option to incorporate these parameters. The Rational method is a simple model of the conversion of rainfall into runoff that can be used to look at the likely effects of different rainfall intensities.
- Overland flow: The main consideration here is not the amount of rainwater that will enter the sewer, but how much time it will take to get there. Clearly the extent to which water entering from one area will overlap with that entering from another will have significant effect on the way the flow in the sewer builds up with time. [50] However, it is certainly the total rainfall driving the eventual severity of flooding.

2.3.2. Theoretical Basis for 1D and 2D hydrodynamical calculations

The Hydrologic Engineering Center - River Analysis System (HEC-RAS) software is a flood modelling software in hydrodynamic simulation. The software allows to perform one-dimensional steady flow, one- and

two-dimensional unsteady flow calculations, sediment transport/mobile bed computations, and water temperature/water quality modelling. A key element is, that all four components use a common geometric data representation and common geometric and hydraulic computation routines. The software uses geometric data representation and geometric and hydraulic computation routines for a network of river channels. While there are a large number of capabilities this model can perform, this research will only focus on HEC-RAS's ability to perform 1D and 2D unsteady flow, including structures such as bridges.

Unsteady fluid flow varies in both space and time. The physical laws which govern this flow of water are: (1) the principle of conservation of mass (continuity), and (2) the principle of conservation of momentum. These laws are expressed mathematically in the form of partial differential equations, which will hereafter be referred to as the Shallow Water Equations (also known as the St. Venants equations). The derivations of these equations are elaborated on and can be found in appendix A. They are based on the equations presented in the HEC-RAS hydraulic reference manual [13].

Assumptions
The 1D and 2D Shallow water equations are based on a set of assumptions and understanding their implications are therefore important. These assumption are the following:

- Fluid is incompressible: the volume is proportional to the mass since the density is assumed constant.
- Pressure distribution is hydrostatic: vertical accelerations are neglected.
- Flow is one- or two-dimensional, vertical variations in flow and velocity are neglected.
- Wave lengths are much larger than water depth.
- Average channel bed slope is small.
- Bed friction can be calculated using Manning's equation, which has been derived for steady flow conditions.
- The flow can be described as continuous functions of the velocity and the water surface elevation H. [12]

One-Dimensional
In 1D river hydraulic modelling, all water flows are assumed to flow in a longitudinal direction. One-dimensional models represent the terrain as a sequence of cross-sections and simulate the flow in order to provide estimates of flow parameters such as flow velocity and water depth. The governing equations that are used in the one-dimensional computations are the continuity and momentum equations, for which the derivations can be found in appendix A.1.

Two-Dimensional
When studying flow over complex floodplains, the assumption that flow is only 1D may no longer be valid. 2D unsteady flow varies in time and along two spatial dimensions. The governing principles of 2D unsteady flow are the same as for 1D flow, the conservation of mass and momentum. Two-dimensional flood models allow water to move in both longitudinal and lateral directions, while velocity is assumed to be negligible in the z-direction. However, unlike 1D models, these models represent the terrain as a continuous surface through a mesh or grid. In order to improve the computational time, HEC-RAS uses a sub-grid approach, which uses a relatively coarse computational grid and finer scale information underlying the topography [13]. The sub-grid bathymetry equations are derived from full shallow water and diffusion wave equations. The 2D continuity and and momentum equation can be found in A.2.

Modelling simplifications
In order to reduce the computation time and reduce numerical instability, the full Shallow Water Equations are often simplified by neglecting different terms in the momentum equation. These simplifications are mostly applied when modelling in 2D. While several different simplifications exist, the main simplification used in HEC-RAS, namely the Diffusive wave approximation is presented in appendix A.2.3. This approximation can be used instead of the 2D full momentum equations. Using the diffusive wave simplification of the shallow water equations, the governing equations for 2D flow (A.5, A.6 and A.7) are simplified to expression A.11. The

advantage of using this approximation is that it leads to a shorter computation time and may reduce model instability. It may be used to describe varying flow in moderate to steep reaches. However, flow separation, eddies as well as momentum transfer cannot be modelled [12].

3

Study area

This chapter aims to elaborate on the characteristics of the study area and to explain why this area is chosen for this research. First, some relevant aspects of Kumasi will be discussed as this is the city where the study area is located. Furthermore, this chapter provides a detailed description of the study area with its relevant characteristics interesting for this research. Last, important features of the study area will be introduced, which will be referred to further in the report.

3.1. Kumasi

The study area is located in Kumasi, the capital of the Ashanti Region in the south-central part of the country. The name of the district the study area is part of is Atonsu, which is a central point where a lot of public transportation comes together. Kumasi is the second largest city in Ghana after the national capital city, Accra. The city is positioned between latitude 6.35-6.40 and longitude 1.3-1.35 and lies at an elevation between 250 and 300 m above sea level with an area of about 254 km^2. The topography is a combination of hilly terrain and agricultural lands. The city falls within the moist semi-deciduous vegetation zone of Ghana which has favourable soil conditions that support green vegetation and farming activities, giving the city its nickname 'the Garden City'. Kumasi has a strategic location, which makes it the principal transport terminal and has assured its essential role in distribution of goods in the country and beyond. The unique central location of the city as a traversing point from all parts of the country, makes it a special place for many to migrate to. Due to this strategic location and political dominance, Kumasi has developed into a major commercial centre with all major trade routes converging on it. [3] In figure 3.1 the position of Kumasi and the study area is indicated.

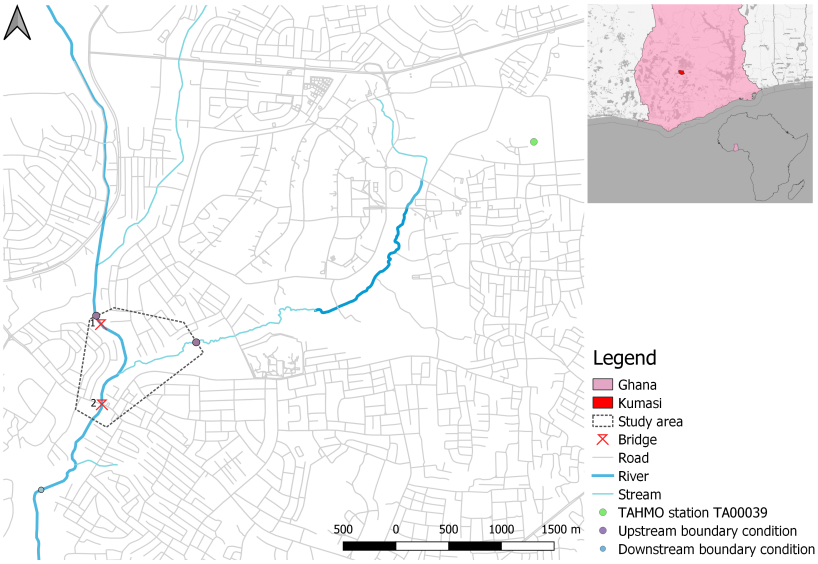

Figure 3.1: Position of Ghana, Kumasi and the study area Atonsu

The population in Kumasi was approximately 2 million in 2010 and was the fastest growing city in the country, as the city itself already contributed for 20.2% of the country's total urban growth between 2000-2010 [39]. As mentioned in section 2.1.2, land use in the city has intensified due to this rapid urbanisation and population pressure. Land use has expanded to the city's public parks and natural vegetation of open spaces, riparian lands and wetlands. Due to this expansion, a lot of large areas are created in the city with impervious surfaces and increased volumes of runoff from precipitation [33].

3.1.1. Climate and weather

Kumasi has a tropical wet and dry type of climate (Köppen climate classification Aw) with hot conditions for the majority of the year. The climate of the city is mostly influenced by the proximity to the equator, the water body of the Gulf of Guinea and the dry Saharan winds. Precipitation wise, the city receives plenty rainfall of 1397 mm annually, of which 90% falls during the rainy season. There is a long wet season, from March to November, where August has a pause in precipitation and separates the two rainy seasons that occur in this region. The annual sunshine records 1952 hours with a peak from February to April and from June to August [4]. In figure 3.2 the annual averages of temperature, rainfall and rain days can be seen. This information was taken into account when planning the fieldwork, for which heavy rainfall was desirable: from begin May to mid June 2019.

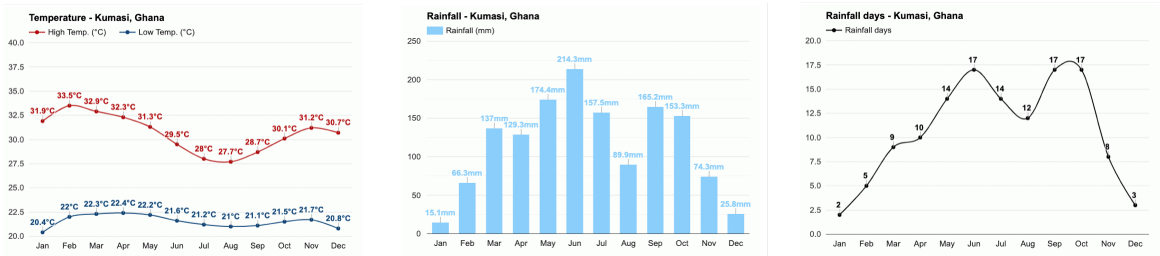

(a) Temperature (b) Rainfall (c) Rain days

Figure 3.2: Annual averages of weather parameters in Kumasi [4]

3.2. Characteristics study area

A flood prone-area has been selected near to the Lake Road Bridge and the Agogo market in Kumasi, which can be seen in figure 3.3. Main arguments supporting the choice of this location was:

- Concerns an urbanised area containing a big market, the Agogo market, which is situated in the selected area
- Different kinds of water infrastructures are present (bridges, drainage canals)
- Alongside the river and in drainage canals a lot of plastic waste is present, causing problems for water discharge at heavy rainfalls causing floods
- The area contains neighbourhoods, swamps and agricultural fields that are regularly flooded in the period of June up to September each year [17].

Figure 3.3: Selected study area [17]

In figure 3.4a and 3.4b an overview and details of the study area can be seen respectively. As can be seen in figure 3.4a, the three sections of the Y-shaped waterbody can be divided in three sections, which will be referred to as 'reach 1' for the upper reach on the left side, 'reach 2' for the upper stream on the right side and 'reach 1-lower' for the lower reach. The blue arrows in the figure indicate the flow direction, from upstream to downstream. Furthermore, figure 3.4b shows an orthomosaic of the study area, where it can be observed that (residential) buildings are located adjacent to the banks of the streams.

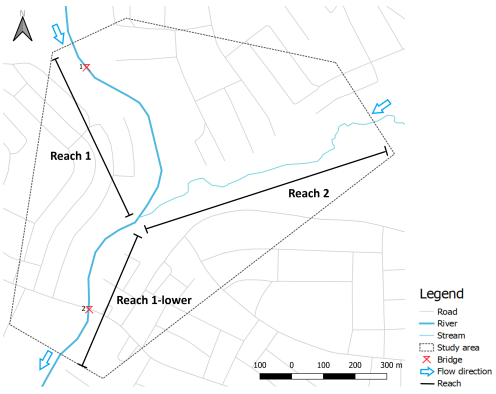

(a) Schematic of study area

(b) Orthomosaic produced by FutureWater

Figure 3.4: River reach where stage and velocity measurements were conducted on 23 May 16:00 PM

4

Methods

This chapter presents the data and methods used to develop the flood model in order to answer the research questions. First, an overview of the framework of analysis is given, which is illustrated by a flow-chart. Then, the input data which consist of open source data and collected data sets are introduced. All collected data was obtained during fieldwork of six consecutive weeks in May-June 2019. Last, the processing of datasets is elaborated on, which is needed for the model developed in chapter 5.

4.1. Framework of analysis

In order to answer the research question, *to what extent does plastic accumulation impact flood severity, in response to rainfall events in the city of Kumasi, Ghana?*, a flood model needs to be developed. This flood model should be able to run simulations of heavy and moderate rainfall events, and simulations with plastic blockages. The software that is able to do this is HEC-RAS, which is composed of two main components: (1) boundary condition data and (2) model geometry setup. An overview of the input data and methods used for model set-up and boundary condition design is illustrated in figure 4.1. Reliable and detailed input data is crucial for modelling in order to be able to produce trustworthy results. All steps that are shown in the figure are necessary to answer the main research question, which is composed of two sub-questions. Left, all data sets used in this research can be seen which exist of open-source (orange) and collected (yellow) data. Furthermore, some datasets are dynamic (filled) and others are static (white). From this, the resulting input data that is needed for the flood model are both dynamic, thus are different for each scenario. The model will simulate different scenarios that are introduced in section 5.7 in order to determine the impact of rainfall events and the impact of the blockages on flood severity respectively. The output will be given as a flood map and can be validated with a flood extent survey for a historic flood event and with discharge measurements from an observed rainfall event, both acquired during fieldwork.

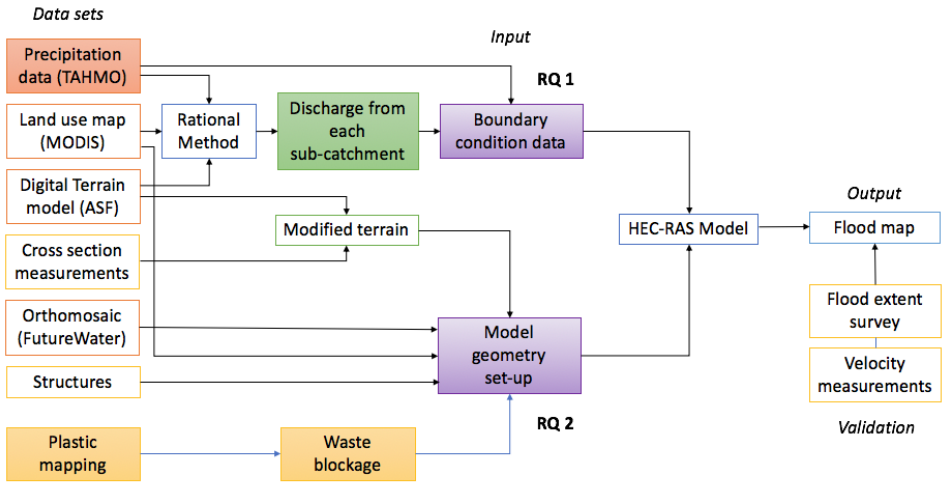

Figure 4.1: Framework of analysis illustrating the use of different data sets in this research and their purpose.

4.2. Applied datasets

As can be seen in figure 4.1 the datasets provide the basis for the geometric setup of the model together with boundary condition data. This section introduces the applied datasets used in this research. These consist mostly of open source datasets, which can be downloaded from the internet. This consists of data of ground elevation, land cover and precipitation. First, an overview of all used GIS datasets is given together with their purpose. Last, the precipitation data that is selected for the model is elaborated on.

4.2.1. Topographic data

Topographic data, such as digital elevation models (DEMs) are essential input in flood modelling. In hydraulic modelling of floods, one of the most fundamental input data is the geometric description of the floodplains and river channels often provided in the form of DEMs[22]. Input data is essential for both 1D, 2D and 1D-2D models. If a 1D model is developed, topographic data is only specified at the cross sections, whereas 2D and 1D-2D models require elevation data covering the entire domain, as provided in a DEM[12]. The differences in the quality of each DEM subsequently result in differences in model output performance. As the flood model is on neighbourhood scale (1500 x 1500 m), the resolution of the terrain should be sufficient to capture details on this scale. In table 4.1 an overview is given of the open source terrain products that are used in this research. A short explanation of these products and their purpose will be given in the following paragraphs.

Table 4.1: Applied GIS data

Product	Facility	Spatial resolution [m]	Date shot
DTM	Alaska Satellite Facility	12.5	July 2007
Orthomosaic	FutureWater	0.1	November 2018
Land cover map	MODIS	500	2017

Digital Terrain Model

The DEM used in this research is developed by Alaska Satellite Facility: ALOS PALSAR. The DEM consists of raster data with a spatial resolution of 12.5 m and is shot in July 2007 [1]. The dataset represents a correct Digital Terrain Model (DTM), as all noise from vegetation and buildings is not present in the model. However, bathymetry of channels and rivers is not included in the terrain representation which is needed for the flood model. River bathymetry has to be incorporated using river cross sectional data. This DTM will therefore be modified with cross section data obtained during fieldwork as described in section 4.3.1, to provide a terrain that includes the bathymetry necessary for modelling. The terrain modifications used in this research are presented in section 5.1.2.

Orthomosaic

From previous actions in the TWIGA project, FutureWater carried out Unmanned Aerial Vehicle (UAV) flights over the selected study area in cooperation with the Ghanaian company Farmerline in November 2018. An Red Green Blue (RGB) orthomosaic was produced with a spatial resolution of 0.1 m. This aerial image shows great detail of the geometric properties of the study area and will be used to determine the geometric properties in the model, such as riverbanks and structures which is presented in section 5.1.1. This image was depicted in section 3.2, figure 3.4b. Furthermore, this product was also converted into a high resolution DEM. However, at time of performing the elevation measurements a GPS was unavailable, thus the DEM could not be geo-referenced with ground control points. The produced DEM therefore showed a bowling effect, which is not suitable for flood modelling. Furthermore, noise from buildings and vegetation was not removed from this DEM, making it not suitable for flood modelling as well.

Land cover map

Land cover data documents how much of a region is covered for example by impervious surfaces, agriculture, and other land and water types and is of interest in determining the runoff in the catchment. The MCD12Q1 V6 product of MODIS provides global land cover types at yearly intervals (2001-2016) derived from six different classification schemes. To determine the land classes, Band 'LC_Type1: Land Cover Type 1: Annual International Geosphere-Biosphere Programme (IGBP) classification' is used, which classifies 17 different classes [23] that

can be found in appendix D. This dataset is extracted from Google Earth Engine. The spatial resolution of this dataset is 500 m. Compared to the size of the study area, this is quite large. However, a higher resolution map which include the study area was not found at time of research.

4.2.2. Precipitation

The precipitation used as boundary conditions described in section 4.5.1 is recorded by the TransAfrican HydroMeteorological Observatory (TAHMO). TAHMO is aiming to build a dense network of hydrometeorological monitoring stations in sub-Saharan Africa. These stations are developed to be inexpensive and robust, suitable for sub-Saharan conditions. The rainfall is measured using an acoustic disdrometer which capture heavy rainfall events better than low intensity events [40]. In Kumasi there are four weather stations installed, relatively close to each other. In figure 4.2 the location of the stations is indicated together with the date they have been monitoring from onwards.

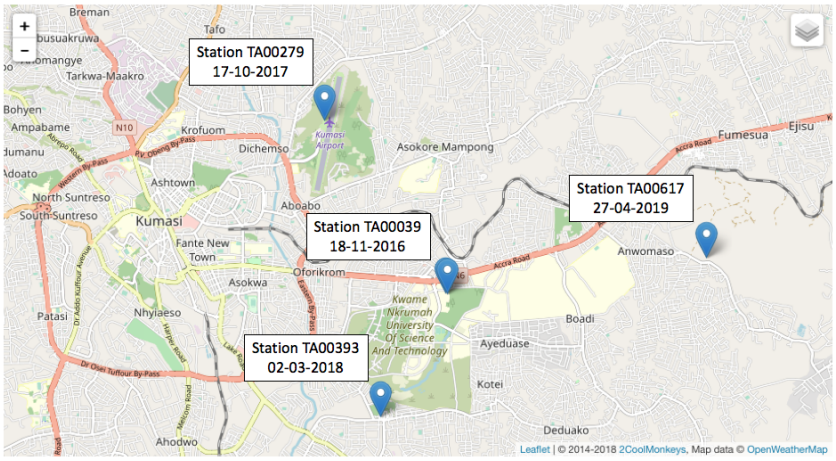

Figure 4.2: Overview of TAHMO weather stations in Kumasi and operational starting date

The longest time series for rainfall data is available for station TA00039, recording consecutively since November 2016. The other stations have been operating less than 2.5 years. As station TA00039 provides the longest time series, data from this station will be used to select rainfall events to explore flood scenarios and validate the model. However, it can be seen that station TA00039 captured high rainfall amounts depicted in figure 4.3, which are not consistent with the amount of rainfall in the following years. Therefore data from this period was discarded, which can be seen in figure 4.4. Furthermore, as the data only spans 3 years it is not relevant to perform statistical analyses, as the timespan is too short. However, it is noteworthy that a heavy rainfall event already causes difficulties and calamities each year in Kumasi, therefore the yearly maxima of the time series are taken into account for the model scenarios. Furthermore, newspaper articles were analysed in order to link flood events with rainfall data.

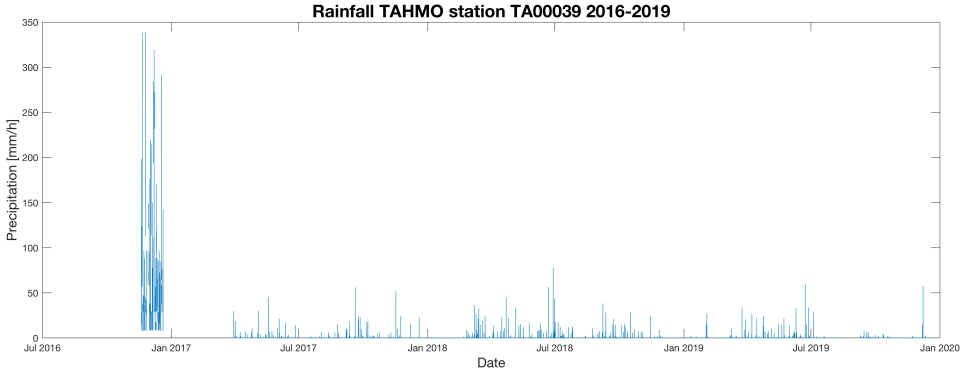

Figure 4.3: Rainfall time series station TA00039

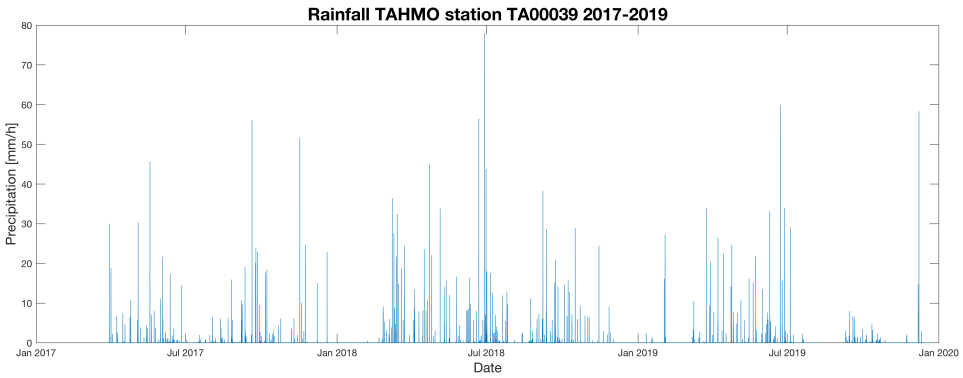

Figure 4.4: Rainfall time series station TA00039 from 2017

The maximum peak intensity for each year can be found in table 4.2. The resolution for which the data has been analysed was hourly precipitation. When analysing the maxima in the rainfall dataset, it can be seen these maxima are part of certain rainfall events depicted in appendix , figure B.1. Comparing the rainfall events from which these maxima are part of, it can be seen that the total precipitation and duration of these events vary significantly from each other which is also summarised in table 4.2. Therefore it is interesting to select all three of these rainfall events, in order to determine their impact on the study area. With varying magnitude and duration of these rainfall events, the simulations can serve as a sensitivity analysis and it can be analysed how the modelled system responds to the variety of events.

Table 4.2: Rainfall maxima of station TA00039

Year	Date	Time	Peak intensity [mm/h]	Total duration event [h]	Total precipitation event [mm]
2017	19-09	19:00	56	3	56.67
2018	28-06	17:00	78	9	102.96
2019	22-06	20:00	60	6	82.81

Furthermore, for the probability of the rainfall events, it is analysed how many times a certain threshold is exceeded in the precipitation dataset. Hourly precipitation is analysed between 2017 and 2020. In table 4.3 it can be seen how many times a particular threshold is exceeded. It can be concluded that the rainfall event larger than 60 and 70 mm/h is only exceeded once in the observed three years. The events larger than 50 mm/h occur 9 times in three years, following an average of 3 times per year. The event larger than 20 mm/h is recorded the most, with 95 times in three years, which means approximately 32 times per year the rainfall is higher than 20 mm/h. These thresholds will not be used in the flood model, however they will be used to discuss the probability of rainfall events.

Table 4.3: Rainfall exceeding threshold between 2017-2020

Threshold	> 20 mm/h	> 30 mm/h	> 40 mm/h	> 50 mm/h	> 60 mm/h	> 70 mm/h
Number of exceedence	95	45	15	9	1	1

4.3. Collected datasets

This section describes the surveys conducted by the author to collect data on flood depth and solid waste in the study area. Data was collected during fieldwork of six weeks from May 6th until June 14th, 2019 in the study area 'Atonsu'. Fieldwork was performed to get a better understanding of the scale and impact of the problems in the study area. As the flood model consist of open source data, it is also improved with in situ measurements. Furthermore, not all data that is needed for the flood model can be obtained from these sources. These have to be collected in the field, and consist of measurements and data from citizen observations. First, it will be explained how cross sectional data was obtained, followed by discharge measurements performed in the river. Next, the plastic sorting will be elaborated on which was done to determine the plastic waste composition in

the study area. Following, the data that was obtained together with local citizens will be discussed. This consist of the plastic mapping and flood survey.

4.3.1. Cross sections

Detailed cross sectional data is essential for hydraulic modelling as the river bathymetry controls the characteristics of the flow as described in section 2.3. Generally, measurements should be taken so that important changes in bathymetry are captured [12].

In this research, cross sections of the main constructed channel have been measured at three locations. From these locations it could be assumed that the constructed part of the channel is consistent along the entire stretch in the study area, from reach 1 to reach 1-lower. However, the smaller natural side river in reach 2 could only be measured at one point from a bridge. Thus only one cross section is obtained in this stretch of the river. While wading is the preferred method for accurate discharge and cross sectional measurements, there are obvious safety considerations that limit the flows at which wading can be accomplished [32]. Wading can usually be carried out safely when water depths are about a meter or less and the maximum stream velocity is no more than about 1 m/s [46]. As it was not possible to enter the natural stream as water levels were too high and other safety concerns were present, it was not possible to perform wading and obtain more cross section data.

4.3.2. Discharge measurements

There are no gauges in the hydrological system in the study area, thus the discharge is estimated by measuring the velocity at different moments and measuring the cross sections at different parts of the river stream. As mentioned previously in section 4.3.1 it was not safe to enter the water, thus velocity measurements could only be performed by using floats. Velocity of the water was therefore measured by the time required for a floating object to travel a certain length of stream. This approach has the obvious limitation of measuring only velocity at or near the water surface. To deal with the variability in stream velocity within any cross-sectional area, studies by the USGS support several general rules of thumb: the mean velocity in a vertical profile is 80-95% of the surface velocity, of which the average of several hundred observations being 85% [32]. Therefore, this factor is taken into account to correct the measured surface velocities. During different conditions, dry, heavy rain and after a rainfall event the velocity of the surface water was measured. This was done 6 times consecutively to get an average and adjust for errors.

Furthermore, conducting the fieldwork in May-June 2019, one heavy rainfall event occurred, during which velocity measurements were done. This particular event will therefore be chosen to serve as a validation scenario for the model, as it can validate the simulation with in situ velocity measurements. In the dataset it can be seen the event started at 14:00 PM with a maximum hourly rainfall of approximately 22 mm on May 23rd, 2019. Measurements in the field were performed around 16:00 PM, during the peak of the event.

4.3.3. Plastic sorting

In order to determine what kind of plastic waste is present in the study area, the plastic was sorted and weighed, following the method of Poon and Chung (2001) [19]. They state that sampling plan should be designed to capture representative waste samples. In theory, the number of samples for field determination of waste characterisation depends on the variation in the waste composition of each sample in the sampling point. With thorough mixing, even a small number of samples can reliably reflect the percentage composition of the waste stream. However, in the field ideal conditions are hard to find, due to seasonal, demographic and customary factors [19]. As they suggest to sort the waste during different times of the year and different conditions, the sampling during the fieldwork could only be done at one time during the year. Thus, it only gives an indication on what kind of waste is present at that particular moment. Furthermore, their methodology also proposes to dry and weigh the waste in a laboratory, which was also not possible for this research. Furthermore, the selected waste piles were not sorted thoroughly, but a square meter was selected for sorting, due to time constraints. The sample selection process started with selecting the residential refuse collection points. Three refuse collection points of the same size in the residential area next to the river stream were randomly selected. From these points, a square meter was measured out and was sorted and weighed. It should be mentioned that the weather was dry and hot at time of sorting. During the sorting process, the contents of any containers or bags found in the waste were emptied. No further cleaning of the plastic waste was performed before weighing. All the materials were weighed within a large plastic bag on a mechanical scale that was calibrated before being

used for the measurements.

4.4. Citizen observations

The use of citizen science is implemented to explore efficiency in data collection. Not only is citizen science a cost-effective way to gather data over a large geographical range, it has the possibility of simultaneously raising public awareness on the problem. To obtain a general knowledge about the amount of plastic waste and how it is distributed through the study area, plastic waste is being 'mapped' together with local citizens. Furthermore, as the local community is regularly subjected to floods, their knowledge is collected by means of a flood questionnaire. In this section first the plastic mapping will be discussed, followed by the flood survey.

4.4.1. Plastic mapping

For this research it is of great interest what kind of plastic waste is present in the area, in order to determine how much can accumulate in the rivers. Items, volumes and their location are important parameters that have been gathered with the mapping. It is investigated how well plastic waste and their volumes can be identified throughout the area, within the riverbed and along riverbanks. From observing what is present in the study area, the plastic waste objects should be identified and tagged with a geolocation. This method is adapted from the Litterati application, which is aiming to photograph plastic items and tagging them with a geolocation, which makes the problem measurable. As it was previously impossible to track plastic waste, it now becomes visible and patterns begin to emerge amongst what lies on the streets and surroundings. The more clear the data on the problem becomes, the more can be done to create effective solutions [30]. However, as plastic waste is abundant in the study area, the tagging in the study area does not only hold for individual objects like in Litterati, but is applicable to waste piles. For this research it is essential to locate these waste piles, determine their size and investigate how these piles develop over time.

To obtain this information, a simple application is developed through ODK collect. The application involves a simple questionnaire, where the geolocation of the waste pile can be saved together with relevant information and a photograph. To bring more structure in the responses, it should also be specified if the plastic waste is on land or in the water. Furthermore, as plastic waste is not only present on land but also in waterways, it is important to know if the plastic is flowing in the stream, or standing still and accumulating in front of a structure such as a bridge pier for example. For this it is important to know how much a river way is blocked with waste. Furthermore, the waste piles can be categorised per size, from small to large. As this is free for interpretation, pictures are additionally asked for. Locating the plastic waste in the area is done together with 4 citizens in the area who have a smartphone with internet access and GPS. These citizens have been instructed to observe a certain area or bridge in the study area. Thus, development of the plastic waste accumulation or distribution can be analysed. Furthermore, it is essential that the questions are unequivocal to avoid any confusion. In figure 4.5 an example of the questions in the application can be seen and the complete set of questions can be found in appendix F. After one week the questions were analysed together with the users and a few questions were altered and some were added. Data collection was performed between May 14th to May 30th, 2019 spanning roughly two weeks. During this period a total of 70 responses were collected.

4.4.2. Flood questionnaire

The flood questionnaire was set up to gain understanding about flooding, its severity and depths throughout the study area. Main questions were adapted from the methodology applied by the Ramani Huria project in Tanzania [36], which also focusses on flood extent and flood modelling. Extra questions were added about flood problems, how people experience floods and how they respond to them. These questions are composed of open questions, thus more information can be given and answers consist of qualitative information. The complete questionnaire can be found in appendix . The questionnaire was carried out in conversational form, with community members throughout the study area. Before starting the questionnaire, participants were asked to consent in giving information. Responses were stored in an application created through ODK collect, which also collects the geolocation and optional photographs. Participants were questioned at a total of 41 different locations throughout the study area.

The reported flood depths can serve as validation of the modelled rain events. However, there was no flood event occurring at time of conducting fieldwork. Thus, the depths reported by the community are maximum

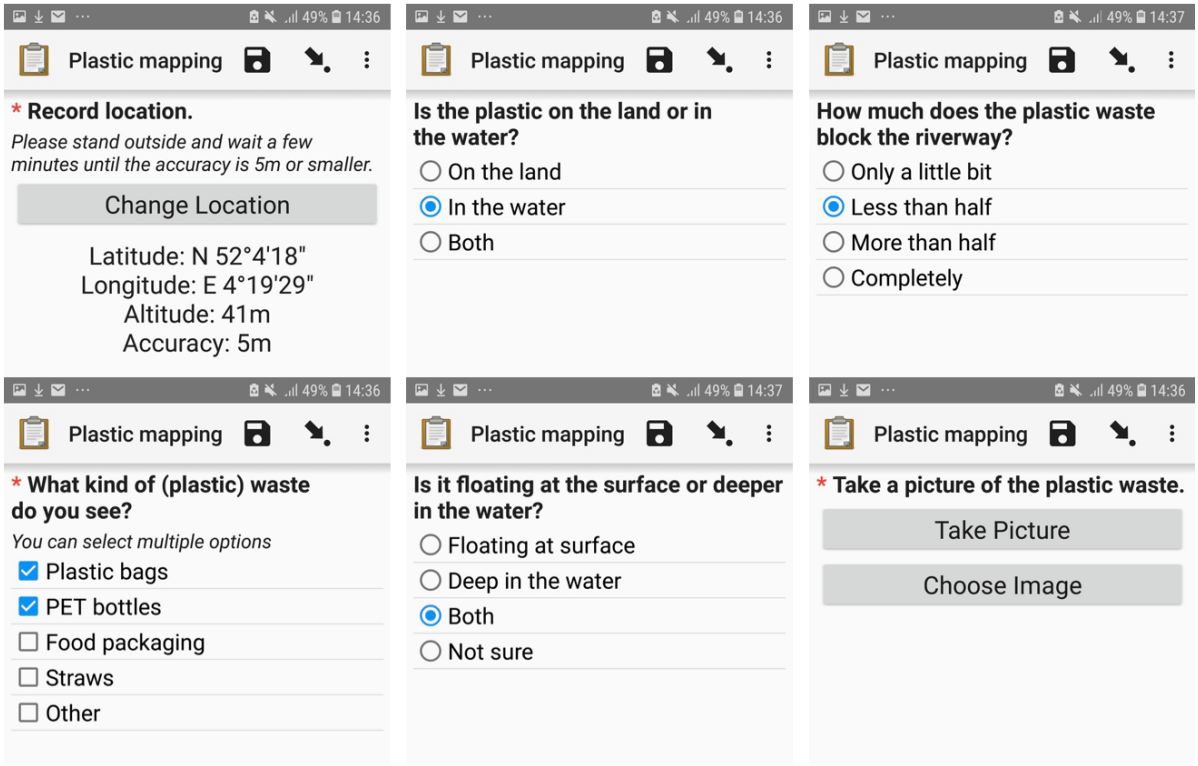

Figure 4.5: Examples of interface and questions plastic mapping application through ODK Collect

flood depths from the last flood event they could remember, thus a historical flood event. The indication of the flood depth was based on a person's body, a schematisation also setup in the Ramani Huria project presented in table 4.4. This reference system was developed, in order to visualise depths clearly during the questionnaire [36].

Table 4.4: Water depth reference system, developed by Ramani Huria and L. Pettersson [36]

Reported depth	Water depth [cm]
Only puddles	0
Finger depth	0-2
Ankle depth	2-10
Mid-shin depth	10-30
Knee depth	30-50
Waist depth	50-100
Chest depth	100-150
Person's height	150-200
Over person's height	> 200

4.5. Data processing

This section focusses on the processing of data in order to serve as input data in the flood model. The boundary condition required in HEC-RAS to model the flow is a discharge time series. As this is not gauged in the catchment, it should be estimated from precipitation data. Therefore, a method converting rainfall to runoff was used. The runoff of this system will be determined with use of an event-based rational method to estimate the runoff from an observed rainfall event. The discharge was also measured during fieldwork, thus the estimates in the model can be validated with in situ measurements for this observed rainfall event.

4.5.1. Discharge

In figure 4.6 a schematic is depicted with all steps to provide an estimation of discharge over time at the upstream boundary condition locations. As can be seen in the figure, the data needed for this estimation are topographic- and precipitation data (orange), which are both static (white) and dynamic (filled). The two main equations used to estimate discharge are: (1) the Kirpich equation, to calculate the time of concentration per grid cell in the upstream catchment and (2) the Rational method to provide the discharge over time. These steps will be elaborated further in the next paragraphs, in consecutive order following the flow-chart.

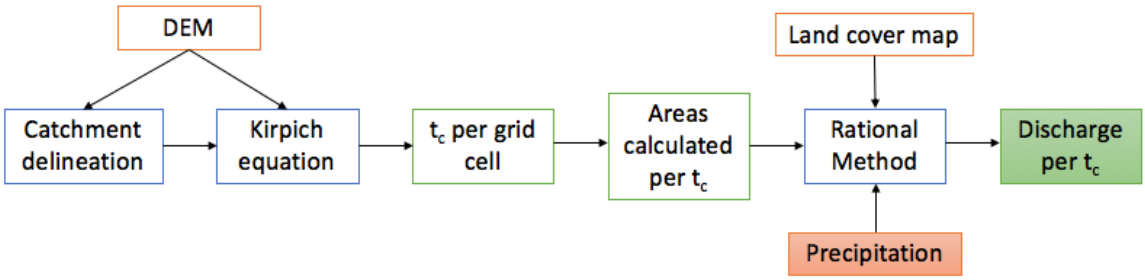

Figure 4.6: Flow-chart illustrating event-based rational method estimation

Catchment delineation

To determine how much runoff the catchment is contributing to the study area, the size of the total upstream catchment area needs to be known. This area was determined by performing a watershed delineation method in QGIS using the Alaska Facility DTM. First, the drainage direction of the DTM was determined. Next, the catchment is delineated to a certain 'pour point' for which the coordinates can be determined on the map. First, the total catchment area was determined by selecting the downstream boundary condition point as pour point. Subsequently, the two upstream boundary condition points were selected as pour points, to determine the individual sub-catchments contributing to the runoff of the two corresponding upstream boundary condition points. This is necessary for the flood model, as in HEC-RAS all upstream reaches need to be specified with a discharge boundary condition.

The area of the total catchment where the study area is part of is approximately 111 km^2. Following from the two upstream boundary condition points, the catchment can be divided into two sub-catchments. Furthermore, the study area itself also contributes to the total runoff. However, comparing this area to the upstream areas, this contribution is considered to be negligible. All areas delineated in this process and their corresponding size can be found in table 4.5 and in figure 4.7.

Table 4.5: Catchment areas

	Area [km^2]
Total catchment	111.4
Sub-catchment 1	64.7
Sub-catchment 2	44.9
Study area	1.8

Kirpich equation

The time of concentration of the upstream catchment areas is calculated with the Kirpich equation. The time of concentration is the time required for a parcel of runoff to travel from the most hydraulically distant part of a watershed to the outlet. It represents the time at which all areas of the watershed that will contribute runoff, are contributing runoff to the outlet. The time of concentration (t_c) is of interest for each point of the catchment. When the time of concentration is known for every point in the catchment, it can be estimated how much area will contribute to runoff in a certain amount of time. As the discharge has to be given over time,

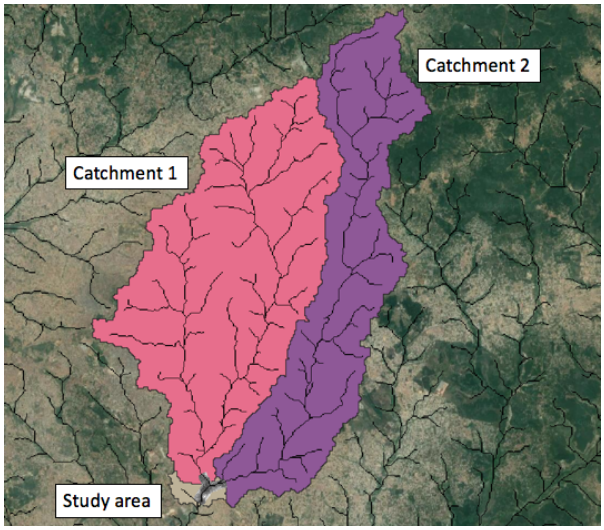

Figure 4.7: Sub-catchments delineated in QGIS

this has to be calculated for each point in the catchment. Therefore, the catchment is divided into grid cells of 100 x 100 m. In QGIS the time of concentration is calculated for each grid cell with the following equation:

$$t_c = \frac{0.21L^{0.77}}{S^{0.385}} \tag{4.1}$$

t_c = time of concentration [min], L = flow length [m], h = average slope of flow path [m/m] [35]

In figure 4.8 it can be seen at what time, which areas are contributing to runoff. These have been grouped per corresponding time of concentration, and it is chosen to do this per hour. Thus, all areas with t_c < 1, 2, 3, 4, 5, have been grouped together and their corresponding areas are calculated per group for each sub-catchment. These areas per t_c will serve as input data for the Rational method.

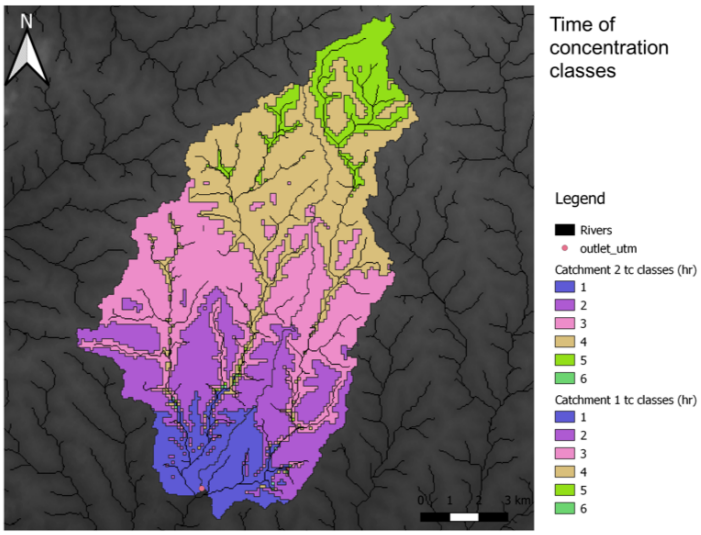

Figure 4.8: Time of concentration calculated per grid cell in QGIS

Runoff coefficient

Another parameter in the equation of the Rational method, is the runoff coefficient. The runoff coefficient

(c) is a dimensionless coefficient relating the amount of runoff to the amount of precipitation received. It is a larger value for areas with low infiltration and high runoff (pavement, steep gradient), and lower for permeable, well vegetated areas (forest, flat land). It is based on the soil type, gradient, permeability and land use. To determine the event runoff coefficient of the catchment, the MODIS land cover map is used. From this land cover map and the catchment shapefiles extracted in the catchment delineation process, the percentage of land use per sub-catchment can be calculated in QGIS. It can be calculated how large the area of a certain class covers the sub-catchment area, subsequently the percentage of this land class will follow. The land use per sub-catchment can be seen in table 4.6. It can be concluded that in both sub-catchments, the class 'Urban and Built-up Lands' is the most dominant class. However, to represent all areas in the sub-catchments, a weighted average is taken to determine the runoff coefficient. In table 4.6 it can be seen how this coefficient is built up. The runoff coefficient for sub-catchment 1 is 0.47, and 0.37 for sub-catchment 2.

Table 4.6: Land use per sub-catchment, runoff coefficient, area and percentage

Class	Coefficient	Catchment 1		Catchment 2	
		Area [km^2]	Percentage [%]	Area [km^2]	Percentage [%]
Savannas	0.2	0.2	0.3	1.63	3.6
Grasslands	0.15	0.83	1.3	6.52	14.5
Permanent Wetlands	0.05	3.51	5.4	4.44	9.9
Croplands	0.3	0.79	1.2	3.77	8.4
Urban and Built-up Lands	0.5	59.40	91.8	26.43	58.9
Cropland/Natural Vegetation Mosaics	0.3	-	-	2.08	4.6

Rational method

Finally the discharge can be estimated with the Rational method, a general method to calculate the discharge. With this method, discharge is determined by the land use and area of runoff, which have both been calculated in the previous paragraphs. Now, for each t_c class, the discharge is calculated. Thus, it will be known how much area is contributing discharge after 1 hour, 2 hours, etc. As this is a very general equation, it can be concluded that the discharge is the biggest uncertainty in the model. All calculated discharge time series can be found in appendix C for each selected rainfall event.

$$Q = C\,i\,A \tag{4.2}$$

A = drainage area [L^2], C = runoff coefficient [-], i = rainfall [L/T], Q = peak storm water runoff rate [L^3/T] [38]

5
Model development

The flood model developed in this chapter is built with software of the U.S. Army Corps of Engineers: Hydrologic Engineering Center's River Analysis System (HEC-RAS). The main reason this software was selected is because it is free. Moreover, coupled 1D-2D models can be developed and detailed structures can be implemented, which is necessary to investigate the impact of floods and plastic accumulation at bridges respectively. All calculations and settings will be done in SI units in HEC-RAS and the 'RAS Mapper' environment is used to setup the geometry.

This chapter will explain all important decisions made in the modelling process. As mentioned in section 2.3, the flood model will be constituted of a coupled 1D-2D model. This will result that all river streams will be modelled one dimensionally and the floodplains, the areas connected to these streams, will be modelled two dimensionally. First, the development in the one dimensional domain will be explained, followed by the development of the two dimensional domain. Subsequently, it is described how these two dimensions are connected to one another. Next, the boundary conditions, parameters and computational settings are elaborated on. Last, the model scenarios to support the research questions will be introduced.

5.1. 1D schematisation

The 1D unsteady computation engine solves the 1D continuity and momentum equations presented in section 2.3.2 using a semi-implicit finite difference scheme [13]. In this section it is presented what data is necessary for this computation and how it is set up to run an unsteady flow simulation. The 1D part of the HEC-RAS model consists of geometric data, describing the geometric properties of the study area. This includes the structures, the two bridges which can be obstructed, which are important to incorporate in order to determine their impact on flood severity.

5.1.1. Geometric data

The geometric data required to describe the system is the river reach connectivity, cross section geometry data and data describing the hydraulic structures in the system. The cross sections consist of station-elevation data describing the terrain profile along a transect perpendicular to the flow direction. These can be divided in the main channel and over-bank sections, which can be specified with different roughness properties. The hydraulic properties of the system are much dependent on the cross sections and these are key elements in the hydraulic simulations [12].

First, the 1D river profile was constructed. This exists of a river centreline, bank lines, junctions and cross sections. As there are two rivers coming together in the study area, a confluence or junction as referred to in HEC-RAS is created where the two rivers meet. As the DTM does not show where exactly the river is positioned, the orthomosaic of FutureWater is used to determine the position of the topographic characteristics. Both maps have been projected to the same coordinate reference system in QGIS, in order to make sure they are both positioned correctly relative to each other. This process is depicted in figure 5.1a where the setup of the geometry follows characteristics in the orthomosaic. In HEC-RAS, each river section is referred to as a 'reach', for which the references were already given in section 3.2, figure 3.4a. Cross sections will be placed with a maximum distance of 8m between each other. This spacing is needed to provide enough nodes to compute the computations and for the model to run stable. This was an iterative process, as cross sections placed to far apart can cause numerical damping of the flood wave and/or model instability. However if they are placed

to close together it can cause wave steepening and model instability on the rising side of the flood wave [16]. However, analysing the profile graphs a compromise between too far away and too close together had to be made, thus a spacing of maximum 8 metres was decided on. When entered cross sections were too far apart from each other, these were interpolated in HEC-RAS. The complete 1D geometry setup can be seen in figure 5.1b.

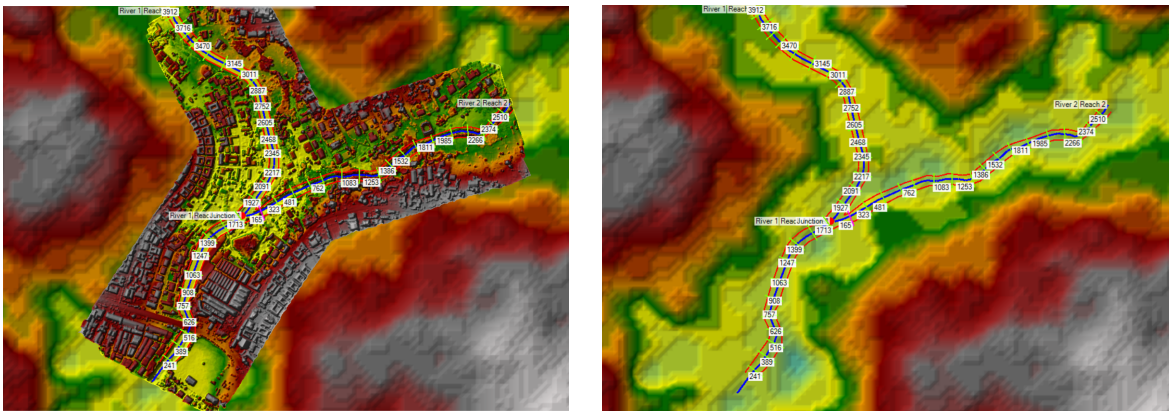

(a) 1D geometry setup following river topography

(b) 1D geometry setup in used terrain data

Figure 5.1: Geometry setup in RAS Mapper environment

5.1.2. Bathymetry

As the DTM only shows the terrain elevation as depicted in figure 5.2a, the bathymetry of the river must be incorporated in this DTM by modifying the terrain data. This was done in the geometry editor of HEC-RAS, by editing the cross sections. During fieldwork, the bathymetry of both the main channel and the stream were observed and measured where possible as described in section 4.3.1. For the main river, the channel is constructed of a rectangular concrete construction, which remains the same from reach 1 to reach 1-lower. However, the natural stream in reach 2, a cross section was only measured at one point. As the smaller river is a natural river without a constructed profile, the same natural measured shape is implemented along the rest of the reach. After all cross sections have been edited to include the bathymetry, these cross sections can be interpolated. HEC-RAS has a function for interpolation, and the new bathymetry terrain can be saved on top of the old terrain. Now, a new terrain is created including the bathymetry of the streams which is depicted in figure 5.2b. The resolution of the bathymetric profile is 1 x 1 m.

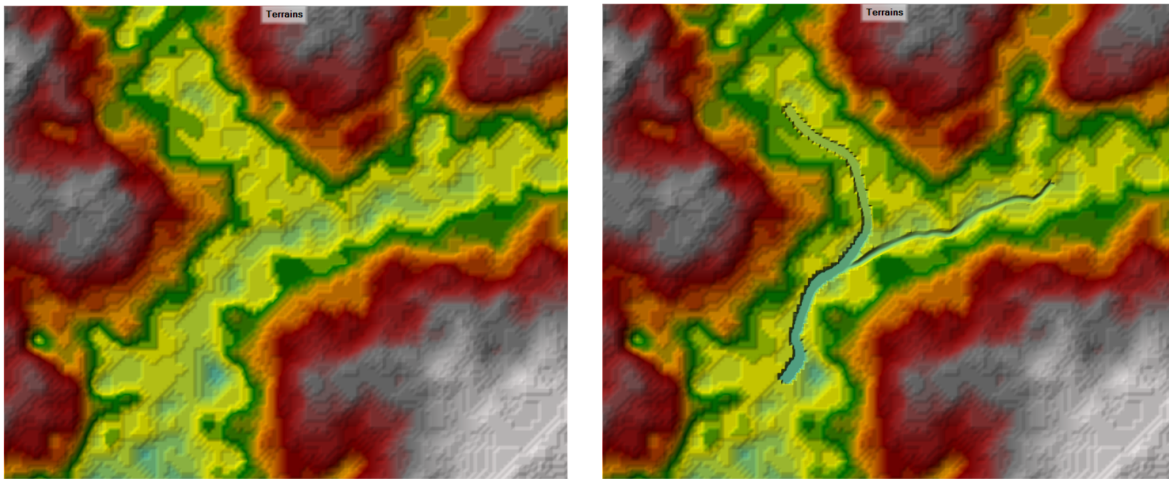

(a) Original terrain without bathymetry

(b) Modified terrain with bathymetry incorporated

Figure 5.2: Modification of terrain data

5.1.3. Modelling levees

The 1D computation engine computes a single water surface elevation for each cross section. For this, the entire cross section area is available for flow at all times and the water surface elevation changes homogeneously over the entire cross section. However, when floodplain flow is confined by a levee this may not be physically accurate [12]. Therefore, HEC-RAS has the option to specify levees for cross sections, to prevent water from getting to certain portions of the cross section, until the water level rises above the specified elevations. When levees are established, no water can go to the left of the left levee station or to the right of the right levee station until either of the levee elevations is exceeded [14]. This has to be defined explicitly, or the programme assumes that water can go anywhere within the cross section as in figure 5.3a. When this is defined for a cross section, which can be seen in figure 5.3b, the right levee is exceeded but the left levee is not exceeded. However, the program can only compute one water surface for the cross section, thus when the levee is exceeded the entire area behind the levee will be filled with water instantaneously [12].

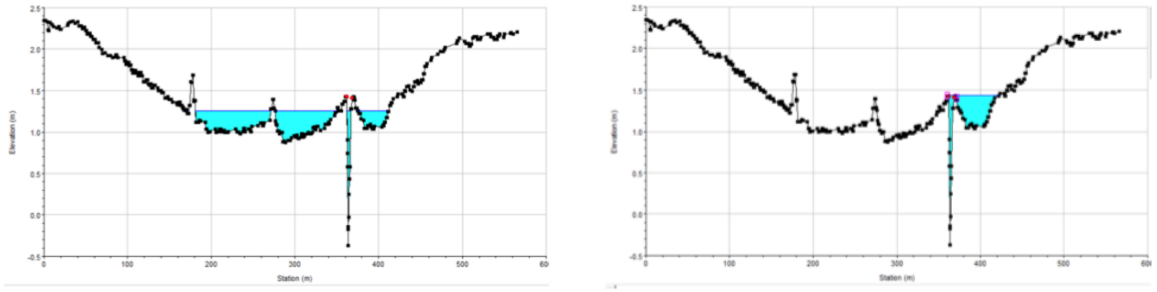

(a) Flow in cross section without levees [12]

(b) Flow in cross section with levees [12]

Figure 5.3: Impact of modelling levees

Furthermore, it is recommended in the HEC-RAS manual for constructed levees where the model would overtop, to end the cross section at the top of the levee. The actual levee should be modelled with a lateral structure, for which the area behind the levee should be modelled with a 2D flow area. This approach is much more accurate for modelling constructed levees, as it allows for different water surface elevations to be computed inside the leveed area, and a much more detailed analysis of levee overtopping and breaching [14].

5.1.4. Structures

HEC-RAS computes energy losses caused by structures such as bridges and culverts in three parts. One part consists of losses that occur in the reach immediately downstream from the structure where an expansion of flow takes place. The second part is the losses at the structure itself, which can be modelled with several different methods. The third part consists of losses that occur in the reach immediately upstream of the structure where the flow is contracting to get through the opening [14].

The method that is chosen to model the flow through a bridge with is the energy equation method. This is applied to high flows in the same manner as it is applied to low flows. Energy losses are based mainly on contraction and expansion losses. As this thesis will model the impact of plastic accumulation at bridges as an obstruction of flow area and not with friction losses, this method is decided on[25]. Structures can best be modelled in the one dimensional domain in HEC-RAS. In the study area, multiple bridges are present. Only two serve as a physical structure in the river stream, which can form blockages. There are two other bridges present in the area, however those bridge decks are quite high above the water surface, and do not have piers underneath. Thus, those bridges do not form an obstruction for the water flow. A total of two bridges are therefore added in the model. Both bridges have piers underneath, which can be specified with detail in the geometric editor. The dimensions of the piers are visually estimated from photographs, as they could not be measured during the fieldwork. However, all other dimensions are measured such as the width and length of the bridge.

Contraction and expansion losses

Losses due to the contraction and expansion of flow between cross sections are determined during the standard step profile calculations. These losses are described in terms of coefficient times the absolute value of the change in velocity head between adjacent cross sections. When the velocity head increases in the downstream

direction, a contraction coefficient is used; and when the velocity head decreases in the downstream direction, an expansion coefficient is used. When specifying these contraction and expansion losses at cross sections, the distance upstream and downstream of the bridge should be accounted for. For this, a general rule is applied, which is depicted in figure 5.4. The contraction loss is set to 0.5 and the expansion loss is set to 0.3.

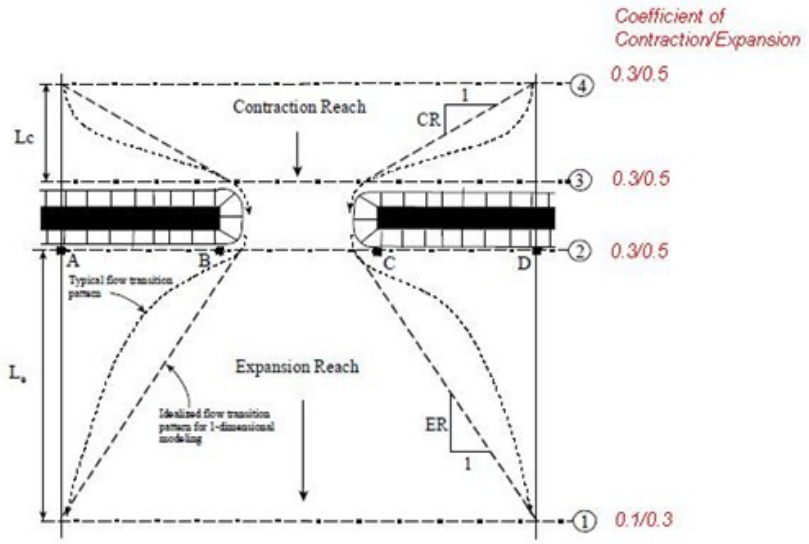

Figure 5.4: Schematisation of contraction and expansion losses an spacing of cross sections

Plastic blockages
The plastic blockages are accumulating at the bottom of the piers under the bridges. This accumulation will therefore be implemented in the model as wider piers, obstructing the flow path. During fieldwork, it was not observed that plastic on land contributes to the plastic accumulation at the bottleneck locations. Furthermore, during the six consecutive weeks, it was visually observed that the accumulation at the piers did not change significantly. However, as it is interesting to what degree a certain accumulation has impact, two discrete values are decided on. These discrete values are 33% and 67%, in order to provide a substantial difference in obstruction of the flow area. These blockages will be implemented individually per bridge, so that their individual impact in the study area can be analysed. In table 5.1 the used dimension of the piers can be seen per bridge and per degree of blockage.

Table 5.1: Bridge pier specifications per bridge and blockage

Scenario	Number of piers	Pier width [m]	Effective width flow [m]	Volume needed for blockage [m^3]
Bridge 1 0%	5	0.35	24.25	0
Bridge 1 33%	5	1.97	16.17	30
Bridge 1 67%	5	3.58	8.08	50
Bridge 2 0%	5	0.5	28.5	0
Bridge 2 33%	5	3.67	19.00	30
Bridge 2 67%	5	6.83	9.50	5s

5.2. 2D schematisation

After the one dimensional schematisation is completely set up, the 2D areas can be added to the geometry. This can be done by connecting the two dimensional area to the one dimensional riverbank with use of a lateral structure. As the study area exists with different streams in it, a schematisation is made on which areas need to be created in order to connect the streams as sufficient as possible. The study area consists of a Y-shaped water body, which can be connected to three different 2D flow areas. The area adjacent to a riverbank is connected to

this particular riverbank. After the areas are setup, the grid cells can be specified, for which a spatial resolution of 10 m is decided on.

5.2.1. Mesh construction

The 2D geometry is built up by a computational grid. Each mesh is built up by interconnected cells that may vary in size and shape, although the maximum cell sides can not be more than 8. Cell faces are similar to 1D cross sections and are used to compute flow between cells, except at the outer boundaries of the mesh. Cell points, located at the connection between cell faces, are used used to connect the mesh to 1D structures and 2D boundary conditions. The cell centre is where the water surface elevation is computed for each cell, but does not necessarily correspond to the cell centroid [15].

Sub-grid terrain representation

Compared to other 2D modelling softwares, HEC-RAS cells and cell faces are not restricted to contain only one elevation value. Instead, detailed geometric and hydraulic property tables, based on the resolution of the underlying terrain, are created during pre-processing of the computational mesh. For each cell face, relationships between elevation and profile, area, wetted perimeter and Manning's n are computed in the hydraulic tables. For each computational cell, a relationship between elevation and volume is computed [15].

5.3. Coupling 1D-2D

Now that the 1D and 2D part of the model are set up, they still need to be connected to one another. As flow moves longitudinal in the flow direction and can flood the floodplains laterally, thus a connection between the two components is needed. The connection between 1D and 2D component consists of a lateral structure, a feature in HEC-RAS that is best used to connect these two [14].

5.3.1. Lateral structures

To setup the lateral structures, the lines they should follow can be drawn and exported as a shapefile using 'profile lines' in RAS mapper. Furthermore, these lines can not extend further than the last cross section of a reach in the study area [15]. Therefore a total of six lateral structures need to be implemented. After all profile lines are exported, they can be imported again in the geometric editor where all 2D geometric processes are handled. Furthermore, the weir width and shape must also be specified, and is chosen to be broad crested and 1 m wide. However, the width does not effect the lateral flow and is just for visual purposes. The lateral structure connecting the two models contains elevation data which can be extracted from the underlying terrain model. When the water level in the 1D cross section or 2D cell exceeds the elevation of the lateral structure, water flows over the structure. Thus, all points must be lower than the weir profile, otherwise it cannot compute the calculations [15]. Points that are higher, need to be manually adjusted, which was a very time consuming process. When all lateral structures are correctly specified, they can be connected to the adjacent 2D flow area. Flow over the structure can be calculated either using a weir equation or using the 2D flow equations. When the 2D equations are used, the 1D water surface profile is added as a stage boundary condition to the 2D cells [15]. Therefore, the condition flow to 2D area is selected using the 2D equations. An overview of the complete geometry data can be seen in figure 5.5.

5.4. Manning's values

The Manning's n values need to be specified in HEC-RAS and represent the roughness or friction applied to the flow. Determining accurate n-values, especially for overland flow, include large uncertainties and often make little sense for modelling purposes as the friction parameter often is the main calibration parameter [12]. Still, for the reliability of the model it is useful to know that the used n-values are within reasonable intervals. For the river stream and banks in the 1D part, this can be specified for the channel and banks. For the 2D part, this can be specified for the entire area or from a spatially varying land cover map. From section it was concluded that the whole study area classified as the same class 'Urban and Built-up Lands', due to the coarse resolution of this map. The Manning's values are selected from literature tables, and can be seen in table 5.2. The hydraulic tables of all points in the geometry can now be computed. However, instabilities arise immediately when entering the manning's values corresponding to their type. Values that are too low can cause model instability, and too high values will increase stage and attenuate the hydrograph more as it

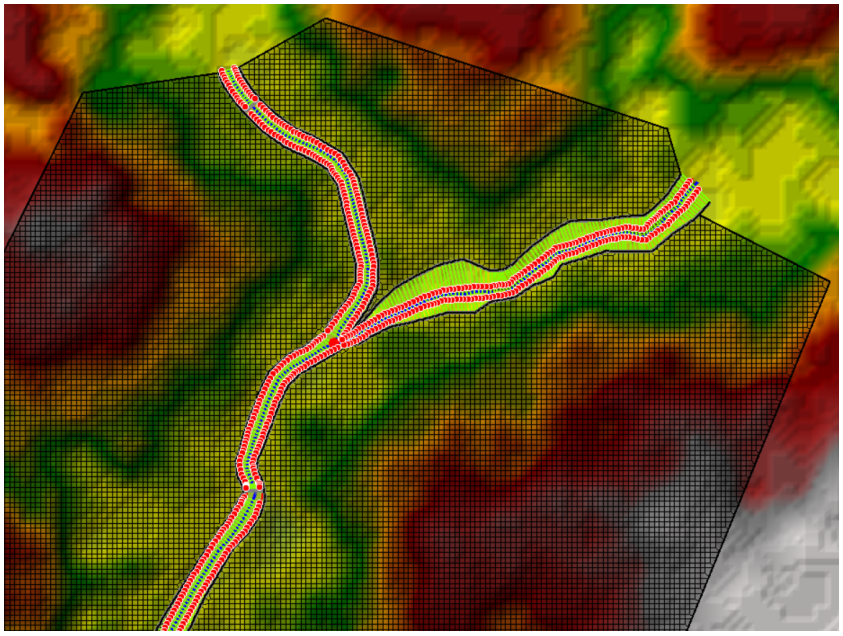

Figure 5.5: Complete 1D-2D geometry setup

moves downstream [16]. Furthermore, HEC-RAS likes changes to occur gradually. As two reaches with quite different manning's values come together in a junction, this can cause for model instabilities. This holds also for the floodbanks which are connected to the 2D areas. As the model will not run stable with the values from literature, it is decided to lower of higher the values of the streams slightly, in order for changes to occur more gradually. Furthermore a limitation is also that the connected areas should have the same manning's n value as their neighbouring floodbanks. Thus, the value of the floodbanks is chosen for the 2D areas.

Table 5.2: Manning's n values [31] [49]

Type	Literature Manning's n value	Modelled Manning's n value
Main constructed channel: concrete	0.02	0.03
Main natural channel: clean, winding, some pools and shoals, some weeds and stones	0.045	0.04
Floodbanks: light brush and trees	0.06	0.06
2D area's: urban land	0.016	0.06

5.5. Boundary Conditions

5.5.1. Upstream

The upstream boundary condition needs to be specified for each reach in the system. This concerns the two reaches that are set up in the model. The boundary condition is given with a flow hydrograph, which specifies the discharge for a given time-step. This is produced from the chosen precipitation events, from which the estimated discharge was calculated per hour. The calculated discharges can be found in appendix C per event.

5.5.2. Downstream

The downstream boundary condition needs to be given for the downstream end of the single reach. Use of Manning's equation with user entered friction slope produces a stage considered to be normal depth if uniform flow conditions existed. This slope is determined from the topography and is set to 0.01. Because uniform flow conditions do not normally exist in natural streams, this boundary condition should be used far enough downstream from your study area that it does not affect the results in the study area [14]. A basic rule in

HEC-RAS is to place this boundary condition downstream at least 5 times the cross section width. In the model it is placed approximately 700 metres downstream, just to be sure. Both upstream and downstream boundary locations are indicated in figure .

5.6. Computation settings

Computation interval

The time step for the model simulations is adjusted based on the Courant number. This method is chosen to overcome stability issues arising form an inappropriate time step. With this method, the time steps are more flexible and adjusted when flow is varying. The methodology it follows Courant = (Velocity*dt/Length) [14]. The settings can be seen in figure 5.6a and b where the maximum Courant number allowed at any 2D cell or 1D cross section is specified. If the maximum number is exceeded, the time step is cut in half for the very next time interval. Because HEC-RAS uses an implicit solution scheme, Courant numbers can be greater than one and still maintain a stable and accurate solution. In general, if the flood wave is rising and falling slowly, thus depth and velocity are changing slowly, the model can handle extremely high Courant numbers, of 5 or even more. However, if the flood wave is changing rapidly, such as in a dam break, the number should be close to one. Therefore it was decided to set the maximum courant number to 3. The minimum Courant number is the threshold for which the the time step will be doubled at all locations if this threshold is exceeded. The time step will only be doubled if the current time step has been used for enough time steps in a row to satisfy the entered criteria of 'Number of steps below minimum before doubling'. The minimum Courant number should be less than half of the maximum Courant number and is decided to be 0.5. The minimum and maximum before doubling were both set to 4. These setting allow the model to run stable, but also run faster [14]. In figure 5.6b and 5.6b the specifications can be seen, for which the 5 second time step is used for most scenarios. For some scenarios, the model was unable to run stable thus the time step was set to 1.

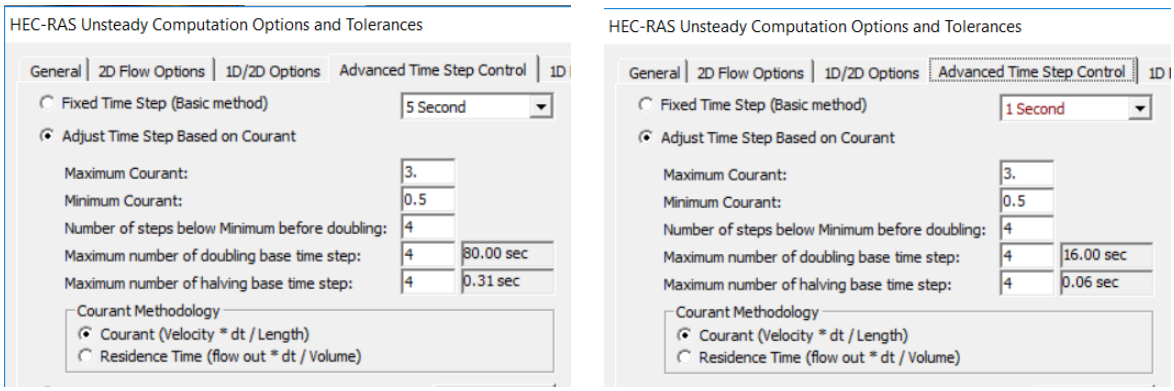

(a) 5 Seconds

(b) 1 Second

Figure 5.6: Courant number settings

Output interval

The interval of mapping-, hydrograpgh- and detailed output is set to 10 minutes. This means that the results are stored every 10 minutes, thus all the output can be analysed with a time step of 10 minutes.

5.7. Model scenarios

To validate the model, an observed rainfall event is chosen to serve as validation run in the model. This rainfall event is a moderate rainfall event, comparing it to other rainfall events throughout the year and is therefore chosen as the first event. In section 4.2.2 yearly maximum peak intensities were determined, which will also serve as scenarios. As described in section 4.2.2 comparing the three rainfall events from which these maxima are part of, it can be seen that the total precipitation and duration of these events vary significantly from each other making it is interesting to determine their impact on the study area. With varying magnitude and duration of these rainfall events, the simulations can serve as a sensitivity analysis and it can be analysed how the modelled system responds to the variety of events. Furthermore, in each event a different bridge will be obstructed with plastic accumulation, in two discrete levels of 33% and 67%. These values are chosen in order

to provide a substantial difference in obstruction of the flow area as described in 6.3.3. These blockages will be implemented individually per bridge, so their individual impact on the environment can be analysed. In table 5.1 the used dimension of the piers can be seen per bridge and per degree of blockage. An overview of the proposed scenarios can be found in table 5.3. Eventually, the model will simulate a total of 20 different scenarios.

Table 5.3: Model scenarios

Rainfall event	No blockage	Bridge 1 blocked 33%	Bridge 1 blocked 67%	Bridge 2 blocked 33%	Bridge 2 blocked 67%
23/05/2019 (peak 22 mm/h, total 27 mm/4h precipitation)	Event 1-0	$Event1-B1\_33$	$Event1-B1\_67$	$Event1-B2\_33$	$Event1-B2\_67$
19/09/2017 (peak 56 mm/h, total 57 mm/3h precipitation)	Event 2-0	$Event2-B1\_33$	$Event2-B1\_67$	$Event2-B2\_33$	$Event2-B2\_67$
22/06/2019 (peak 60 mm/h, total 83 mm/6h precipitation)	Event 3-0	$Event3-B1\_33$	$Event3-B1\_67$	$Event3-B2\_33$	$Event3-B2\_67$
28/06/2018 (peak 78 mm/h, total 103 mm/9h precipitation)	Event 4-0	$Event4-B1\_33$	$Event4-B1\_67$	$Event4-B2\_33$	$Event4-B2\_67$

6

Results and discussion

This chapter presents the results of the surveys, citizen observations and most importantly the results of the modelled scenarios presented in section 5.7. First, the outcome of the flood- and plastic waste survey is presented. Next, the main results of the flood model will be presented with additional analyses that are needed to support the research questions. Subsequently, the discussion of the results is elaborated on at the corresponding sections.

6.1. Citizen observations

This section presents the results of the flood- and plastic waste surveys. These were carried out in the study area as described in section 4.3.3 and 4.4. The questionnaires used in these surveys can be found in appendix E and F respectively. First, the most important findings from the flood survey will be presented. Furthermore, the results from the plastic mapping survey is presented, followed with results of plastic waste composition in the study area.

6.1.1. Flood survey

Figure 6.1 depicts the flood depth as reported by citizens at 41 different locations throughout the study area during the flood extent survey. As there was no flooding event experienced in the time span fieldwork took place, information was gathered referring to the last main flood event people could remember. More than half of the respondents (23 out of 41) specifically mentioned a severe flooding event that took place in June or July 2018, which was the last severe flooding event they could remember. Relating these responses to newspaper articles and rain gauge data, it was concluded the last main flood event took place on June 28th, 2018. This coincides with the maximum peak intensity found in 2018, which is part of rainfall Event 4 in section 4.2.2. Because the flood event is more than one year ago, a lot of information was gathered from flood marks on buildings which can be seen in figures 6.2a, 6.2b and 6.2c. In general, the water is reported as deeper along almost all river- and stream sides. Along reach 2 less respondents were questioned, as the area consists of a large open workplace and a small agriculture field. It can also be seen that respondents with a distance of approximately 200 meters from a river or stream do not observe any floods. However, around bridge two mixed responses can be seen, where at both sides of the river both high and low flood depths are responded. This can be due to the local elevation differences in topography, which occur a lot in the study area.

During the survey, questions related to the perception and understanding of the floods were asked. Analysing the responses per question, some general remarks can be made about the flood events. The most important results from the questions to understand the flood events are about:

Flood perception: Most respondents have been living in the area for already a few decades. Almost all respondents have experienced floods and mentioned that the floods are occurring more regularly and with a greater impact than decades ago. Furthermore, the main river seems to have expanded and several years ago, around 2015, the government has constructed a channel of the main river and made it wider. This has helped to reduce the severity of the floods, but at the same time making the channel closer to existing buildings and houses. Furthermore, there are two bridges in the area which serve as bottleneck locations as they have pillars underneath that accumulate a lot of solid (plastic) waste. It is mentioned that a lot of people dump their trash in the river, however none of the respondents claim to do so. A lot of respondents link the waste accumulation to the flood events and furthermore that the river's capacity is not sufficient to runoff water.

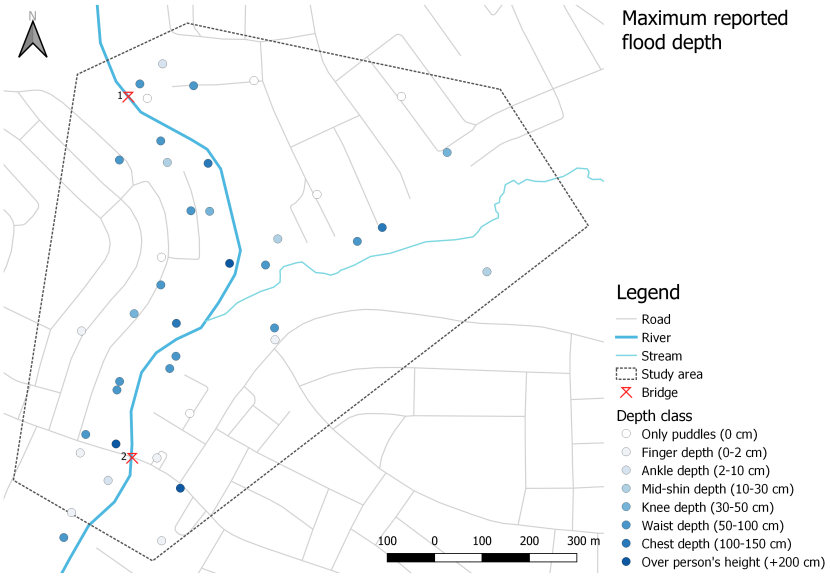

Figure 6.1: Reported maximum flood depth of historic flood event on June 28 2018

When it is raining heavily, water from overland flow cannot join the river because it is already full. It can be observed the water level rises in the river, when this happens people around it know it is about to flood. When the water is inundating the area, respondents mention it is sometimes flowing or standing still. Once it was mentioned the water was streaming heavily, close to the main river. Furthermore, it was mentioned that after the inundation, water flows back to the river to runoff to downstream areas.

Response time: When the water level rises in the river, the people near and around it know it is about to flood. Most respondents mention they only have a few hours to pack their most valuable things and flee to higher ground. They receive no warning about when it will rain heavily or for example when it is raining heavily in upstream areas. Currently, there is no warning system whatsoever in place. Sometimes, the rain unpleasantly surprises residents in the middle of the night, when their homes are already flooding as they are still sleeping. As people do not have any reference about when heavy rainfall events are expected and only see the water coming when the rivers are already almost overflowing their banks, they are often caught off guard and have no time to prepare or flee. When it was asked if people thought it would help if perhaps a service would notify them when heavy rainfall is expected or happening upstream, it would already give them more time for preparations. Perhaps a sms-service could warn a community member, which will further spread the news.

Damage: As it was mentioned by respondents that there are only a few hours to react when they know it is about to flood, people do not have a lot of time to prepare. Most houses only have a ground floor, thus items in the household can not be secured to a higher place. Furthermore, people can only carry their most valuable items with them and all other things are left behind. However, if people are surprised with rains, they have no time to pack anything at all. This means a lot of valuable items, household materials and houses are left with a lot of damage after a flood event. Houses, furniture and personal belongings are unfortunately often left to flood.

6.1.2. Plastic mapping

A total of 70 responses were collected between a two week time period of May 15th until May 30th, 2019. From all responses, only responses with a geolocation accuracy of 5 meters were taken into account. This was done to compare the same waste piles with each other, to determine their development over time. Some responses had a accuracy of a few hundred meters, thus their approximate location could not be determined. Hence, only 40 responses were left to analyse. From these responses it was analysed which referred to the same waste pile, in order to analyse the development of that waste pile in the time range of the responses. In the time span of two weeks, it could be concluded there are locations in the study area that serve as main waste piles. Figure

(a) Chest depth (b) Person's height (c) Chest depth

Figure 6.2: Floodmarks throughout the study area indicating flood depths

6.3 shows the locations of the main mapped plastic waste piles. Their location did not change at all and their size stayed more or less the same, concluding from attached pictures. Thus, all duplicate points were removed in order to quantify the volume of waste present in the study area. In figures 6.4a, 6.4b and 6.4c it can be seen what kind of pictures classify to the relevant waste categories. From the responses, it can be seen that bags are the most common plastic item in the study area, followed by bottles and packaging.

This thesis only takes into account how much a bridge is blocked with plastic waste. However it is interesting to know how much plastic waste is present in the study area, to determine how much can eventually accumulate at these bridges. From the mapped waste piles, it can be concluded there are 8 small piles, 8 medium piles and 2 large piles. Furthermore, there is a large dump site placed close to the junction of the two rivers, which has an area of about 20 x 20 m. However, this dump site is located at higher elevation, thus the waste will not go easily into the water. Additionally, it was observed that a lot of plastic waste is also coming from upstream areas, flowing through the system. This flux was not determined precisely, and would be interesting to know how much goes through and how much exactly accumulates in a certain time span.

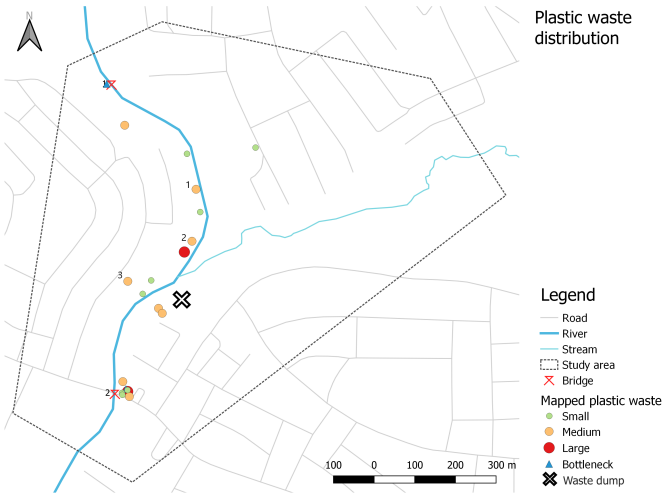

Figure 6.3: Mapped plastic waste points after duplicate removal

(a) Small waste pile (b) Medium waste pile (c) Large waste pile

Figure 6.4: Example response of waste pile sizes

6.2. Plastic sorting

From sorting three randomly selected waste piles in the study area as described in section 4.3.3, an indication can be given about the plastic waste composition. The selected piles depicted and numbered in figure 6.3. In figures 6.5a, 6.5b and 6.5c the composition is depicted in a pie chart per sampling location. It can be concluded that the largest portion of plastic waste consists of plastic bags. It should be noted that this category consists of mainly single use plastic bags, but the drink sachets which are widely used for drinking water also fall in this category. From all three piles, it composes more than half of the total plastic weight sorted from the piles. This gives a rough estimation about the composition of plastic items in the area.

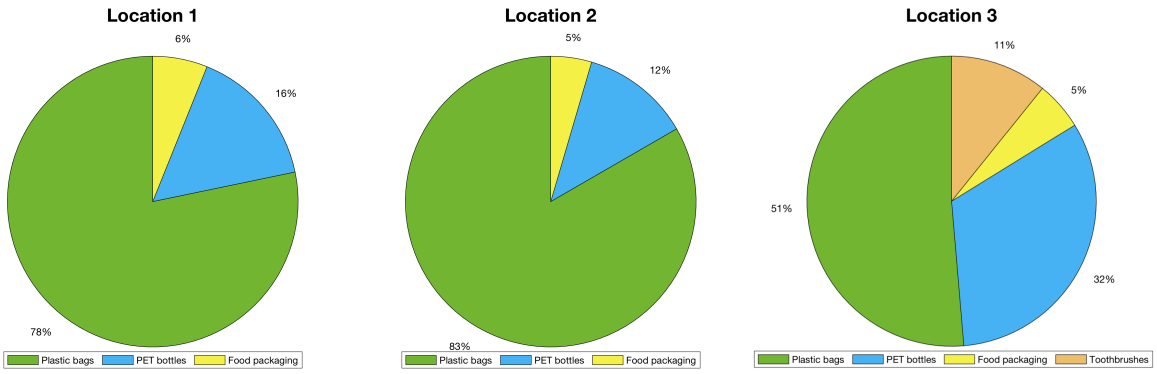

(a) Pile 1 (b) Pile 2 (c) Pile 3

Figure 6.5: Plastic composition of three waste piles

Representation As mentioned in section 2.2.1 products that are packaged in polyethylene, forms about 70% of the plastic waste in the municipal waste stream. It is not further specified if this is Low Density or High Density Polyethylene, however polyethylene is the most common plastic. Its primary use is in packaging such as plastic bags, containers, bottles etc. Probably all items that were found are made of this type of plastic, but this was not further researched. However, it gives a good indication that this is indeed the most common plastic in the waste stream which is not properly disposed of.

6.3. Flood model results

In this section the model results of the different scenarios are presented and analysed. The impact of the rainfall events and introduced blockages will be compared with each other by analysing the flood extent, depth, velocity, distribution and local hydraulic impact. For these analysis only flood depths with a minimum of 10 cm are taken into account, as lower depths of standing water are not considered as problematic inundation. Thus, all flood maps and plots visualised in this section and in appendix H only show the extent of flooding with depths of minimal 10 cm. Main findings of the scenarios are covered, which are supported with relevant maps, plots and graphs. The complete results per scenario can be found in appendix H. Furthermore, for a short recap, the abbreviations referenced to the scenarios are depicted in table 6.1. Firstly, the flood model will be validated with in situ measurements and reported flood depths of a historic flood event. Following, the impact of heavy and moderate rainfall events will be analysed. Last, the impact of the introduced blockages will be analysed per rainfall event. Furthermore, the discussion of relevant results are included in their corresponding section.

Table 6.1: Scenarios and abbreviations

Rainfall event	No blockage	Bridge 1: 33% blocked	Bridge 1: 67% blocked	Bridge 2: 33% blocked	Bridge 2: 67% blocked
Event 1	$Event1-0$	$Event1-B1\_33$	$Event1-B1\_67$	$Event1-B2\_33$	$Event1-B2\_67$
Event 2	$Event2-0$	$Event2-B1\_33$	$Event2-B1\_67$	$Event2-B2\_33$	$Event2-B2\_67$
Event 3	$Event3-0$	$Event3-B1\_33$	$Event3-B1\_67$	$Event3-B2\_33$	$Event3-B2\_67$
Event 4	$Event4-0$	$Event4-B1\_33$	$Event4-B1\_67$	$Event4-B2\_33$	$Event4-B2\_67$

6.3.1. Model validation

Validating the model is important in order to determine if the results of the model are trustworthy. Therefore, the model is validated by a scenario of an observed rainfall event during which measurements were taken in the field. Secondly, the model is also validated by a scenario of a historic rainfall events, from which community reported flood depths were collected through a flood survey.

Observed rainfall event

The rainfall event on May 23rd, 2019 was observed during fieldwork and therefore selected as the first model scenario *Event 1-0*. In order to validate the model, the results of this model scenario are compared to measurements of velocity and stage as described in section 4.5.1. During the peak of the event, around 16:00 PM local time, velocity measurements and stage observations were carried out. After the rainfall event, civilians throughout the study area were asked if flooding was experienced due to this specific event. This clarified that no flooding was experienced throughout the entire area due to the particular rainfall event that day.

Analysing figure 6.8a, it can be interpreted that the modelled result of this particular event produced floods along reach 2, reach 1-lower and at the upper part of reach 1. Thus, it follows that the model underestimates the capacity of the river, or the estimated discharge is too large, especially for the side river at reach 2. However, in the upper reach of the constructed river as indicated in 6.6a, the water level is approximately the same as measured during the rainfall event. With modelled water depths around 2 m at this stretch of the river, which concurs with measurements performed in this study of 2-2.5 m depth. Furthermore, the velocity is in the same order of magnitude as measured during the rainfall event as indicated in 6.6b. In this part of the reach water flows are modelled with a velocity of 1.66 m/s compared to measured surface velocity of 2.4 m/s, which after correction described in section 4.5.1 becomes 2.04 m/s in the same stretch of the river. Interpreting this validation from comparing the model scenario to the observed event, it should be kept in mind that the result of the main constructed upper stretch of the river corresponds to the observed event, but the side stretch of the natural stream overestimates the flood event as there was none experienced. Hence, the modelled capacity of reach 2 is underestimated and the estimated discharge for this boundary condition is estimated too large, reach 1 is greatly modelled according to observations except for the most upper part and the capacity of reach 1-lower is also underestimated.

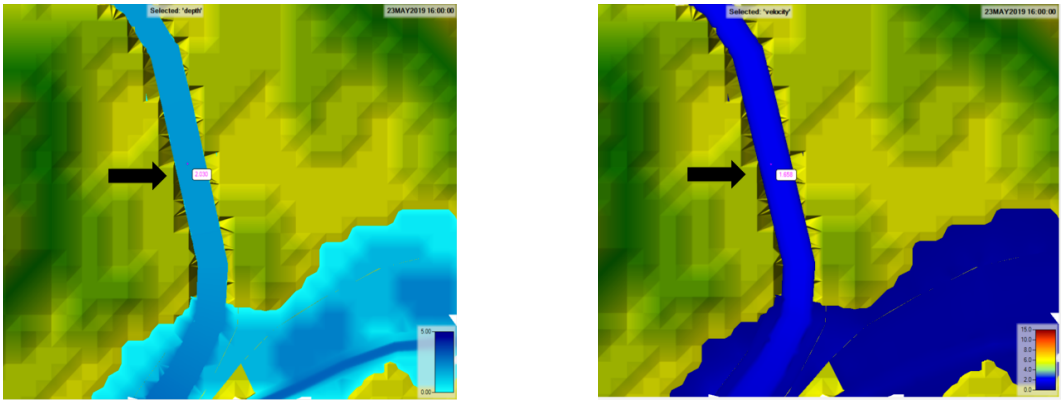

(a) Modelled depth

(b) Modelled velocity

Figure 6.6: River reach where stage and velocity measurements were conducted on 23 May 16:00 PM

Reported flood depth historic rainfall event

During the surveys, the maximum flood depth was reported by the community at 41 different locations. However, some respondents did not remember the exact date of the flood, but from analysing newspapers and rainfall data, it was determined it was most likely the event on June 28th, 2018 *Event4-0* as described in section 6.1.1. Comparing the reported flood depths from the surveys with the maximum simulated depth of the rainfall event, it can be determined how many of the point measurements correspond to the same simulated depth class as depicted in 6.7.

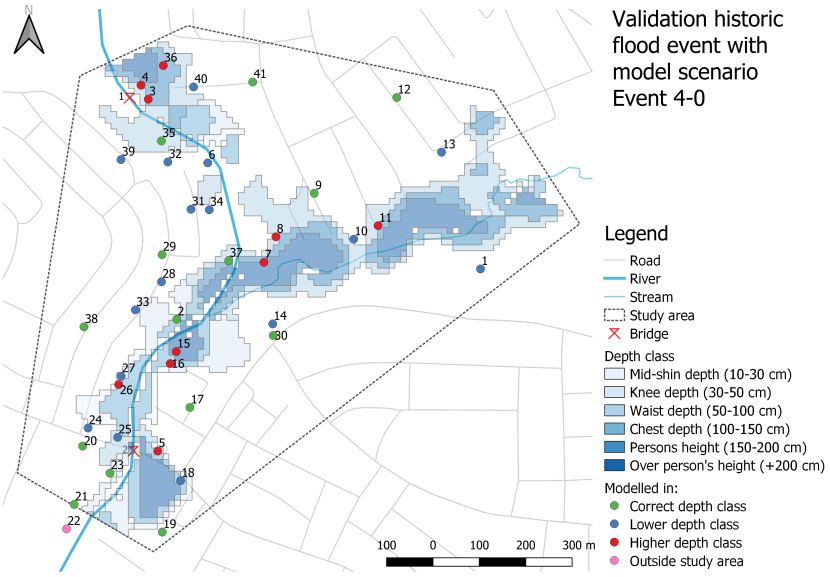

Figure 6.7: Reported maximum flood depth of historic flood event on June 28 2018 compared to simulation

Comparing the reported flood depths to scenario *Event4-0*, it was determined that 35% of the points correspond to the correct depth class, indicated in green. However, 40% of the points are simulated with a lower depth class in blue and 25% simulated with a higher depth class in red. In appendix G all points' reported and simulated depth class can be found. Comparing these points together with the flood extent and -depth of *Event4-0*, it can be interpreted that most points modelled in the correct depth class are not inundated during the event and simulation and are mostly at locations further away from the streams. However, some points are closer to the streams such as 21 and 23 which show the inundated area downstream at reach 1-lower is modelled correctly and the inundation does not extend far from the channel. Furthermore, points 35, 37 and 2 at the left side of reach 1 are modelled in their correct depth classes close to the stream. Looking at the points modelled in a lower depth class it can be seen that most points lie outside the simulated inundated area

with a maximum distance of 150 m from the streams at point 13. This implies that the modelled flood extent does not cover enough area, compared to reported in the flood survey. However, some points are also located in inundated areas closer to the streams (points 18, 25 and 27) and are modelled 2 or 3 depth classes lower. Looking at the points that were modelled with a higher depth class, it can be seen that these are all relatively close to the streams and are all placed in inundated areas. Points 3,4 and 36 are in upper reach 1 for which point 3 and 36 it was reported there are no floods at all or below 10 cm. Points 7,8 and 11 in reach 2, differ 2 to 5 depth classes. Along reach 1-lower, points 16 and 26 differ one depth class, point 15 3 depth classes and point 5 differs 4 depth classes.

For this scenario, it can be concluded that the flood extent of reach 1-lower is modelled most accordingly to the responses, however at the upper part of the stream depths close to the stream are overestimated. Furthermore, at upper reach 1 the depths are overestimated and further down the same reach the extent is underestimated. At reach 2 the flood extent is also underestimated and flood depths closer to the streams are overestimated.

However, it should be considered the flood event was more than a year ago, thus some answers might not be remembered correctly. Even more, the estimated discharge of this event is the highest uncertainty since this was estimated roughly with a rational method. However, as 40% of the response points are estimated too low, it can be concluded that the floods occurring in the area have an even bigger impact, than the simulated maximum flood event of *Event4-0*. This is quite striking, since this event already covers the area with 25%, from which 20% have depths higher than 'knee depth', thus higher than 50 cm.

6.3.2. Impact of heavy and moderate rain events

To determine the impact of the individual rainfall events in the study area, the four different rainfall events which vary from moderate (event 1) to heavy (event 2, 3 and 4) have each been simulated without blockages, which can be seen as a null scenario for the selected rainfall events. The maximum flood extent of the four scenarios with their corresponding maximum depth classes can be seen in figures 6.8a, b, c and d. All simulated events show flood occurrence adjacent to the streams. Reach 2 is affected the most, where the stream overflows its banks in every simulated rainfall event. As mentioned before, this can be due to the estimated capacity of the stream or the estimated discharge from the upstream catchment, which has the largest uncertainty. The simulated maximum depth of *Event1-0* has the least impact in the area, producing mostly floods along reach 2 and reach1-lower as depicted in figure 6.8a. Furthermore, the heavy rainfall events 2, 3 and 4 as depicted in figures 6.8b, 6.8c and 6.8d respectively more or less show the same flood extent, especially around reach 2 and downstream of the junction in reach 1-lower. The main differences can be found at the upper part of reach 1, where *Event3-0* and *Event4-0* have a larger flood extent than *Event2-0*. Furthermore, it can be seen that *Event4-0* has more areas in higher depth classes than the rest of the events. For these rainfall events, it becomes clear the entire river is not capable of conveying the estimated runoff, as almost all banks overflow and produce inundated areas along the river. These results show that the areas directly adjacent to the channel and stream are experiencing the most impact due to flooding.

The flood extent of the four individual events can be compared with each other when visualising them in the same figure, as depicted in figure 6.9. In this figure it can clearly be seen that event 2, 3 and 4 have the same flood extent along reach 2 and a the upper part of reach 1-lower. Furthermore, analysing the ground elevation from the ASF DEM it shows that the areas with higher elevations are not impacted by the floods. For event 2, 3 and 4 it seems that all low laying areas are saturated and do not extent further than the covered area. This means that topography is an important factor influencing the flood extent.

For each simulated event it was calculated how much of the maximum flood extent in the study area belongs to a certain depth- and velocity class in QGIS. This is calculated relative to the extent of the study area, which is indicated in the flood maps as a dotted line. The analysed study area is $918850 m^2$, thus for each class it can be calculated how much area it covers, followed by the percentage of each depth- and velocity class. From this, the total inundated area can be expressed as percentage of the study area per scenario. These results are depicted in bar graphs in figure 6.10. In the bar graph of figure 6.10a, it can be seen that event 4 has the most area with the highest depth class, 'over person's height'. Furthermore, it can be seen that almost the same amount of area that is inundated during event 1, covers the three lowest classes in the other three simulated events. Comparing the three heavy rainfall events, it can be seen that event 2 and 3 have a larger

(a) Event 1

(b) Event 2

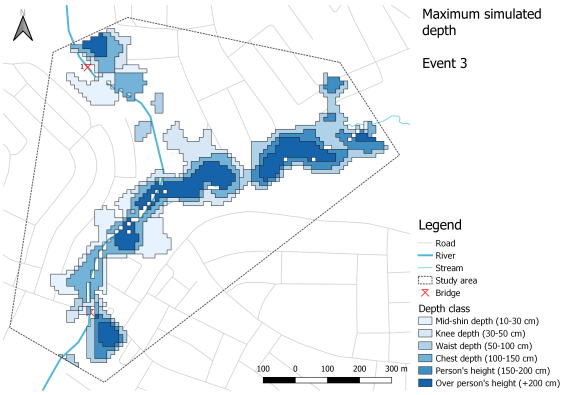

(c) Event 3

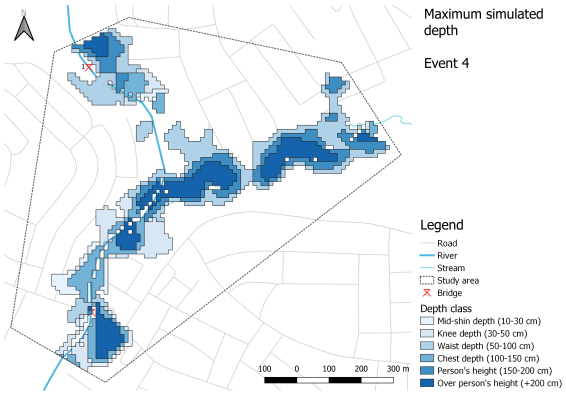

(d) Event 4

Figure 6.8: Maximum simulated depth of the moderate and heavy rainfall events

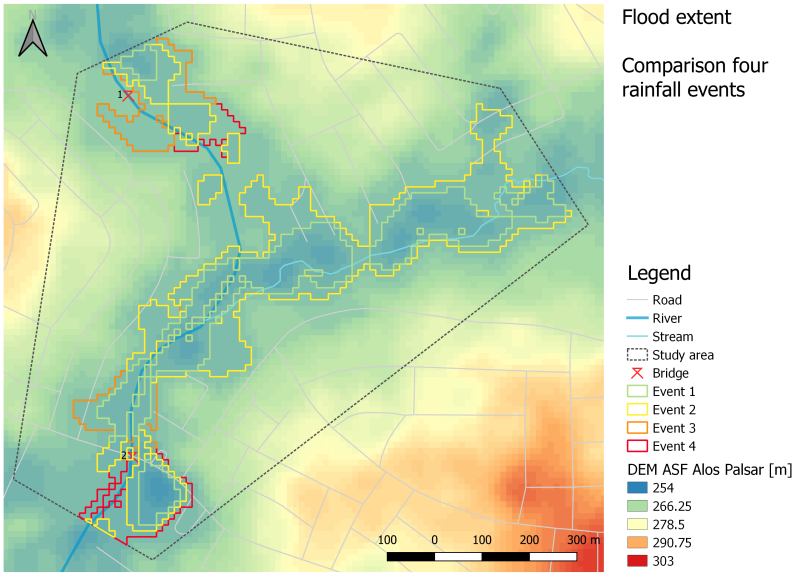

Figure 6.9: Comparison flood extent four selected rainfall events

area with class 'mid-shin depth' and 'knee depth' than event 4. Whereas event 4 has remarkably more area in class 'waist depth' than events 2 and 3. The flood depths in event 4, consist for almost 21% of depths larger than 'knee depth', thus 50 cm. Comparing this to event 2 and 3, these classes cover approximately 13% and

16%. The depths higher than 50 cm seem to be increasing proportional to the increase in precipitation. Furthermore, for all events half of the total inundation are depths higher than 1 m covering the area between 5-13%.

Looking at the velocity in figure 6.10b, it can be seen that for all events, class 1 with velocity ranges between 0-1 m/s is the most dominant class. However, the larger events increase slightly in higher velocity classes. The proportion of higher classes present in the velocity increases proportional with the total area that is inundated. The higher classes can be found directly next to the river in almost all events. For event 4, some of the higher velocities are found a bit further in the floodplain along reach 2.

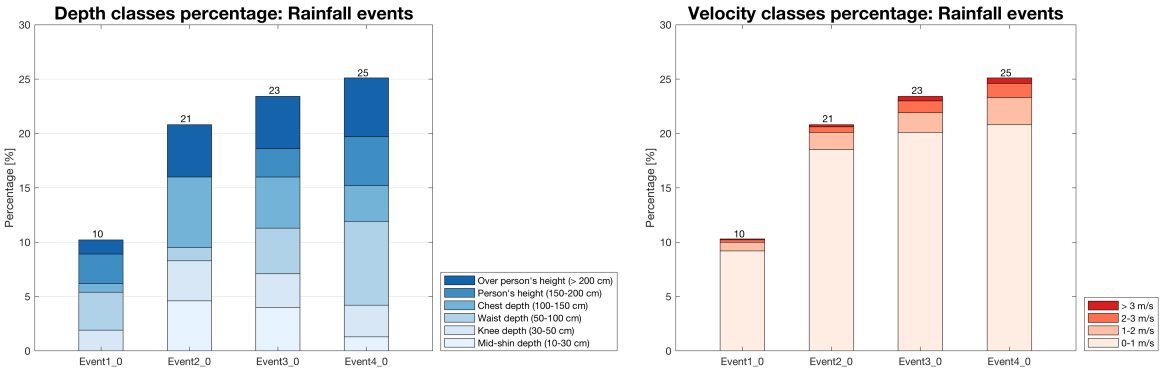

(a) Depth classes

(b) Velocity classes

Figure 6.10: Bar graphs of depth- and velocity classes covering study area per simulated event

Analysing the percentage of inundation in figures 6.10, it can be seen that for a higher total rainfall, the inundated area increases. Comparing the four rainfall events in magnitude it can be stated that the total rainfall volume increases almost linearly from each other, varying from an increase of approximately 20 to 29mm per event. Looking at the graphs that represent the inundated areas per event, it can be seen that the difference between a low and moderate event is large. Furthermore, when moving from moderate to heavy rainfall events, the surface does not increase much, thus the inundation reaches a certain threshold. These results are shortly elaborated on: Event 1 with a total precipitation of approximately 28 mm in four hours, has as result to inundate maximum 10% of the study area. Event 2 with a total precipitation of approximately 57 mm in three hours inundates almost 21% of the study area. Event 3 with total precipitation of approximately 83 mm in six hours inundates 23% of the study area with water. Event 4 with total precipitation of approximately 103 mm in nine hours inundates 25% of the study area. From this it can be seen that the biggest increase in inundated area is between event 1 and 4 resulting in almost 15% difference, which are the lowest and highest total precipitation. However the difference between event 1, 2 and 3 respectively is approximately 11% and 13%. Especially the difference between event 3 and 4 is minimal, with only 2% difference. The total rainfall between these two events differ approximately 20 mm from each other, and event 4 is 3 hours longer than event 3.

What might influence this small increase is the topography of the area. As mentioned before all lower lying areas are affected during the floods. When all the lower lying areas are affected, the water needs to move somewhere else and it will flow to other lower lying areas more downstream. This is what can be seen when comparing event 3 and event 4 with each other from the depth maps in figure and respectively. The upstream parts of the study area remain unchanged in terms of inundated area, however small changes can be seen along reach 1, where event 4 has different depth classes and slightly more inundated areas. Along reach 1-lower, it can be seen the inundated area has increased the most for event 4. Thus it seems that the upper areas are already saturated, in terms of areas that are prone to inundation, as the inundated area is larger downstream and upstream only small differences occur. The highest flood depths occur along reach 2.

Model reliability

Following from the model validation and the results of the different rainfall events, it can be questioned if the modelled discharge portrays the rainfall events correctly. The estimated discharge is the main boundary condition in the model for flow, however at the same time this is the biggest uncertainty in the entire research.

No measurements in the upstream catchment were available whatsoever, thus the reliability of this estimation remains unknown. However, a few discharge measurements were done in fieldwork, and the discharge seems in the right order of magnitude for the peak flow of event 1, as stage and velocity were approximately the same modelled and measured. However, the validation of the historic flood event with community reported flood depths concluded mainly that the flood extent was underestimated along reach 1 and reach 2 and that inundated areas close to the stream at the upper part of reach 1, at the middle of reach 1-lower and at the north side of reach 2 are overestimated. As most point (40%) were modelled in a lower depth class, it can be concluded that the flood extent is underestimated in the model. Furthermore, the response time of the catchment is also unknown. Furthermore, the precipitation data for this discharge was taken constant over the entire area, averaged with an aerial reduction factor. However, as upstream are also no rain gauges available, this method remains further unsure. Thus the main boundary condition in the model, forms a big uncertainty in this research.

6.3.3. Impact of blockages

To determine the impact of the blockages introduced at the two bridges in the area, the scenarios will be analysed per rainfall event. In order to identify what the impact is of partially obstructing the river, two discrete levels of 33% and 67% blockage are introduced as mentioned in section . These blockages are located at the two bridges, which form a bottleneck location in the study area, accumulating plastic waste at their piers. The results will be analysed on different parameters such as, flood extent, depth, velocity, water level, flow distribution and volume accumulation. Per scenario, the relevant parameters will be analysed to support the results. All maps, plots and graphs can be found in appendix H for all scenarios per event.

Event 1

The impact of *Event 1* in the study area is the least of all four rainfall events, with a maximum inundation extent covering approximately 10% of the study area with water depths higher than 10 cm. The impact of the introduced blockages on the inundated area can be seen in figure 6.11, which depict the maximum flood extent per scenario. Comparing the flood extent from the different scenarios based on the same rainfall event with different blockages, only small changes can be seen. Mainly, the blockages have impact on the direct area around the bottleneck locations which are indicated as bridges 1 and 2 in the map.

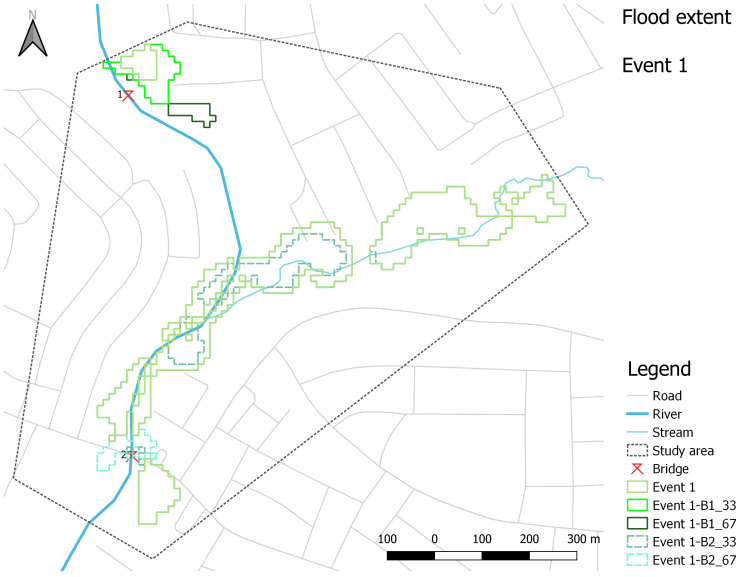

Figure 6.11: Comparison flood extent scenario's Event 1 with and without blockages *Event1-0*

Upstream in the study area at reach 1, where the first bottleneck location is situated, the differences in flood extent of scenario *Event1-0*, *Event1-B1_33* and *Event1-B1_67* is depicted in figure 6.12. The scenario without blockage, *Event1-0*, only covers a small area on the right side of the bridge. The scenario with the blockage

downstream shows the similar result upstream as *Event1-0*. When the blockage of 33% is introduced in figure 6.12c the inundated area around the blockage expands locally, with water depths around 'knee depth'. When the blockage of 67% is introduced in figure 6.12c, the area expands even more and even higher depth classes are present. Now, the largest class present around the bottleneck location is 'waist depth'. However, looking at the rest of the study area, no changes are seen in flood extent at other inundated areas. Thus, the introduced blockages at the first bridge only impact the direct areas in terms of flood extent and depth. Looking at the DEM, this can be explained as the low elevations are not completely inundated around the bridge when it is not yet obstructed.

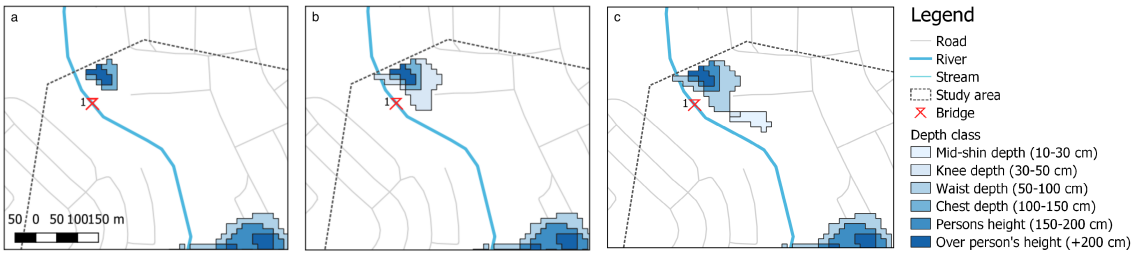

Figure 6.12: Maximum flood depth upstream area for scenario's: a) textitEvent1-0, b) textitB1_33, c) *B1_67*

Comparing the scenarios where the second bridge is blocked *Event1-B2_33* and *Event1-B2_67*, with the initial scenario of *Event1-0*, show different results than when the first bridge is partially blocked. First, it is very interesting that scenario *Event1-B2_33* simulates less inundated areas than all other scenarios. Analysing the flow time series of this scenario, it can be seen that the flow of this scenario is greater than the other scenarios. The computation log file from HEC-RAS is used to do another check on the scenario results, for which especially the inflow and outflow amounts are further examined. Based on the water balance, these amounts should be equal to each other. However, scenario *Event1-B2_33* shows that the outflow is greater than the inflow, which should not be possible. Looking at the other events with this scenario, it becomes clear all scenarios with 33% blockage at the second bridge show the same peculiar result in the water balance. Thus, this scenario will not be compared to the other scenarios of this event, as the result and computation log do not make sense. However, in section 6.4, the problem of an incorrect water balance will be further elaborated.

Furthermore, it is remarkable the scenario with 67% blockage at bridge 2 introduced seems to be running without this numerical error. Looking at the maximum flood extent, it simulates a larger maximum inundation in the area around the second bridge, compared to the other scenarios. When the second bridge is blocked to 67% the inundated area in the study area increases, almost to the same extent as when the first bridge was blocked to 33%. However, the inundated areas are occurring at a different place when comparing the two flood maps with each other. When the second bridge is blocked to 67% the areas around that bridge area inundated, as depicted in figure 6.13. Upstream, the inundation extent remains the same compared to the scenario without blockage. Furthermore, when observing the inundated areas around the junction of the reaches, it can be seen that the depth classes of scenario *Event1-B2_67* are lower than the depth classes of scenario *Event1-0*. In this part of the study area, scenario *Event1-0* has more area with depths around 'person's height' and 'waist depth', than scenario *Event1-B2_67* where the same areas are respectively in the classes 'chest depth' and 'knee depth', thus one depth class lower. Thus, upstream the flood extent remains the same, but the flood depth is decreasing. This implies that water ends up more downstream than upstream for scenario *Event1-B2_67*.

This local flooding around the partially blocked bridges, can be supported with graphs of the water level of the particular reach. Looking at the first bridge, the graphs of maximum water level of scenario *Event1-0*, *Event1-B1_33* and *Event1-B1_67* can be seen in figures 6.14a, 6.14b and 6.14c respectively. Focussing on the structures the water level difference, due to the bridge and extra blockage, increase for the scenarios where the blocked areas increase. For *Event1-0* the water level difference due to the structure is 10cm, for scenario *Event1-B1_33* 40cm and for scenario *Event1-B1_67* 78cm. When the conveyance area decreases, the water level upstream of the bridge increases. Downstream of the bridge, a drop in water level can be seen. This supports the occurrence of increase in local inundation, as the banks of the channel overflow at this point, in this case upstream from the bridge due to a higher backwater curve.

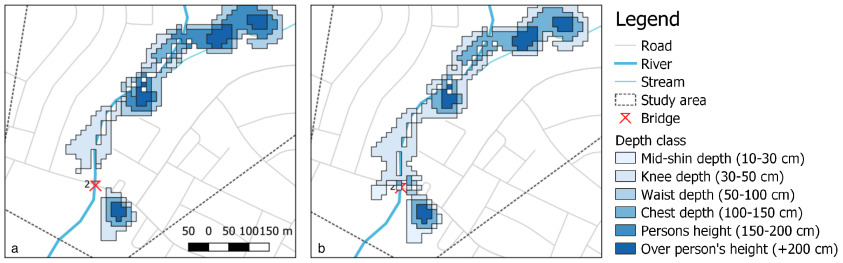

Figure 6.13: Maximum flood depth downstream area for scenario's: a) Event1-0, b) Event1-*B2_67*

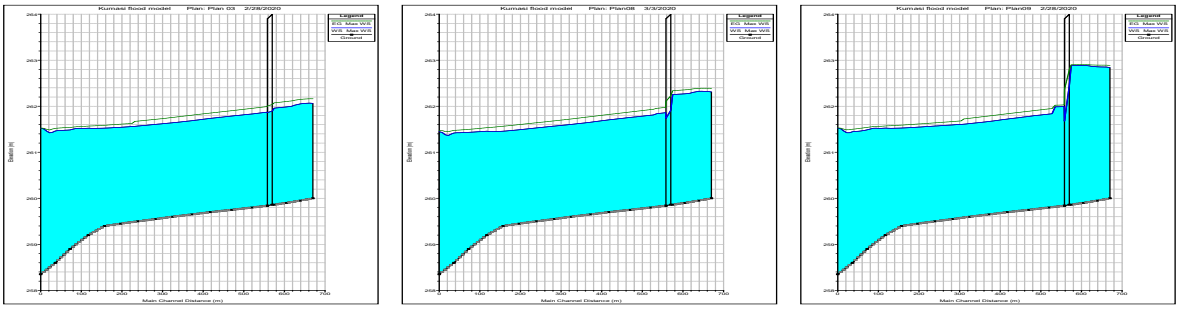

(a) *Event 1* (b) *Event 1-B1_33* (c) *Event 1-B1_67*

Figure 6.14: Water level reach 1

The same effect can be seen downstream, when the water levels around the second bridge from scenarios *Event1-0* and *Event1-B2_67* are compared with each other in figures 6.15a and b. The water level difference is even larger around this reach, which can be seen already a few hundred meters upstream of the bridge. *Event1-0* already shows a very high water level, which abruptly drops a few metres as depicted in figure 6.27. This wave is present due to the sudden drop in riverbed, which influences the water level and energy grade line to also drop very sudden. Thus, this sudden change in water level is not due to the structure, but is already present in the initial scenario. However, looking at figure 6.15 depicting scenario *Event1-B2_67*, this sudden change occurs slightly later just in front of the bridge, which makes it difficult to determine the effect of the introduced blockage of 67%.

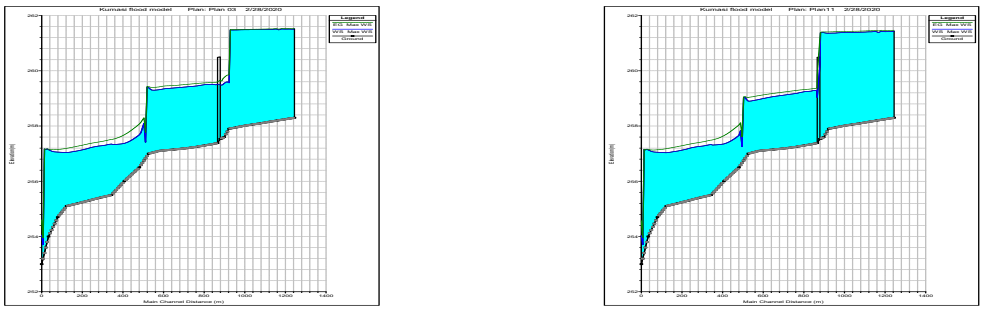

(a) *Event 1* (b) *Event 1-B2_67*

Figure 6.15: Water level reach 1-lower

Looking at the flow distribution over time at different cross sections in figure H.13, the behaviour of flow in the system can be analysed from the different scenarios. For all scenarios the boundary conditions are the

same, except for the amount of blockage per bridge. Thus, this is the only influence on the flow distribution in the study area. The graph of cross section 2, just after the first bridge, does not show much difference between the scenarios. However at the beginning of the simulation scenario *B1_67* shows a smaller flow due to the introduced blockage of 67%, but the difference is minimal and not significant. In reach 2 at cross section 7, the flow distribution of each scenario looks very different. Scenario *Event1-0*, *B1_33* and *B1_67*, show a big dip in the graph, implying water is leaving the cross section around 15:00, which is due to flooding of the area upstream. When both streams come together at the junction, the distribution of the simulated flows follow the same trend again. The scenarios of *Event1-0*, *B1_33* and *B1_67* have a wider peak, thus the flow is more consistent over a longer time, without reaching an absolute maximum. However, the scenarios of *B2_33* and *B2_67* do show a peak in their distribution. Observing the flow distribution of cross section 12 and 14 the impact of the second bridge can be seen. This only affects scenario *B2_33* and *B2_67*, which can be seen as they both have a lower and more spread out 'peak', creating a more spread out distribution. Furthermore, the lower peak downstream of the bridge, implies that water between these two cross-sections has left the stream. In these graphs, it can clearly be seen that the scenario of *B2_33* has a much higher flow than the other scenarios, which does not correspond to the boundary conditions. Furthermore, at cross sections 12 and 14 *Event1-0* and *B1_33* show a small peak around 18:10. This looks like an instability, however in the flood maps and log files nothing suspicious is found in these events.

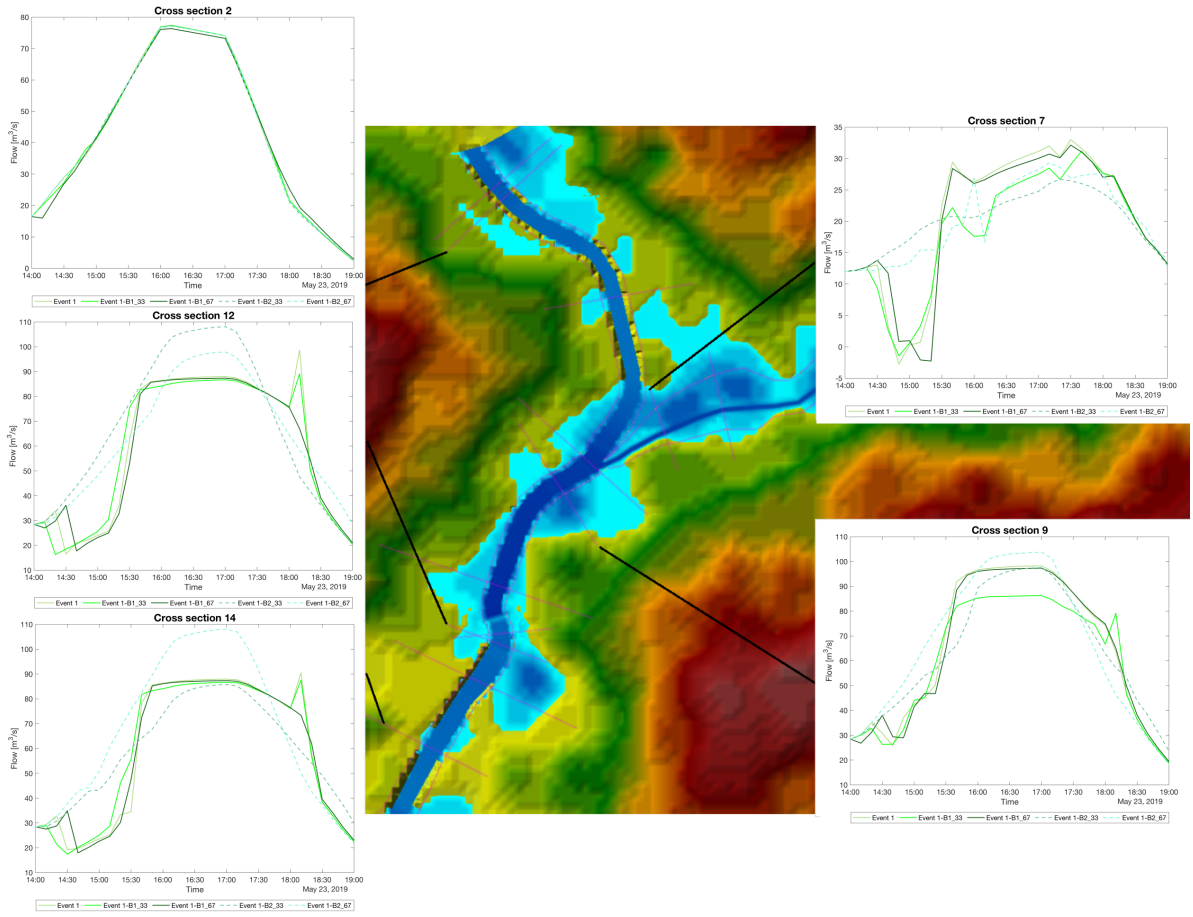

Figure 6.16: Event 1: Flow time series at different cross-sections

Event 2

Comparing the flood extent maps of scenario *Event2-0*, *Event2-B1_33*, *Event2-B1_67* and *Event2-B2_67* in figure 6.17, it can be seen that the differences between the scenarios are minimal. Looking at the scenarios with the first bridge blocked it can be seen that the inundated areas increase around the blocked bridge,

where the most increase around that area occurs when the bridge is blocked for 67% as depicted in figure 6.18. However, for the scenario with 67% blockage, the inundated areas also extend a bit downstream of the junction. Furthermore, a few areas along reach 2 change to a higher depth class, meaning the water level rises around these areas for *Event2-B1_67*.

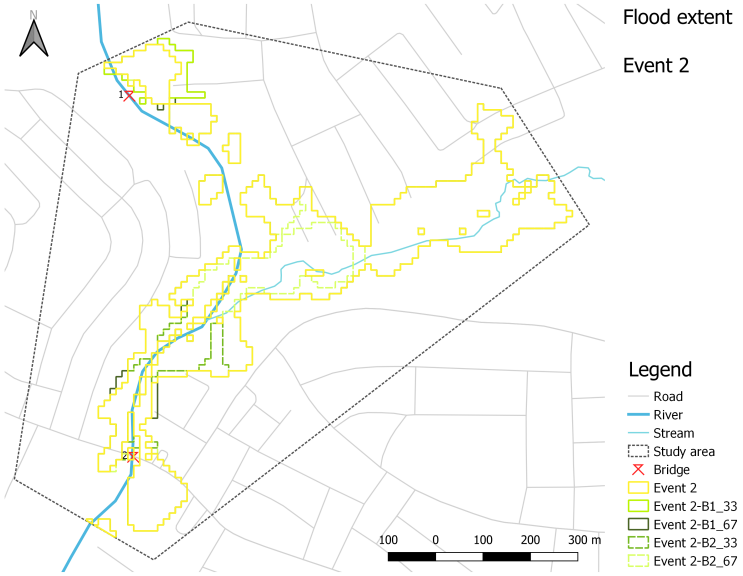

Figure 6.17: Comparison flood extent scenarios Event 2 with and without blockages

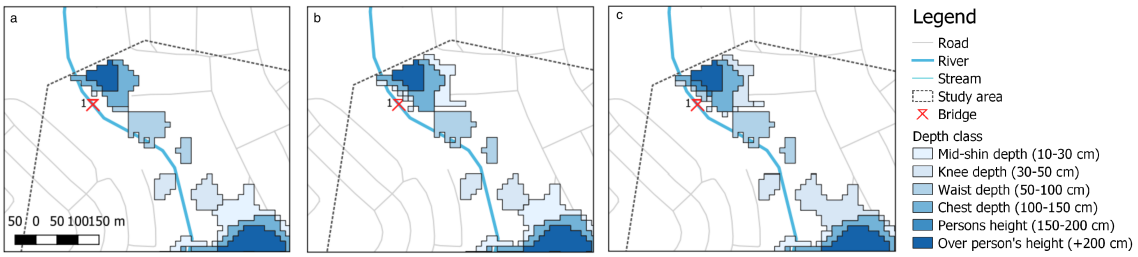

Figure 6.18: Maximum flood depth upstream area for scenario's: a) *Event2-0*, b) *Event2-B1_33*, c) *Event2-B1_67*

What immediately stands out looking at the flood extent of the scenarios of event 2 is that *Event2-B2_67* has the smallest inundated area. This area is approximately 3% smaller than the initial scenario without blockage. As depicted in 6.19 the differences in reach 2 are clearly visible between these two events. Not only has the flood extent decreased, a lot depth classes are also lower for *Event2-B2_67*. However, analysing the velocity, distribution and computation log file, a logical explanation could not be found. Furthermore, it was suspected the same error of the water balance occurred in this simulation, however this was not the case.

Comparing the different depth classes from the bar graphs in figure 6.20a, it can be seen that for the first three scenarios the changes in depth class are minimal. Especially the higher depth classes, from 'waist depth' upwards seem to be presented more or less the same for scenarios *Event2-0*, *Event2-B1_33* and *Event2-B1_67*. However, the greatest difference between these scenarios is in the lower depth classes, where 'knee depth' is more present than 'mid-shin depth' for scenario *Event2-B1_67*, compared to *Event2-0* and *Event2-B1_33*. Furthermore, the main difference is that scenario *Event2-B2_67* has the lowest total inundation as mentioned before, however the highest class 'over person's height' is almost the same as the other scenarios. Thus, *Event2-B2_67* consists of less lower classes, compared to the other scenarios. Concluding from figure 6.20b, the lowest velocity class is dominant in all scenarios, just as in event 1. The higher velocity classes, are also represented more or less the same proportion for every scenario, hence the velocities are not affected.

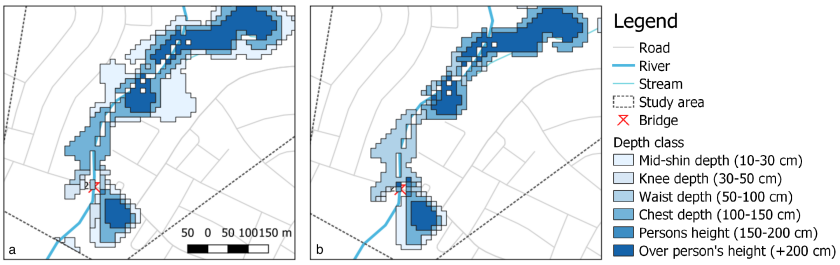

Figure 6.19: Maximum flood depth downstream area for scenario's: a) *Event2-0*, b) *Event2-B2_67*

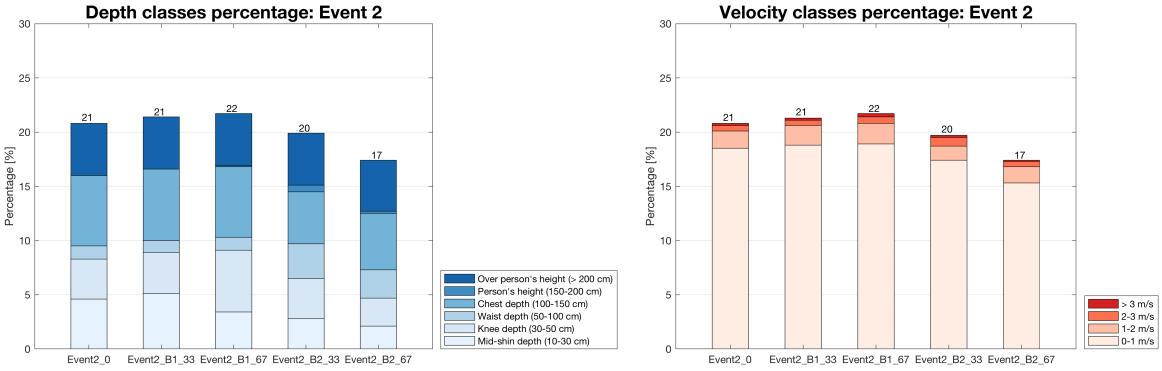

(a) Depth classes

(b) Velocity classes

Figure 6.20: Bar graphs of depth- and velocity classes covering study area for Event 2

Analysing the hydraulic impact of the structures and introduced blockages, changes in water level differences can be seen. The initial impact of the structures, is a water level difference of 10 cm and 5 cm for the first and second bridge respectively. For scenario *Event2-B1_33* the water level difference is 25 cm, thus an extra difference of 15 cm due to the blockage of 33% is induced. For scenario *Event2-B1_67* the water level difference is 45 cm, which is 35 cm more compared to the initial scenario. At the second bridge, it seems that the blockage of 67% has impacted the water level to overtop the bridge deck. Here, the flow is rising almost 1.5 m above the bridge deck. Another general observation that can be made is that the sudden changes in water level due to the river bed are less present in reach 1-lower due to a higher discharge, depicted in figure 6.21a and 6.21b.

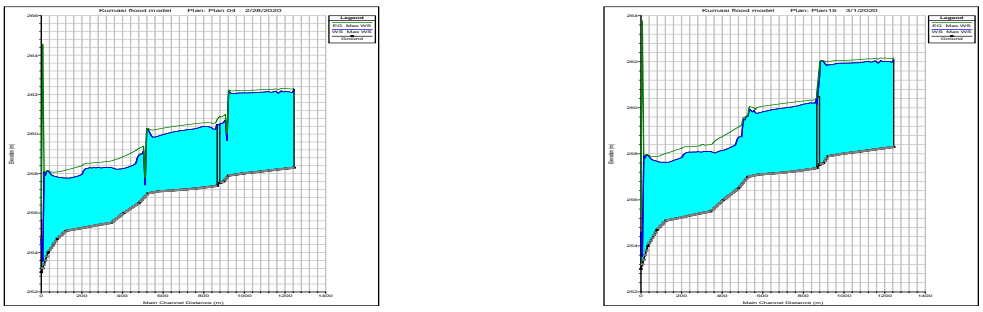

(a) *Event 2*

(b) *Event 2-B2_67*

Figure 6.21: Water level reach 1-lower

Analysing the flow distribution at different cross sections in the area, it was concluded that the flow distribution follows the same behaviour as the scenarios of Event 1. However, Event 2 has higher discharge

rates, as it is a larger rainfall event. No significant changes are present compared to the flow distribution of event 1 at the different cross-sections.

Event 3

Looking at the results of event 3 it can be seen that along almost all sides of the channel and stream inundated areas arise, as depicted in figure 6.22. The rainfall event with a total precipitation of 83 mm in 6 hours, has the impact to flood approximately 23% of the study area. When introducing a blockage of 33% at the first bridge, it can be seen the total inundated area stays more or less the same. Observing the flood map, it can be seen that the direct environment of the bridge is again impacted most. The inundated area increases slightly, but more significant is that maximum water levels around the bridge are higher for scenario *Event3-B1_33*. As the initial scenario *Event3-0* shows already water levels that are more than 'person's height', the second highest class that is present is 'chest depth'. Looking at the flood map of scenario *Event3-B1_33*, cells with class 'chest depth' are now 'person's height' and more cells belong to the class 'waist depth', which was barely present in the initial scenario. Thus, introducing the blockage of 33% affected the flood extent slightly, however standing water has higher depths. When blocking the same bridge to 67%, the flood extent around the bridge slightly increases again. Furthermore, the higher depth classes are more present in the same area. These changes are depicted in figure 6.23. For both scenarios, downstream a few cells change to a lower depth class compared to *Event3-0*, but not significantly. However, for scenario *Event3-B1_67*, the flooded area downstream decreases slightly compared to *Event3-0*.

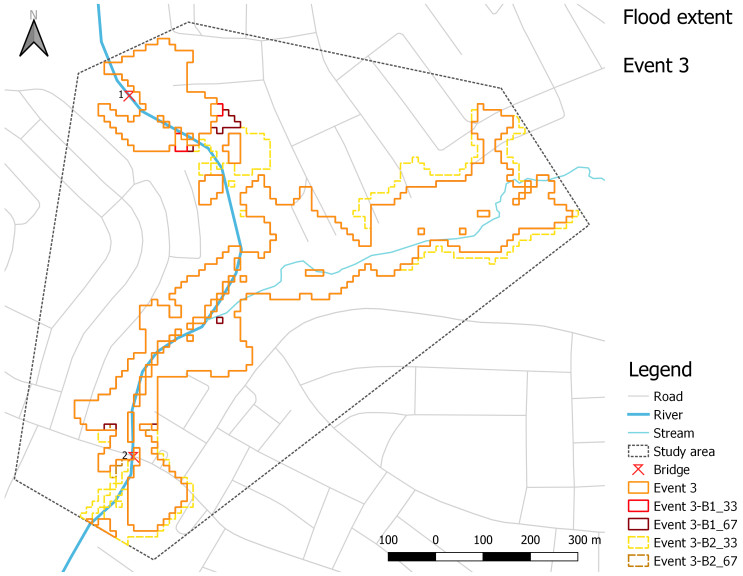

Figure 6.22: Comparison flood extent scenarios Event 3 with and without blockages

In figure 6.24 the changes in flood extent and depth can be seen for the downstream area. Looking at the flood extent of scenario *Event3-B2_67* it can be seen that the area around the second bridge extends slightly. Furthermore, in the same area higher depth classes are present compared to scenario *Event3-0*. However, upstream the inundated areas also seem to be affected in terms of flood depth. Around bridge 1 lower classes are present, and around the junction a few cells have higher flood depths. It seems the blockage downstream influences the flow distribution, making the water shift to locations more downstream. It is remarkable that the scenarios of *Event3-B1_67* and *Event3-B2_67* have almost the same flood extent, covering an area of approximately 24%. As their individual impact in the study area is notable at different locations, the flood extent throughout the area in general remains approximately the same.

Looking at the local hydraulic impact due to the structures, with- and without blockages, water level differences can be seen. *Event3-0*, shows a water level difference of 15 cm at the first bridge. At the second bridge, it can already be observed the water level is already overtopping the bridge. This makes clear the channel is not capable of conveying the flow anymore at this part of the reach. Observing the first bridge, it can

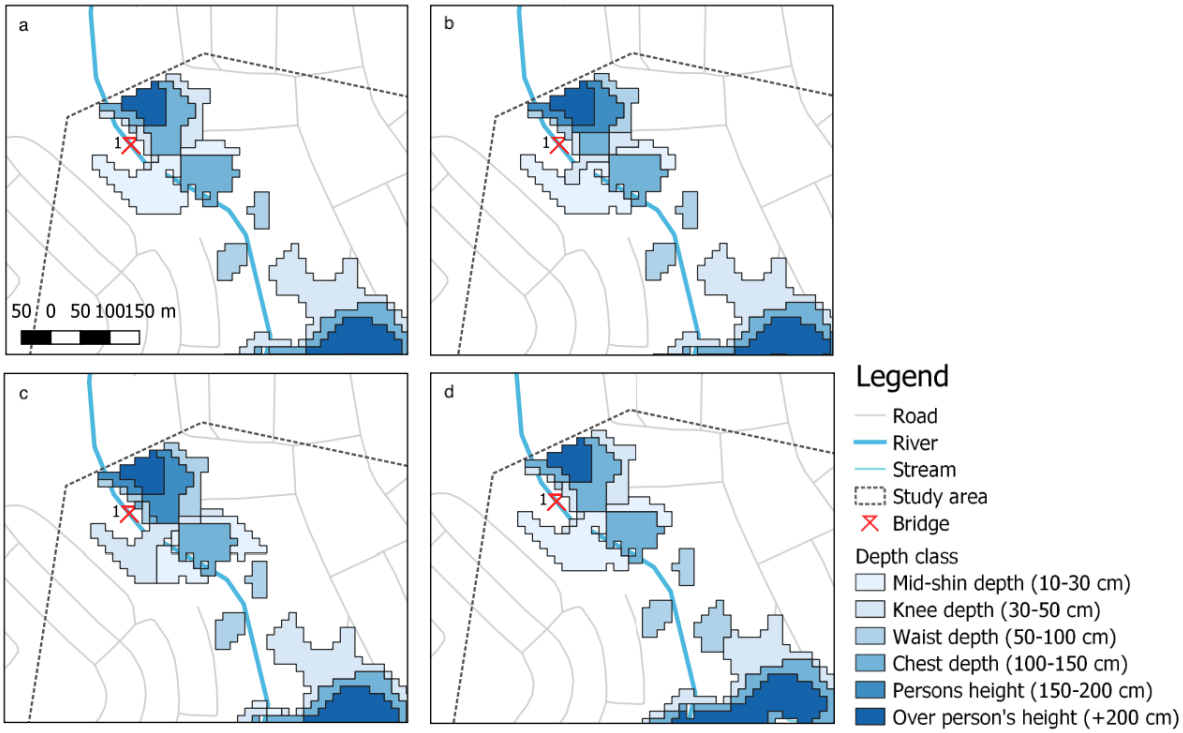

Figure 6.23: Maximum flood depth upstream area for scenario's: a) *Event3-0*, b) *Event3-B1_33*, c) *Event3-B1_67*

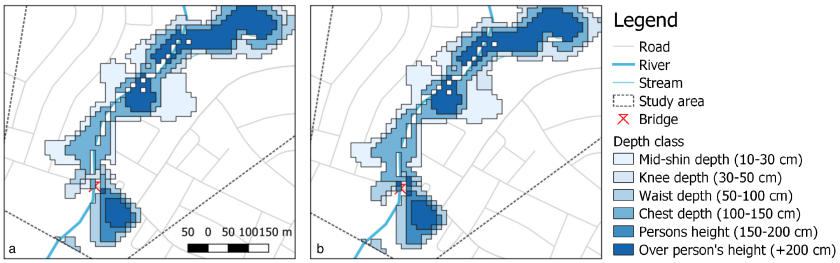

Figure 6.24: Maximum flood depth downstream area for scenario's: (a) *Event3-0*, (b) *Event3-B2_67*

be seen that with a blockage of 33% the water level difference is 30 cm and with 67% 40 cm. Compared to the previous events, Event 1 and 2, the difference in water level between the scenarios is less. This means with higher discharge rates, the structures with blockages have less impact than with lower discharge rates. For scenario *Event3-B2_67* the water level difference introduced by the structure of the first bridge remains the same as for the scenario of *Event3-0*, and downstream of the first bridge as well. At the second bridge, the flow is already overtopping the bridge. Comparing *Event3-0* with *Event3-B2_67*, it can be seen that the water level drops more abruptly downstream of the bridge. The water level stays approximately the same, however this drop proceeds more gradually.

The flood distribution of rainfall event 3, shows a different distribution than for event 1 and 2. For all graphs, the flow reaches a maximum, which can be seen as the peak. After cross section 1, the graphs all still look the same, a small decrease in maximum flow can be observed for event *Event3-B1_67*, which was also for the scenarios of event 1 and 2. However, at reach two the flow varies per scenario from each other, but roughly follow the same trend. At the junction, scenario *Event3-B2_67* is much lower than the other scenarios. The impact of the second bridge can clearly be seen on the flow distribution of *Event3-B2_67* depicted in cross section 12 and 14. Before the bridge the flow is more than after, indicating that water is leaving the channel. This also occurred for this particular scenario during event 1 and 2.

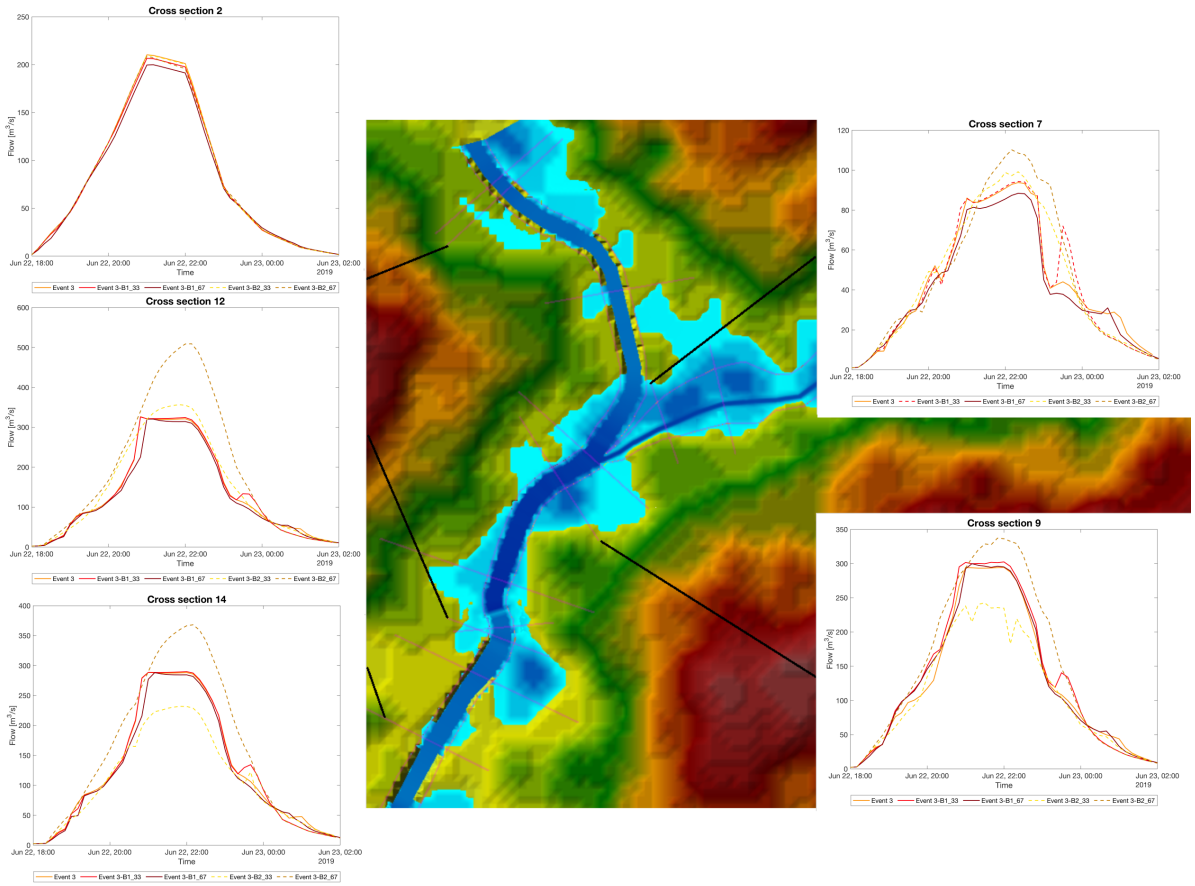

Figure 6.25: Event 3: Flow time series at different cross-sections

The results of this rainfall event seem more straightforward than the results of event 1 and 2. None of the unexpected features that were observed in the results of event 1 and 2 occur during this event, except for the numerical error for scenario *Event3-B2_33*. A possible explanation for this could be that this scenario simulates a larger rainfall event, with more higher consistent discharge rates as boundary condition. As HEC-RAS can not handle low flows very well, the magnitude of this event is significantly larger than the previous two events.

Event 4

Rainfall event 4, has the highest total precipitation and the longest duration of all selected rainfall events, with approximately 103 mm spread out over 9 hours and a maximum precipitation rate of 78 mm/h. From all events, this impacts the study area the most with a maximum flood extent covering 25% of the total study area. Comparing this to the scenarios where the first bridge is blocked, the inundated area again stays more or less the same. However, the depth classes around the first bridge become slightly higher. What stands out more, is that the rest of the study area shows lower depth classes compared to *Event4-0*. Especially the area around the junction shows lower depth classes and even more downstream the inundated area decreases. This has as result that the inundated area for scenario *Event4-B1_33* decreases with almost 1% relative to the initial scenario. Looking at scenario *Event4-B1_67*, more differences can be seen throughout the area. The direct area around the blocked bridge extends the inundated area and shows the deeper classes expand compared to scenario *Event4-0* and *Event4-B1_33*. Furthermore, the inundated area around reach 2 increases with depths up to 'mid-shin.' Furthermore, a lot of cells that belong to 'waist depth' are now 'chest depth' in that area. However, around the junction the opposite effect is seen, the inundated areas have moved down a class. More downstream at the study area along reach 1-lower, the flooded area has even decreased. Thus, this introduced blockage of 67% upstream in the study area, impacts all reaches. This scenario also has the largest flood extent,

covering 27% of the study area. Looking at the scenario where a blockage is introduced of 67% at the second bridge, a decrease in inundated areas can be observed compared to the initial scenario. Furthermore, upstream a small change can be seen, where the depths seem to be decreasing slightly. However, the total inundated area stays more or less the same, with almost 1% decrease in area than scenario *Event4-0* without blockages.

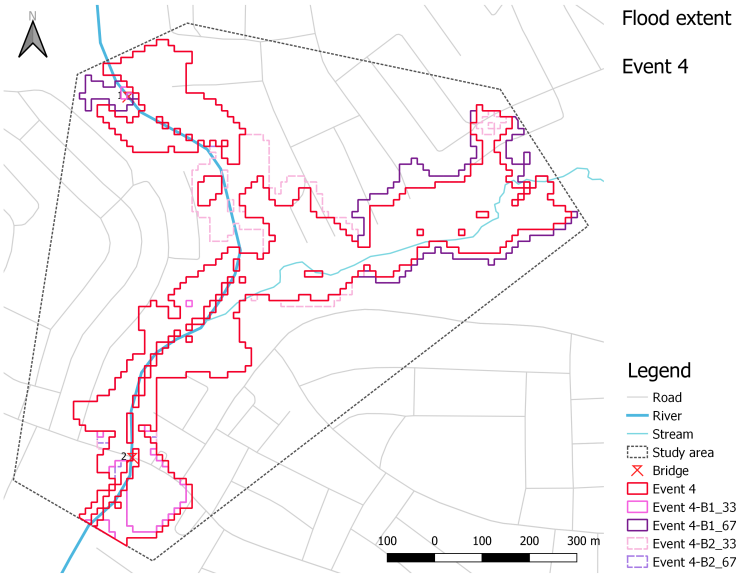

Figure 6.26: Comparison flood extent scenarios Event 4 with- and without blockages

Locally, the change in water level difference is not significantly impacted compared to the previous rainfall events. Downstream at the second bridge, this effect can be seen more clearly. Looking at the flow distribution over time at the different cross-sections, it can be seen that the first bridge again does not have much impact on the flow, as all scenarios follow the same trend. Cross section 7 shows a different result than for the previous events, event 1 and event 2. Now, all scenarios greatly follow the same shape, with a peaked distribution, whereas previously the scenarios of the null-event, *Event4-B1_33* and *Event4-B1_67* had a flattened top. Around 16:00 the scenarios of *Event4-B1_33* and *Event4-B1_67* show again a large dip, which might be due to water leaving the stream and flooding the area more than entering. After the junction, at cross section 9, the scenarios of *Event4-0*, *Event4-B1_33* and *Event4-B1_67* again follow the same trend, however the scenarios of *Event4-B1_33* and *Event4-B1_67* have a slightly wider base, implying more flow is distributed over a longer time. Furthermore, it is interesting that scenario *Event4-B2_67* has a lower maximum flow. Looking at cross section 12 and 14, which are before and after the second bridge respectively, it can be seen the flow of *Event4-B2_67* is only impacted, as the other scenarios follow the same trend.

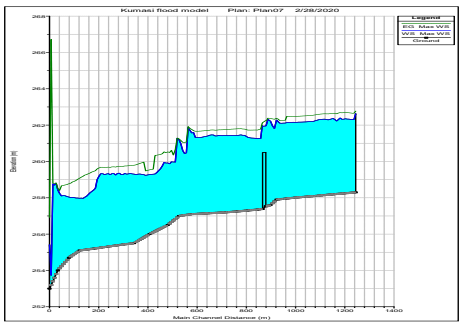

Figure 6.27: Event 4: water level reach 1-lower

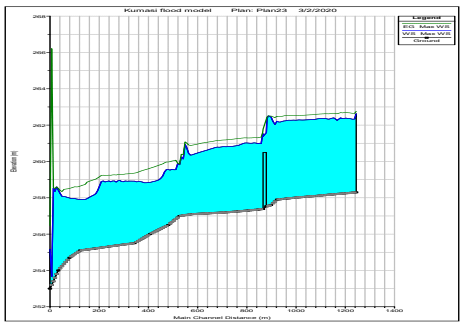

Figure 6.28: Event 4 *B2_67*: water level reach 1-lower

Probability of waste blockage scenarios During fieldwork, the bottleneck locations were observed during a time span of six weeks. During these six weeks, it was not observed the blockages change in size. Furthermore from the plastic mapping results, to what the degree a certain bridge was blocked the response 'less than half' was mostly responded for both bridges. However, during another fieldwork of the TWIGA team, it was also observed that the bridge was completely blocked. Thus, the occurrence of both discrete levels seem realistic. Furthermore, looking at the mapped plastic waste piles, it becomes evident that there is abundant plastic waste available close to the river streams. As it was also observed a lot of waste comes from upstream, this amount is not even taken into account in this research which is also an extra flux that should be taken into consideration.

However a rough estimation can be made about the total volume of waste in the area. As mentioned in section 6.1.2 there are 8 small piles, 8 medium piles, 2 large piles and a large plastic waste dump of approximately 20 x 20 m located in the study area. From the pictures collected in the plastic mapping survey, a volume could be estimated per pile category of small, medium and large.

$$N * V = V_{total} \tag{6.1}$$

Where N = number of waste piles, V = volume of pile category, V_{total} = total volume per waste pile category.

Estimating a small waste pile is roughly 20 m^3, a medium pile is 100 m^3 and a large pile is 500 m^3 a total volume of 1960 m^3 is present as plastic waste in the area following the straightforward approach of equation 6.1. Furthermore the volume of the plastic waste dump is not accounted for yet. It can also be estimated roughly that for blocking a bridge of 33% a volume of approximately 30 m^3 is needed and for 67% 50 m^3 waste is needed. It becomes clear this is a fraction of of the total waste in the area, with 1.5-2.6% of the total waste needed in order to block to a certain degree. Thus, it is not unlikely for the scenarios to occur. However, the volumes have been estimated very roughly in the field thus they might be overestimated. But, the large plastic waste dump has not been taken into account yet for this approximation. Furthermore Kumasi has been visited several times in the TWIGA project and sometimes it was observed the bridge was completely blocked, to a degree of 100%.

6.3.4. Summary of model results

A summary is given of the model results, grouped per parameter and either focussed on the impact of the moderate and heavy rainfall event, or on the scenario's with blockages.

Incorrect water balance for scenario *B2_33*

Analysing the results of scenario *B2_33* for all events, it became clear this scenario produced incorrect results. From the computation log file, the resulting outflow is greater than the inflow for this scenario, for all events. This should not be possible, as from the water balance it follows that the inflow should be equal to the outflow, or smaller, implying water is still left in the system. However, a greater outflow should not be possible and implies a numerical error occurred during the computation. However, it remains uncertain what caused this error. Thus, all results of this scenario are not compared to the other scenarios.

Flood extent

- The maximum flood extent of the moderate (event 1) and heavy (event 2, 3, 4) rainfall events vary from covering 10% to 25% of the observed study area, with depths higher than 10 cm taken into account. The maximum flood extent increases linearly with increasing precipitation of rainfall events. The flooded areas are adjacent to the river streams, and inundate flat and low laying areas. Analysing the topography, it is concluded that all low elevations are impacted by the floods. Areas with a higher elevation are not impacted by inundation.

- The introduced blockages influence the flood extent per event differently. However, it can be concluded that the total inundated area in the study area changes only slightly. Blocking the first bridge with 33% result in a total increase or decrease of maximum 1% for all events compared to their corresponding null scenario. Blocking the first bridge with 67% result in a total increase of maximum 2% for all events compared to their corresponding null scenario. Blocking the second bridge with 67% result in a total increase or decrease of maximum 3% for all events compared to their corresponding null scenario. The scenario of blocking the second bridge with 33% were not simulated correctly and result in a total

increase of maximum 4% compared to their corresponding null scenario.

The total maximum flood extent increases or decreases only slightly per scenario. However looking at local flood extent, it is concluded the local flood patterns shift in the area. When a bridge is partially blocked, the flooded area around the bridge extends. This limited impact is due to the topography around the blocked bridges, as the low lying areas become steeper within a distance of 100 m. Comparing this to the rest of the area, upstream or downstream less flooded areas arise, making the change in total flood extent only change slightly. Varying the discrete levels of 33% and 67% per bridge, it can be concluded that the inundated areas around the blockage increase with the blockage, producing a larger flood extent and higher depths for the higher discrete level.

Flood depth

- The flood depths of the moderate (event 1) and heavy (event 2, 3, 4) rainfall events, increase linearly for the heavy events (event 2, 3, 4) for depth classes higher than 'knee depth'. The percentage of depths higher than 'knee depth' are 8% for event 1, 12% for event 2, 16% for event 3 and 21% for event 4. The highest depth class 'over person's height' does not increase significantly for the larger events, however the class 'waist depth' is significantly increasing for larger rainfall events from 3.5% to 8%. It can be concluded that for larger rainfall events, the depths of inundated water are of higher depth classes, and less of lower depth classes. Furthermore, for all events half of the inundated areas consist of depths higher than 1 m.

- Comparing the flood depths of the scenarios of blockages per event, small changes can be seen in the overall depth classes. For event 1, especially the scenario of blocking the first bridge to 67%, show an increase areas of depth class 'waist depth', and the highest depth class stays exactly the same for all scenarios. For event 2, a similar effect is visible where depth class 'knee depth' is increasing more in area for event B1_67, and the highest depth class again is represented more or less the same for all scenarios. For event 3, it is remarkable that all four simulations show almost the same distribution in depth classes. Event 4 shows the largest increase of the highest and lowest depth class when blocking the first bridge to 67%. However, locally around the blocked bridges, water depths are higher when blocking the particular bridge in the two discrete levels. Furthermore, shifts in depth classes in the rest of the area are also influenced slightly.

Flood velocity

- For the moderate (event 1) and heavy (event 2, 3, 4) rainfall events, the most dominant velocity class of the inundated areas is the lowest class, with velocities between 0-1 m/s. The higher classes increase slightly for the higher rainfall events, however it can be concluded that only cells close to the stream have higher velocities and they are a in lesser extent present compared to the dominant class. The higher classes make up for only 1% for event 1, 2% for event 2 and 3% for event 3 and 4% for event 4. Thus, this increase is proportional to the increase of the rainfall event. However, it can be concluded that the velocity is not an extra dangerous parameter in the inundated areas.

- Comparing the distribution of velocity classes per scenario per event, it can be seen no significant changes arise between the scenarios for all events.

Local hydraulic impact

The local hydraulic impact is summarised in table 6.2 for which the water level differences due to the structures and introduced blockages can be seen per scenario. It can be concluded that in general the structures and blockages have more impact on smaller discharges, in terms of water level difference. When the discharge of the event is already large itself, the structures including blockages have less impact on the water level difference upstream and downstream of the bridge. Furthermore, when discharge is large, especially at the second bridge, it will just flow over the structure.

Flow distribution

Table 6.2: Local hydraulic impact in terms of water level difference due to obstructions per scenario

Rainfall event	Water level difference bridge 1 [cm]	Water level difference bridge 2 [cm]
Event 1-0	10	+2
$Event1 - B1\_33$	40	+2
$Event1 - B1\_67$	78	+2
$Event1 - B2\_33$	15	+15
$Event1 - B2\_67$	10	210
Event 2-0	10	5
$Event2 - B1\_33$	25	5
$Event2 - B1\_67$	45	overtops bridge deck
$Event2 - B2\_33$	5	overtops bridge deck
$Event2 - B2\_67$	5	165
Event 3-0	15	overtops bridge deck
$Event3 - B1\_33$	30	overtops bridge deck
$Event3 - B1\_67$	40	overtops bridge deck
$Event3 - B2\_33$	15	overtops bridge deck
$Event3 - B2\_67$	15	overtops bridge deck
Event 4-0	20	overtops bridge deck
$Event4 - B1\_33$	35	overtops bridge deck
$Event4 - B1\_67$	50	overtops bridge deck
$Event4 - B2\_33$	20	overtops bridge deck
$Event4 - B2\_67$	25	overtops bridge deck

- From the results, it follows that the first bridge does not seem to influence the flow distribution significantly. Analysing the flow upstream, and downstream of the first bridge it can be concluded that the flow distribution of all events and scenarios stay more or less the same. The only slight change is that the scenario of *B1_33* for all events seem to be a bit influenced, producing a smaller peak in all events. However, this impact is not significant.
- At the second bridge, the impact of the structure is more significant. The impact due to the blockage of 67% seems evident. Analysing the cross section upstream and downstream of this bridge, it can be concluded that the flow peak is lower for the scenarios with this bridge blocked downstream of the bridge, implying flow has left the stream between the cross sections as the area under the graph is reduced. The accumulated flow at the downstream cross section is smaller when the blockage of 67% is introduced, compared to the flow accumulation of no blockage at all.
- The different impact of the bridges on the flow distribution cannot be explained. It seems the second bridge has much more impact on the flow, as the scenario of B2-33 for all events also seem to be not simulated correctly. The difference between the two bridges are in the riverbed, which influence the flow in the stream.

6.4. HEC-RAS Limitations

6.4.1. Scenario bridge two blocked with 33%

Analysing the results of scenario *B2_33* for all events, it became evident that the results were very different than the results of other scenarios for these events. Comparing the flow distribution graphs, it became clear the amount of flow was out of line compared to the other scenarios of the corresponding events. From the computation log file, it became clear the outflow for all events was larger than the total inflow. For all other scenarios of the events, the outflow however was smaller than the inflow. This means some water is left in the system, which could also be seen in the flood maps. Thus, the flood map at the end of the simulations are in line with the information of the outflow being less than the inflow of an event. The only explanation that could be found when the outflow is higher than the inflow is that HEC-RAS puts in extra flow in the stream when cells run dry, as the software cannot handle low flows very well. However, it was not observed that low flows are occurring in the system, during the entire simulation of all events. The flow velocity in the river stream for scenario *B2_33* at the end of the system seemed slightly higher than the other scenarios thus it might

be possible a different flow pattern arises during this simulation. However, it cannot be explained why this scenario produced such different results than the other scenarios and why this problem arises at this bridge with this particular amount of blockage. As the first bridge is also blocked to the same extent, the simulations of those scenarios do not produce an ambiguous result.

6.4.2. Bridge modelling method

As the impact due to the bridges was sometimes difficult to determine, it can be discussed if the right bridge modelling method was chosen to model the scenarios. The other bridge modelling methods, such as pressure and weir flow method, are perhaps more realistic taking into account the high flows and low flows of the bridge. However, following from the results where the impact of the bridges and blockages are less impacting the events with large discharge, this result is logical. When flow is smaller, the backwater curve due to the structures is larger, which is in line with expectation. When the flow is already large itself, for which water elevation is already higher than its banks and thus flooding the area, the water body will eventually just flow over the structure.

6.4.3. Accumulation modelling method

The method of modelling the accumulation for this thesis can be discussed as well. Currently, it was only looked at obstructing the flow area in the stream. However, as the debris accumulation with plastics will change the friction factor of the existing bridge, it would have been more realistic to take this into account. Now, the results have only been influenced by the obstructions, and the local impact seems evident. Furthermore, it is also important what kind of accumulation takes place and how this develops over time. Sometimes the blockage occurs on the water surface, then friction has to be taken into account definitely. As the type of accumulation is not really incorporated in this research, it would be interesting to do a comparison in more detail.

6.4.4. Different impact at two bridges

From the results of the different scenarios it became clear the two different bridges have a different impact in the flow. The first bridge did not influence the flow in the streams as much as the second bridge. This was actually not as expected, since both bridges have been blocked to the same degree. Furthermore, the local hydraulic impact from the two bridges are different. However, as the flood wave in reach 1-lower was already much higher, and dropped abruptly due to a sudden drop in bed level, this explains why the water levels are very different from each other. However, the local flooding of the areas directly around the bridges were impacted to the same degree more or less. Furthermore, when this local flooding took place, the distribution of floods through the rest of the area also changed. This can be explained, because the flow is impacted differently at some locations were flood is occurring. Thus, this has impact in the general flow distribution of the system, as these obstructions cause for example by accelerations at certain points and flooding at different areas making volumes of water leaving the flow. These processes impact how flow behaves. However, both bridges have been modelled with the same factors and methods, thus not sure where all these differences come from. Perhaps the design of the bridges impact the flow differently. Bridge 1 has 5 piers which are thinner than the 3 piers at bridge two. Perhaps this also has impact in the flow. Furthermore, bridge 1 is more upstream and bridge 2 is more downstream, which is influenced by the local topography of the area.

6.4.5. Precipitation, infiltration and evaporation

Another limitation in the modelling process was that infiltration and evaporation can not be accounted for in the modelling process. As the events that are modelled are relatively short, the influence of infiltration and evaporation in the study area on the water balance are expected to be small, given the small size of the study area compared to the total catchment. However, information on these processes have been taken into account for the upstream catchment by using the runoff coefficient in the rational method. Detailed information about precipitation, infiltration and evaporation were not available for the upstream catchment, thus might improve the estimation of the discharge. Furthermore, local precipitation was not taken into account as a boundary condition of the 2D flow areas anymore. First, this was taken into account in the model as well. However, including this extra boundary condition in the model, the model would not run stable. As the precipitation in the study area is negligible compared to the total rainfall runoff by the upstream catchment, this will probably not affect the simulated inundation much.

7

Conclusion and recommendations

7.1. Conclusion

The research context of this thesis was to explore if an integrated flood model based on satellite data and in situ measurements can be produced, in order to determine the impact of plastic accumulation on flood severity, in response to rainfall events in the city of Kumasi, Ghana. First, the two sub-questions will be answered whereafter a general conclusion on the main research question is given.

7.1.1. RQ 1: What is the impact of moderate and heavy rainfall events on flood distribution in the study area?

The impact of the moderate (event 1) and heavy rainfall (event 2, 3, 4) events on the study area have a flood extent covering between 10% to 25% of the observed study area, with depths higher than 10 cm. The maximum flood extent increases reaching a certain threshold with increasing total precipitation of rainfall events. The flooded areas are adjacent to the river streams, and inundate flat and low lying areas, from which can be concluded that the topography of the area is an important parameter influencing the flood extent. Areas with higher elevation are not impacted by inundation. From the observed study area, 5% to 13% is inundated with depths higher than 1 m, which is half of the total inundated area per event. It can be concluded that for larger rainfall events, the depths of inundated water consist of higher depth classes, and less of lower depth classes. Furthermore, the greatest part of these inundated areas, 80% to 90%, have velocities ranging from 0-1 m/s, the lowest velocity class. The higher classes increase slightly for the higher rainfall events, however it can be concluded that mostly cells close to the stream have higher velocities.

Taking into account certain thresholds for flood depth and velocity, of flood depths of maximum 1 meter and with velocities until 1 m/s of flow, it can be concluded how dangerous the impact of these flood events are. Half of the maximum inundated area have depths higher than 1 meter, which means it is not safe to enter this area. Furthermore, it should be taken into account that for the maximum reported flood depths of the historic flood event, 40% of the points were estimated with lower depths indicating the flood extent should cover more of the study area. Thus, the impact of the maximum flood extent might be even larger. This could be due to the main boundary condition of discharge in the model, which forms a big uncertainty in this research. However, in terms of velocity the higher velocity classes are only occurring close to the stream and in less extent than the lowest velocity class. The impact for all events is greatest directly adjacent to the streams, and with increasing distance from the streams, the impact becomes less. However, as people are living at close distance to the rivers, these impacts will greatly form inconveniences. Taking into account the probability of these floods are likely to return every year, the impact of moderate and heavy rainfall events is significant on flood occurrence in the study area. Furthermore, as the city is most likely to expand the urbanised area even further, this impact will only become larger in the future.

7.1.2. RQ 2: How does the occurrence of plastic accumulation impact the magnitude of flood events in terms of flood extent, depth and distribution?

The distribution of inundated areas through the area is impacted by the blockages, however compared to the impact of the rainfall event itself, the aggravation of the floods seem not significant in terms of total maximum flood extent. Analysing local flood extent of the scenarios, it is concluded the local flood patterns shift in the area. When a bridge is partially blocked, the flooded area around the bridge extends. Varying the discrete

levels of 33% and 67% per bridge, it can be concluded that the inundated areas around the blockage increase linearly with the blockage, producing a larger flood extent and higher depths for the higher discrete level locally. Furthermore, shifts in depth classes in the rest of the area are also influenced slightly.

The introduced blockages influence the flood extent per event differently. However, it can be concluded that the total inundated area in the study area changes only slightly. Blocking the first bridge with 33% result in a total increase or decrease of maximum 1% for all events compared to their corresponding null scenario. Blocking the first bridge with 67% result in a total increase of maximum 2% for all events compared to their corresponding null scenario. Blocking the second bridge with 67% result in a total increase or decrease of maximum 3% for all events compared to their corresponding null scenario. The scenario of blocking the second bridge with 33% result in a total increase of maximum 4% compared to their corresponding null scenario, however they were not simulated correctly due to a numerical error. For the moderate rainfall event, the water level upstream of the blockage seems to rise, having impact on areas around by flooding it. For heavy rainfall events, the blockage seems to have less impact making the water convey over the bridge deck. Furthermore, at the blockage downstream of 33%, the model simulates extra flow, which might arise due to acceleration of the flow or changing flow patterns. This causes the model to produce impossible results, with more flow leaving the area than entering.

As it can be concluded from this research that plastic waste is very much abundant in the study area, the occurrence of plastic accumulation at the bottleneck locations seem inevitable. The probability of the two discrete levels obstructing the flow paths are not unlikely given the citizen observations, and seem to impact the direct areas around the bottleneck location greatly.

7.1.3. General conclusion

To finalise a general conclusion on the main research question *To what extent does plastic accumulation impact flood severity, in response to rainfall events in the city of Kumasi, Ghana?* can be given.

The results of this research have shown that the main contribution to flooding is flow from upstream areas exceeding river capacity, while local blockages mainly aggravate flooding around the blocked location. This is due to the steep topography and higher elevations at a small distance from the bridges and river stream. The flood extent from the different blockage scenarios stay more or less the same, varying in 1-3% in maximum inundated area. However, this impact is minimal compared to the flood contribution of the occurring rainfall events.

7.2. Recommendations

As this thesis could only cover a certain scope of the ongoing issues regarding to plastic waste, flooding and flood modelling in the study area, recommendations for future research are given in this section. However, the results seem promising and there are possibilities within HEC-RAS to investigate this topic. Furthermore, this thesis stresses the ongoing problems in Kumasi regarding plastic waste and flooding and made a first step engaging the local community. Exploring the option to collect data on plastic and flooding together with citizens, shows detailed information could be gathered using low-cost technologies. Including citizens in the research, can increase both the scale of environmental research and public engagement in this environmental issue. The collected information on waste is valuable to indicate main waste piles and bottleneck locations throughout the area. This could help with waste management in the city, not only improving the flood problems, but also general environmental and health regarding issues. Furthermore, the flood model gives an indication on the response time of the catchment, which could serve as basis for a potential early warning system. As mentioned in the interviews, such a system would be very valuable, as no warning on rainfall or floods are now in place. To help improve the problems regarding plastic waste, flooding and flood modelling, recommendations are given to continue research in this field.

Discharge and precipitation measurements

- The biggest uncertainty in the model, which is actually one of the most important parameters in flood modelling is the discharge. In this research discharge at the boundary of the study area has been estimated very roughly, with a constant precipitation over the total upstream area with the rational

method. However, the only way to determine the actual discharge in the two modelled streams, is to measure them at different points in the catchment. As there are currently no gauges in the catchment, it would be very valuable if this can be monitored. Furthermore, the response time of the catchment should be investigated. Measurements upstream and downstream in the catchment are recommended to determine the real response time. This information is also very valuable for the local community, as they currently have no indication in rising water levels or whatsoever.

- Furthermore, the rainfall should also be measured at more points upstream. Currently there are 4 rainstations in Kumasi, which are all placed very close to each other. It would also be valuable information to measure this more spread out over the total catchment area, in order to perform interpolation techniques between these stations. Currently, this can not be done as all rain stations are placed almost at the same location, compared to the rest of the catchment.

Topographic improvements

- As topographic maps are crucial for flood modelling, two datasets in this research can be improved. It follows from the results that ground elevation is an important parameter influencing flood occurrence. Thus, a DTM with a higher spatial resolution could offer more detailed results, providing more accurate estimations in flood extent and depth. Especially because the study area is hilly terrain and relatively large local differences were observed during fieldwork. As there is already a high resolution DEM available, without ground control points, it is recommended to improve the model with this terrain data once the DEM is accurately processed with ground control points. Furthermore, noise such as trees and building should also be removed from this DEM, in order for it to represent the terrain correctly. Furthermore, the land cover map used in this research has a very coarse spatial resolution of 500 x 500 m, it is recommended to use a spatial resolution more in proportion to the observed study area. Both of these suggestions, would improve the resolution and the topographic characteristics in the flood model.
- Another important dataset which forms an uncertainty, was the bathymetric data of the natural side stream in reach 2. As mentioned in section 4.3.1 there were limitations in measuring the river due to safety considerations. However, this information is crucial for the flood model, as the cross sectional data determine the capacity and the conveyance of the stream and its floodplain. As it followed from the results that the inundation around this reach was not simulated as observed, it becomes clear the bathymetry of this river should be improved. As fieldwork was performed in the rainy season, when water levels in the river are higher, a suggestion could be to measure the cross sections in the river outside of the rainy season, when water levels will become lower.

Model validation

The flood model could only be validated with an observed rainfall event without occurring floods and a historic rainfall event with community reported flood depths. As they both show promising results, it would improve the model if a simulation could be validated with an observed flood event, after which immediately flood depths can be observed or questioned in the area. Moreover, extra fieldwork measurements, regarding discharge and stage measurements during different rainfall events can validate more model scenarios.

Modelling of bridges and accumulation

As it was the first time to perform bridge modelling for the author, it is recommended to explore further options of modelling bridges with accumulation in HEC-RAS or a different software. As the used method to calculate bridges in this thesis was performed with the energy equation, the pressure and weir flow method in HEC-RAS might seem more realistic as it takes high and low flows into account. Thus it can be recommended to compare the bridge modelling methods in HEC-RAS. Furthermore, it should also be explored if modelling accumulation in terms of obstruction of the flow path is the most realistic method or not. As this thesis only focussed on bridge bottlenecks only, it would also be interesting to analyse how reduction in overall stream conveyance capacity due to solid waste impacts flooding in the area.

Duration of datasets

- When precipitation data becomes available over a longer time span, it is interesting to calculate the return periods of events. When this can be determined, the capacity of the channel can be determined and the return periods of certain flood events can be calculated. When this is known, precautions can be taken for these storm events. Furthermore, it will be more interesting to run the model with these events, as the impact per event can then be simulated more accurately. This can help with the design and implementation process of channels in Ghana.
- The dataset on plastic can also be extended. As the fieldwork took place during a few weeks in a certain time of the year, it would be interesting to map plastics during different times of the year, with different weather conditions. Now, the timespan was very short, thus it is more of an instantaneous measurement. Furthermore, it is also interesting to research the plastic flux in the stream. When observing this, it should be determined how much of the flux is flowing through bridges to downstream areas, and how much of the flux is caught at the pillars of the bridge. For this, it is recommended to observe this in a longer time span, as more information on how this plastic accumulates will become visible. Duration of a time span could be several weeks throughout the whole year, capturing the main characteristics of every season.

A

Derivations for 1D and 2D hydrodynamical calculations

A.1. One-Dimensional

A.1.1. 1D continuity equation

The continuity equation describes the preservation of mass in a given control volume. This means that the net mass flux equals the change in storage. The 1D form of the St. Venant continuity equation can be written as:

$$\frac{\partial A}{\partial t} + \frac{\partial Q}{\partial x} - q = 0 \tag{A.1}$$

Where Q s the flow rate, A is the cross sectional area, and q is the lateral inflow.

A.1.2. 1D momentum equation

The momentum equation is based on Newtons second law of motion, stating that the sum of forces acting on an element equals the rate of change of momentum. The formulation of the momentum equation is dependent on the forces that are being considered. Taking pressure, gravity and friction into account, the 1D momentum equation can be written as:

$$\frac{\partial Q}{\partial t} + \frac{\partial QV}{\partial x} + gA\left(\frac{\partial z}{\partial x} + S_f\right) \tag{A.2}$$

To simplify the computation, HEC-RAS assumed a horizontal water surface at each cross-section normal to the direction of the flow such that the momentum exchange between the channel and the floodplain can be neglected [13]. The one-dimensional equations of motion then become:

$$\frac{\partial A_t}{\partial t} + \frac{\partial(\Phi Q)Q}{\partial x_c} + \frac{\partial[(1-\Phi)Q]}{\partial x_f} = 0 \tag{A.3}$$

$$\frac{\partial Q}{\partial t} + \frac{\partial(\Phi^2 Q^2/A_c}{\partial x_c} + \frac{\partial\left[(1-\Phi)^2 Q^2/A_f\right]}{\partial x_f} + gA_c\left[\frac{\partial Z}{\partial x_c} + S_{fc}\right] + gA_f\left[\frac{\partial z}{\partial x_f} + S_{ff}\right] = 0 \tag{A.4}$$

where Q is the total flow, A is the flow area, Φ is the quotient of channel conveyance over the total conveyance, z is the elevation of water surface, and S is the friction slope, in which the subscripts c and f refers to the channel and floodplain, respectively.

A.2. Two-Dimensional

A.2.1. 2D continuity equation

The 2D form of the continuity equation states, as in 1D, that the net mass flux into the control volume equals the change in storage in the control volume. The only difference is that mass fluxes are now calculated in 2 dimensions. The 2D continuity can be written as:

$$\frac{\partial H}{\partial t} + \frac{\partial(hu)}{\partial x} + \frac{\partial(hv)}{\partial y} + q = 0 \tag{A.5}$$

Where H is the water surface elevation, h is the water depth, u and v are the velocity componets in the x- and y- direction respectively and q is the source term, representing inflow from external sources such as precipitation [12].

A.2.2. 2D momentum equation

The momentum equation, just as in 1D, is based on the principle that the sum of forces acting on an element equals the rate of change of momentum. Considering forcing from gravity, eddy viscosity, friction and the Coriolis effect, the 2D momentum balance equations can be written as:

Momentum balance in the x-direction:

$$\frac{\partial u}{\partial t} + u\frac{\partial u}{\partial x} + v\frac{\partial u}{\partial y} = -g\frac{\partial H}{\partial x} + \nu_t\left(\frac{\partial^2 u}{\partial x^2} + \frac{\partial^2 u}{\partial y^2}\right) - c_f u + f v \tag{A.6}$$

Momentum balance in the y-direction:

$$\frac{\partial u}{\partial t} + u\frac{\partial v}{\partial x} + v\frac{\partial v}{\partial y} = -g\frac{\partial H}{\partial y} + \nu_t\left(\frac{\partial^2 v}{\partial x^2} + \frac{\partial^2 v}{\partial y^2}\right) - c_f v + f u \tag{A.7}$$

where H is the water surface elevation, vt is the eddy viscosity coefficient, cf is the friction coefficient , f is the Coriolis parameter and v and u are velocity components in the x and y directions respectively [13]. The first term in the momentum equations represents the local acceleration, the second term the convective acceleration. The next terms describe the forcing from gravity, eddy viscosity, bed friction, and Coriolis force. Using the Manning's formula, the friction coefficient cf can be expressed (in the x-direction) as following:

$$c_f = \frac{n^2 g|u|}{R^{4/3}} \tag{A.8}$$

where n is Manning's n, g the gravitational constant, u the velocity in the x-direction and R the hydraulic radius.

A.2.3. Diffusive wave approximation

The momentum equation can be simplified to the so called diffusive wave approximation, if gravity and friction are assumed to be the dominant forces acting on the control volume. The following derivation follows from the HEC-RAS Hydraulic reference manual [13].

When gravity and friction are assumed to be the dominant forces in the momentum equation, the acceleration terms as well as the eddy viscosity and Coriolis terms are neglected. Following, the momentum balance can be written as a balance between the gravitation and bottom friction forces:

$$g\nabla H = -c_f V \tag{A.9}$$

Where V is the flow velocity in vector form V = (u,v)

If the bottom friction is evaluated using the Manning formula, equation A.9 can be written as:

$$V = \frac{-[R(h)]^{2/3}}{n}\frac{\nabla H}{|\nabla H|^{1/2}} \tag{A.10}$$

Where R(h) is the hydraulic radius at the water surface elevation H, ∇ is the differential operator, and n is the Manning friction coefficient.

Inserting equation A.10 into the continuity equation A.5 and writing in vector form gives:

$$\frac{\partial H}{\partial t} + \nabla \cdot \beta \nabla H + q = 0 \tag{A.11}$$

Where

$$\beta = \frac{-[R(H)]^{2/3}}{n} \tag{A.12}$$

B

Rainfall events

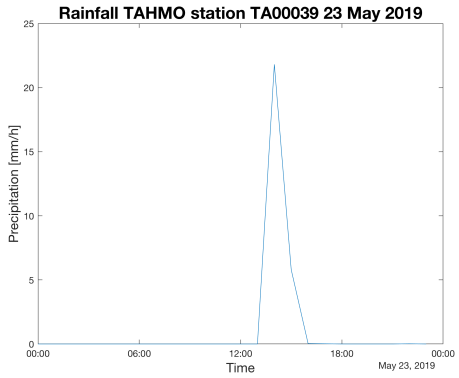

(a) Event 1

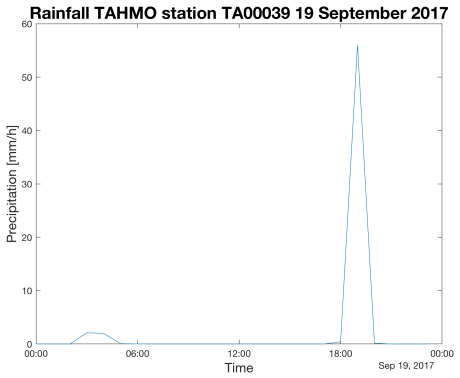

(b) Event 2

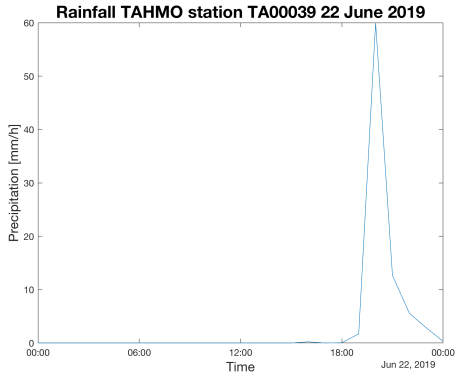

(c) Event 3

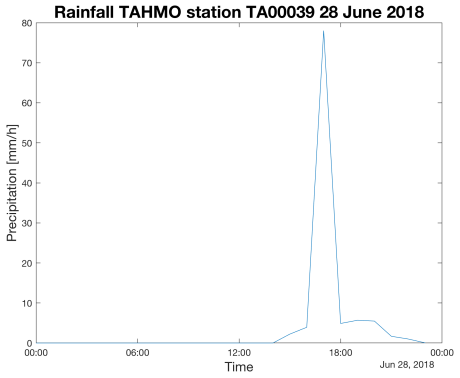

(d) Event 4

Figure B.1: Selected rainfall events

C

Discharge

C.1. Event 1

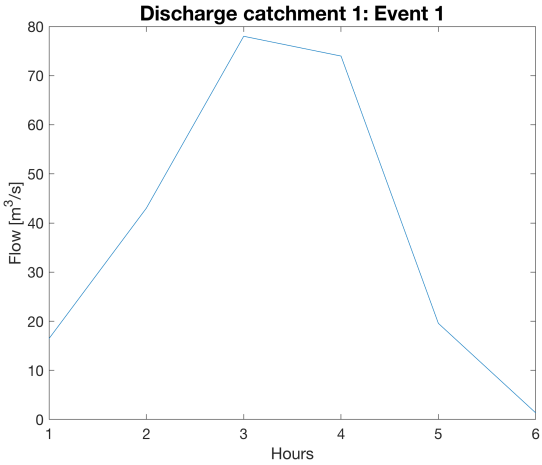

Figure C.1: Estimated discharge per hour of sub-catchment 1

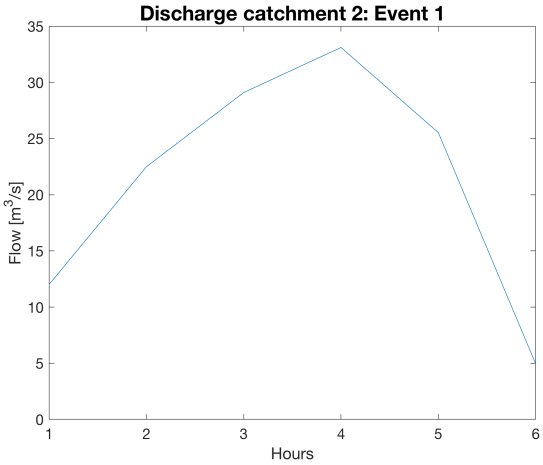

Figure C.2: Estimated discharge per hour of sub-catchment 2

C.2. Event 2

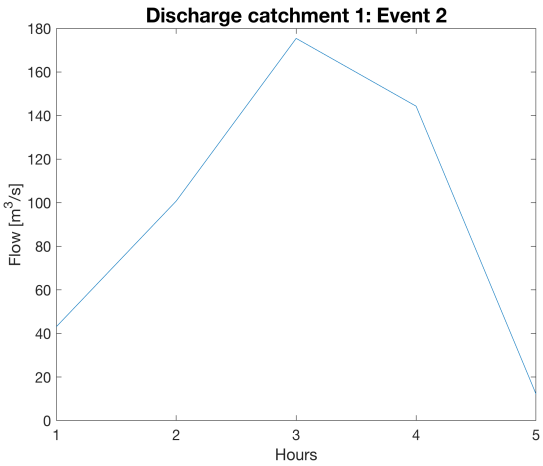

Figure C.3: Estimated discharge per hour of sub-catchment 1

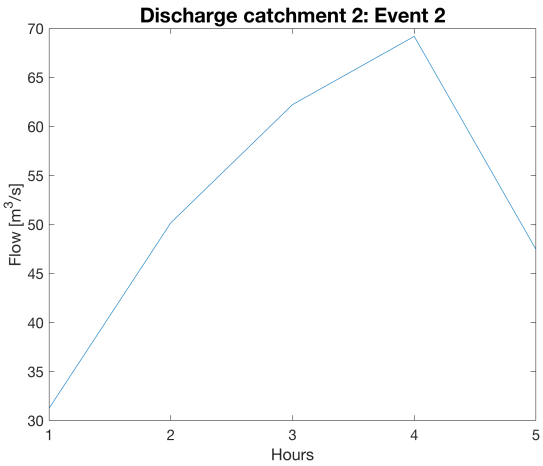

Figure C.4: Estimated discharge per hour of sub-catchment 2

C.3. Event 3

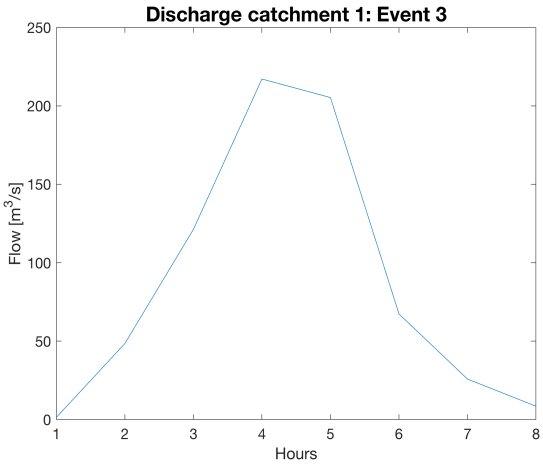

Figure C.5: Estimated discharge per hour of sub-catchment 1

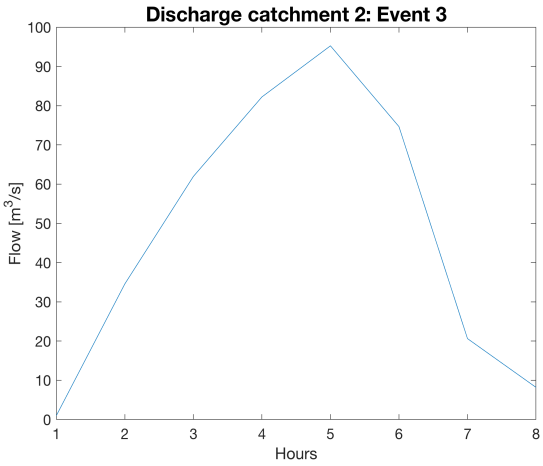

Figure C.6: Estimated discharge per hour of sub-catchment 2

C.4. Event 4

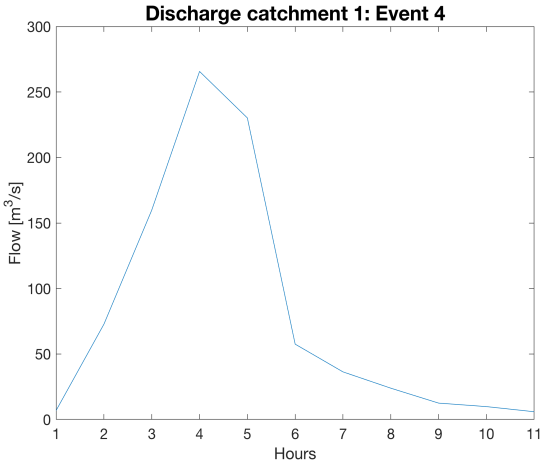

Figure C.7: Estimated discharge per hour of sub-catchment 1

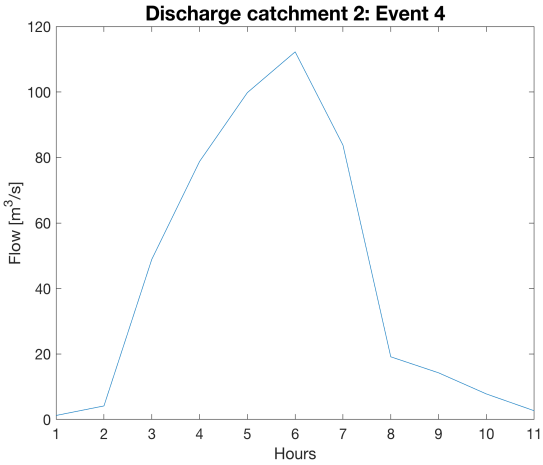

Figure C.8: Estimated discharge per hour of sub-catchment 2

D

MODIS Land Cover - Product MCD12Q1

Table D.1: LC_Type1 Class table [2]

Value	Color	IGBP global vegetation classification description
1	05450a	Evergreen Needleleaf Forests: dominated by evergreen conifer trees (canopy >2m). Tree cover >60%.
2	086a10	Evergreen Broadleaf Forests: dominated by evergreen broadleaf and palmate trees (canopy >2m). Tree cover >60%.
3	54a708	Deciduous Needleleaf Forests: dominated by deciduous needleleaf (larch) trees (canopy >2m). Tree cover >60%.
4	78d203	Deciduous Broadleaf Forests: dominated by deciduous broadleaf trees (canopy >2m). Tree cover >60%.
5	009900	Mixed Forests: dominated by neither deciduous nor evergreen (40-60% of each) tree type (canopy >2m). Tree cover >60%.
6	c6b044	Closed Shrublands: dominated by woody perennials (1-2m height) >60% cover.
7	dcd159	Open Shrublands: dominated by woody perennials (1-2m height) 10-60% cover.
8	dade48	Woody Savannas: tree cover 30-60% (canopy >2m).
9	fbff13	Savannas: tree cover 10-30% (canopy >2m).
10	b6ff05	Grasslands: dominated by herbaceous annuals (<2m).
11	27ff87	Permanent Wetlands: permanently inundated lands with 30-60% water cover and >10% vegetated cover.
12	c24f44	Croplands: at least 60% of area is cultivated cropland.
13	a5a5a5	Urban and Built-up Lands: at least 30% impervious surface area including building materials, asphalt and vehicles.
14	ff6d4c	Cropland/Natural Vegetation Mosaics: mosaics of small-scale cultivation 40-60% with natural tree, shrub, or herbaceous vegetation.
15	69fff8	Permanent Snow and Ice: at least 60% of area is covered by snow and ice for at least 10 months of the year.
16	f9ffa4	Barren: at least 60% of area is non-vegetated barren (sand, rock, soil) areas with less than 10% vegetation.
17	1c0dff	Water Bodies: at least 60% of area is covered by permanent water bodies.

E

Flood questionnaire

1. Record location.
2. Age
   (a) Child
   (b) Adult
   (c) Elderly
3. Gender
   (a) Female
   (b) Male
4. What type of house is this?
   (a) Residential building
   (b) Commercial building
   (c) Mixed residential/commercial
   (d) Public building
   (e) Other
      i. Specify other:
5. How long have you been at this location?
6. What is your experience with floods here?
7. When was the last time you experienced a flood here?
8. How much standing water do you usually get on the street outside in the rain season?
   (a) Only puddles
   (b) Finger depth [0-2cm]
   (c) Ankle deep [2-10cm]
   (d) Mid-shin deep [10-30cm]
   (e) Knee deep [30-50cm]
   (f) Waist deep [60-100cm]
   (g) Chest deep [100-150cm]
   (h) Person's height [150-200cm]
   (i) Over person's height [+200cm]
9. How long does the water usually stay on the street outside after a rainfall during the rainy season

(a) Shorter than 30 min
(b) One hour
(c) Several hours
(d) One day
(e) Several days
(f) One week
(g) Several weeks

10. How often did you experience standing water outside of your house last year(2018)?
11. In which month(s) do you experience the most standing water on the street?
12. How many days has there been standing water on the street in this month(s)?
    (a) 1 to 10
    (b) 10 to 20
    (c) 20 to 30
13. How deep was the deepest water on the street in this month?
    (a) Only puddles
    (b) Finger depth [0-2cm]
    (c) Ankle deep [2-10cm]
    (d) Mid-shin deep [10-30cm]
    (e) Knee deep [30-50cm]
    (f) Waist deep [60-100cm]
    (g) Chest deep [100-150cm]
    (h) Person's height [150-200cm]
    (i) Over person's height [+200cm]
14. When there is standing water on the street, is it standing still or flowing?
    (a) Standing still
    (b) Flowing
    (c) Other
        i. Specify other:
15. Do you know where the water comes from?
    (a) Rainfall
    (b) It comes from upstream
    (c) It comes from a nearby river/stream that overflows
    (d) I don't know
    (e) Other
        i. Specify other:
16. Do you know where the water goes to?
    (a) It goes back to the river
    (b) It flows to other areas downstream
    (c) It stays on the ground and disappears (infiltration/evaporation)
    (d) I don't know

(e) Other
    i. Specify other:

17. Do you know what usually causes water on the street during rainy season?
    (a) Waste blockage of drains
    (b) Waste blockage in nearby river/stream
    (c) Overflow of nearby river/stream
    (d) Other
        i. Specify other:
18. Did the water get into your house during rainy season 2018?
19. How deep was the water inside your house?
    (a) Only puddles
    (b) Finger depth [0-2cm]
    (c) Ankle deep [2-10cm]
    (d) Mid-shin deep [10-30cm]
    (e) Knee deep [30-50cm]
    (f) Waist deep [60-100cm]
    (g) Chest deep [100-150cm]
    (h) Person's height [150-200cm]
    (i) Over person's height [+200cm]
20. Do you remember in which month(s) this happened?
21. What do you do when the water comes into your house?
22. Do you have damage to your house after such an event and if so, what kind of damage?
23. Do you know when it is about the flood?
24. How much time do you have to prepare/flee for the flood?
25. Would it help if you would get a warning about heavy rain events?
26. Is there anything other you would like to share about flooding events?
27. Take a photo (for example floodmarks)

F

ODK - Plastic mapping

1. Record location.
2. Take a picture of the plastic waste.
3. What kind of (plastic) waste do you see?
    (a) Plastic bags
    (b) PET bottles
    (c) Food packaging
    (d) Straws
    (e) Other
        i. Specify other:
4. Is the plastic on the land or in the water?
    (a) On the land
    (b) In the water
    (c) Both
5. Is the plastic deep in the ground or loose on the surface?
    (a) Deep in the ground.
    (b) Loose on the ground
    (c) Both
6. How big is the pile?
    (a) Small
    (b) Medium
    (c) Large
7. Is it floating at the surface or deeper in the water?
    (a) Floating at surface
    (b) Deep in the water
    (c) Both
    (d) Not sure
8. Do you see plastic flowing in the water stream?
    (a) Yes
    (b) No

9. How large is the area covered with plastic at the water surface?
    (a) Small
    (b) Medium
    (c) Large
10. How much does the plastic waste block the riverway?
    (a) Only a little bit
    (b) Less than half
    (c) More than half
    (d) Completely
11. Was the plastic waste here yesterday?
    (a) Yes
    (b) No
12. Do you have any other remarks about the plastic waste?

G

Overview validation points figure 6.7

Table G.1: Validation Event 4-0 historic flood event comparison points in QGIS

Point	Reported maximum flood depth	Modelled maximum flood depth	Modelled in ""
1	Mid-shin depth	0	Lower depth class
2	Chest depth	Chest depth	Correct depth class
3	0	Person's height	Higher depth class
4	Waist depth	Person's height	Higher depth class
5	Puddles	Chest depth	Higher depth class
6	Chest depth	0	Lower depth class
7	Waist depth	Over person's height	Higher depth class
8	Mid-shin depth	Person's height	Higher depth class
9	0	0	Correct depth class
10	Waist depth	0	Lower depth class
11	Chest depth	Person's height	Higher depth class
12	0	0	Correct depth class
13	Knee depth	0	Lower depth class
14	Waist depth	0	Lower depth class
15	Waist depth	Over person's height	Higher depth class
16	Waist depth	Over person's height	Higher depth class
17	0	0	Correct depth class
18	Over person's height	Chest depth	Lower depth class
19	Puddles	0	Correct depth class
20	Puddles	0	Correct depth class
21	Puddles	0	Correct depth class
22	Waist depth	Outside study area	Outside study area
23	Ankle depth	0	Correct depth class
24	Waist depth	0	Lower depth class
25	Over person's height	Waist depth	Lower depth class
26	Waist depth	Chest depth	Higher depth class
27	Waist depth	Mid-shin depth	Lower depth class
28	Waist depth	0	Lower depth class
29	0	0	Correct depth class
30	Puddles	0	Correct depth class
31	Waist depth	0	Lower depth class
32	Mid-shin	0	Lower depth class
33	Knee depth	0	Lower depth class
34	Knee depth	0	Lower depth class
35	Waist depth	Waist depth	Correct depth class
36	Ankle depth	Person's height	Higher depth class
37	Person's height	Person's height	Correct depth class
38	Puddles	0	Correct depth class
39	Waist depth	0	Lower depth class
40	Waist depth	0	Lower depth class
41	0	0	Correct depth class

H

HEC-RAS Results

H.1. Event 1

H.1.1. Maximum flood extent, depth and velocity

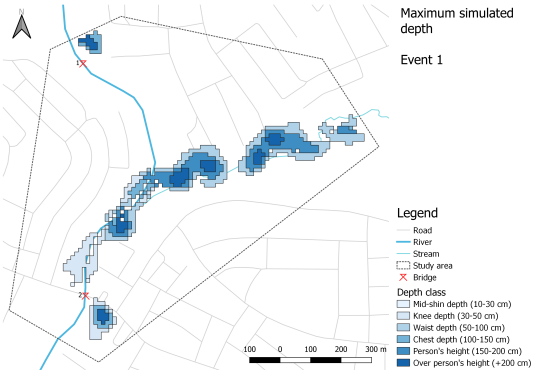

Figure H.1: Event 1: Maximum simulated depth

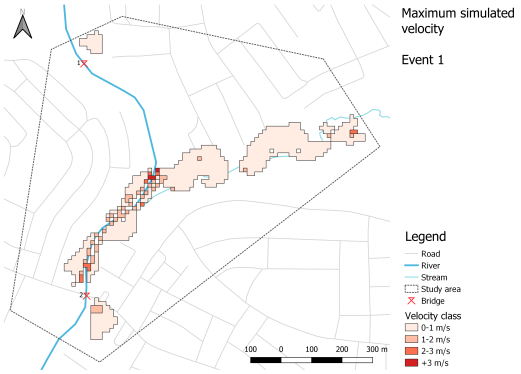

Figure H.2: Event 1: Maximum simulated velocity

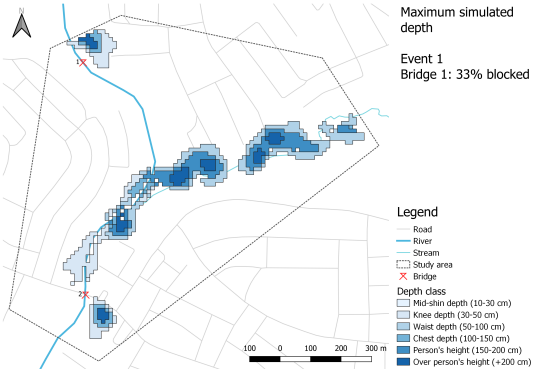

Figure H.3: Event 1 - bridge 1 33% blocked: Maximum simulated depth

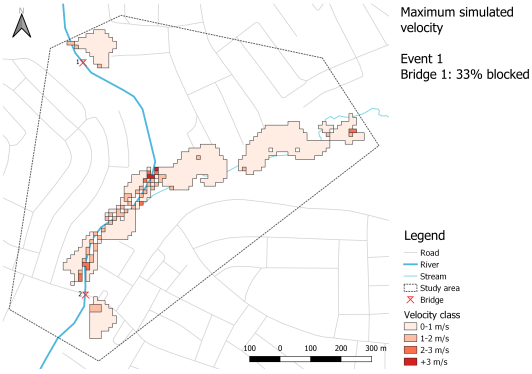

Figure H.4: Event 1 - bridge 1 33% blocked: Maximum simulated velocity

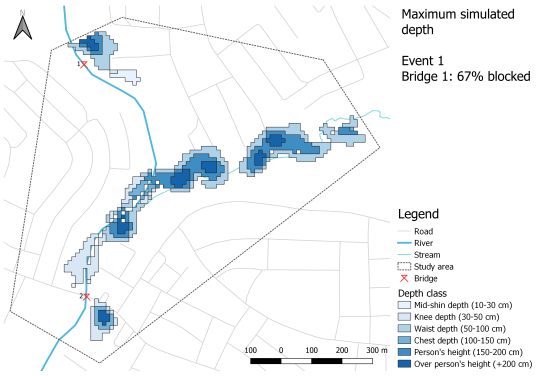

Figure H.5: Event 1 - bridge 1 67% blocked: Maximum simulated depth

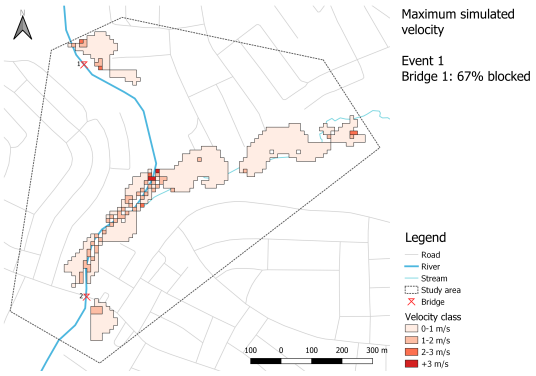

Figure H.6: Event 1 - bridge 1 67% blocked: Maximum simulated velocity

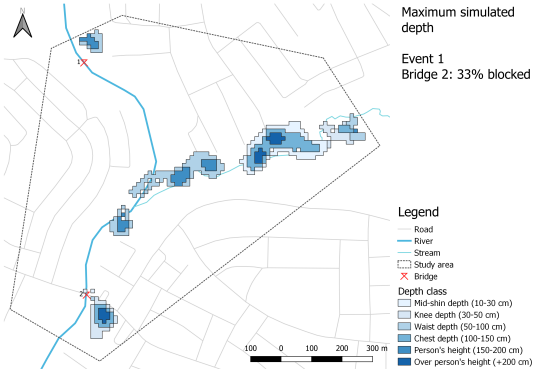

Figure H.7: Event 1 - bridge 2 33% blocked: Maximum simulated depth

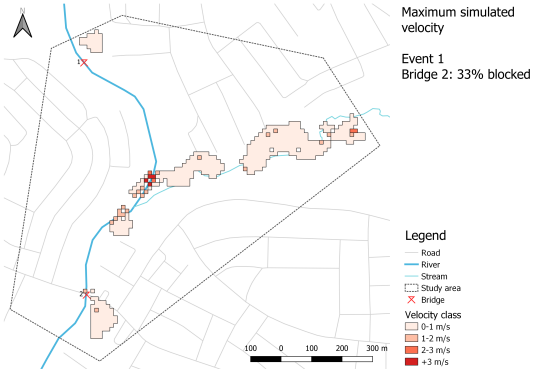

Figure H.8: Event 1 - bridge 2 33% blocked: Maximum simulated velocity

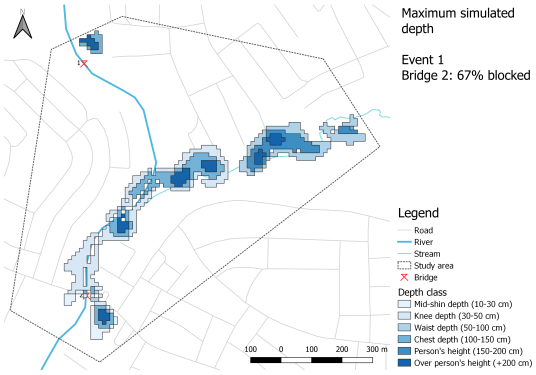

Figure H.9: Event 1 - bridge 2 67% blocked: Maximum simulated depth

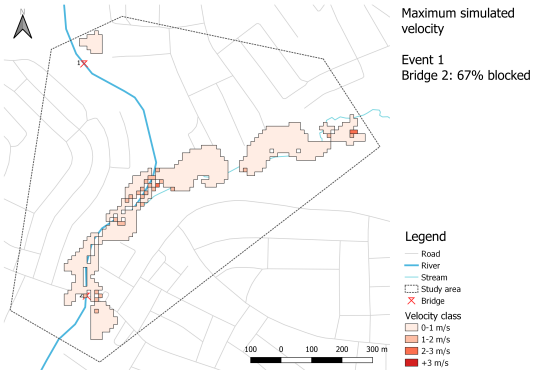

Figure H.10: Event 1 - bridge 2 67% blocked: Maximum simulated velocity

H.1.2. Distribution of depth and velocity classes per simulation

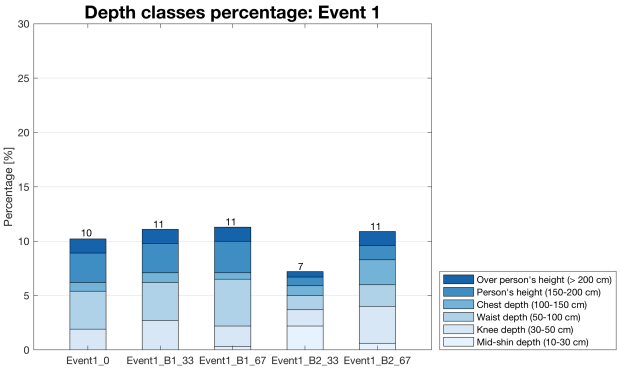

Figure H.11: Event 1 - Depth classes percentages

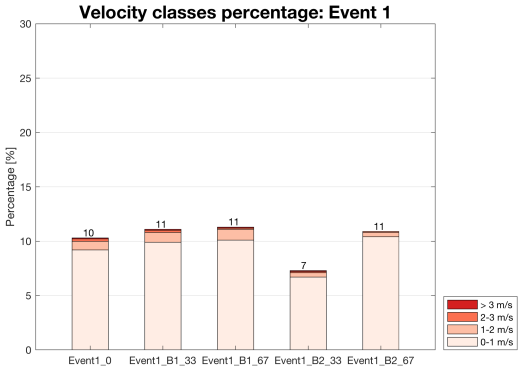

Figure H.12: Event 1 - Velocity classes percentages

H.1.3. Flow distribution over time

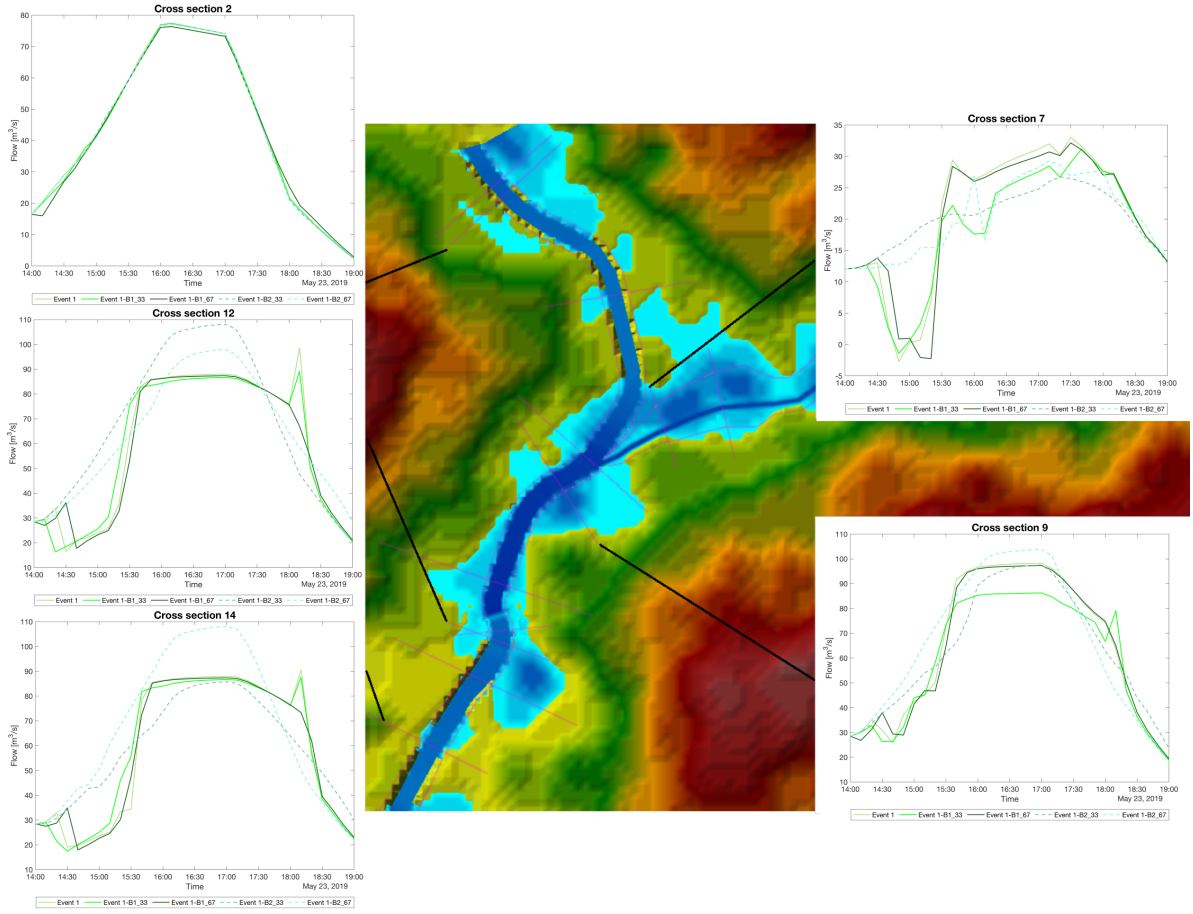

Figure H.13: Event 1: Flow time series at different cross-sections

H.1.4. Maximum water surface profile

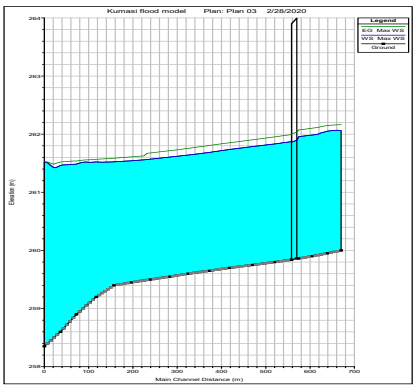

Figure H.14: Event 1 - Reach 1: Maximum WS and EG profile lines

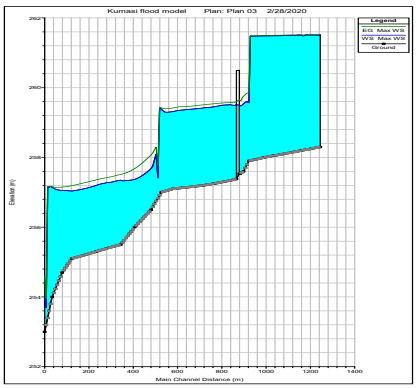

Figure H.15: Event 1 - Reach 1 lower: Maximum WS and EG profile lines

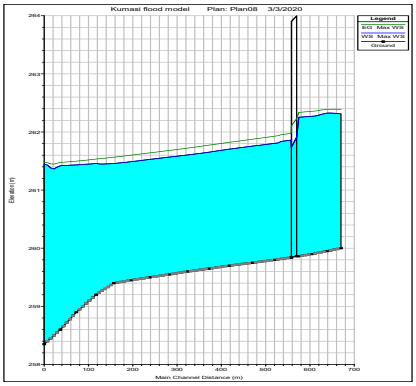

Figure H.16: Event 1 B1 33% - Reach 1: Maximum WS and EG profile lines

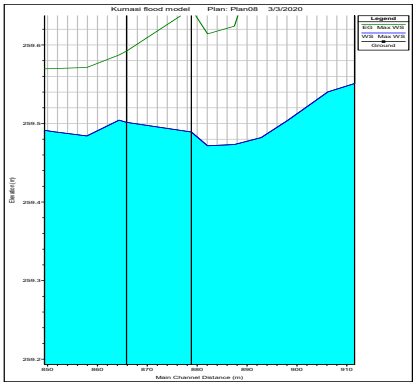

Figure H.17: Event 1 B1 33% - Reach 1 lower: Maximum WS and EG profile lines

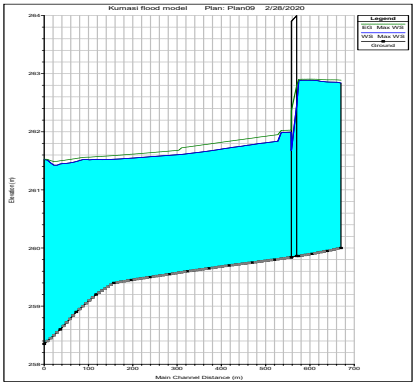

Figure H.18: Event 1 B1 67% - Reach 1: Maximum WS and EG profile lines

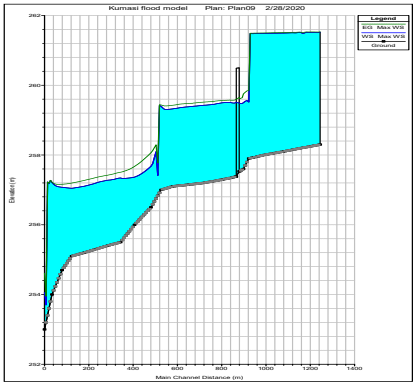

Figure H.19: Event 1 B1 67% - Reach 1 lower: Maximum WS and EG profile lines

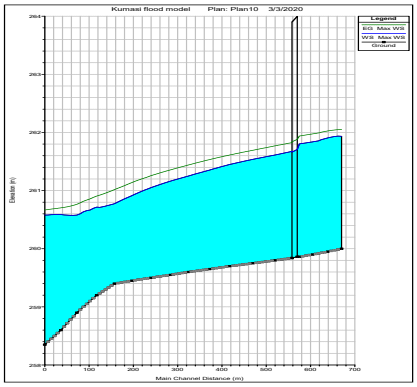

Figure H.20: Event 1 B2 33% - Reach 1: Maximum WS and EG profile lines

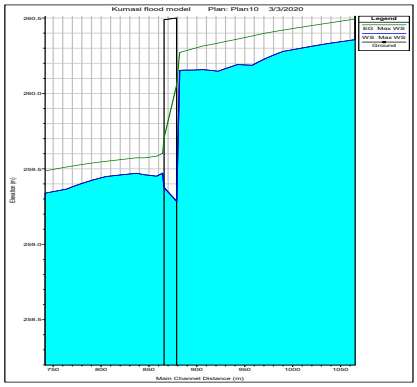

Figure H.21: Event 1 B2 33% - Reach 1 lower: Maximum WS and EG profile lines

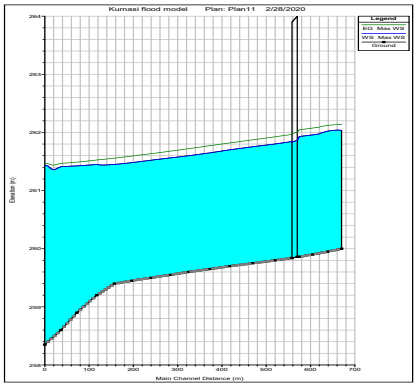

Figure H.22: Event 1 B2 67%- Reach 1: Maximum WS and EG profile lines

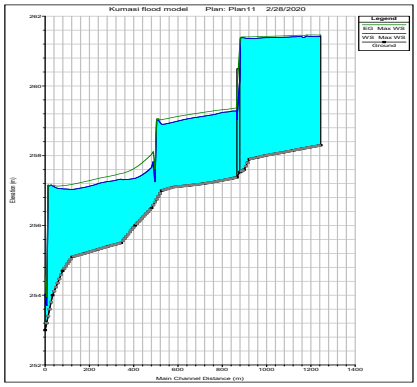

Figure H.23: Event 1 B2 67%- Reach 1 lower: Maximum WS and EG profile lines

H.2. Event 2

H.2.1. Maximum flood extent, depth and velocity

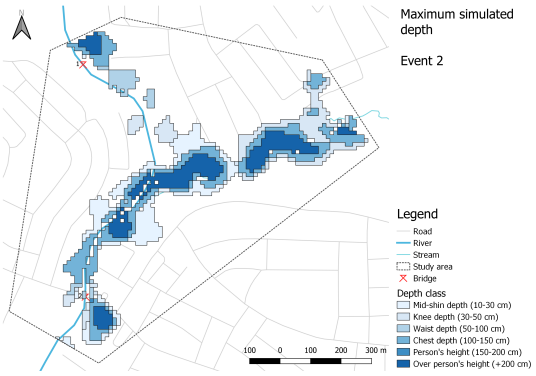

Figure H.24: Event 2: Maximum simulated depth

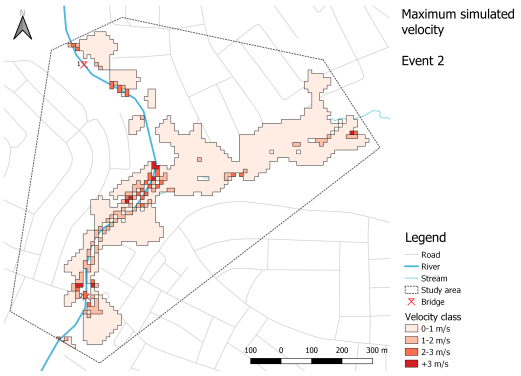

Figure H.25: Event 2: Maximum simulated velocity

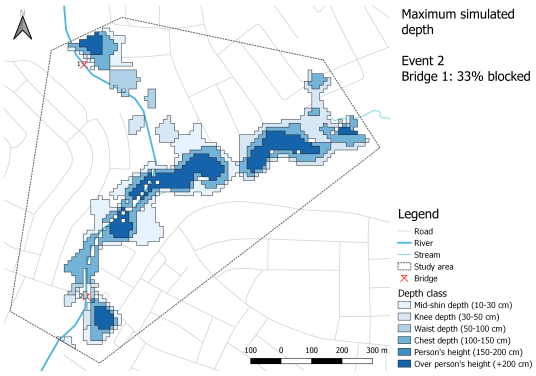

Figure H.26: Event 2 - bridge 1 33% blocked: Maximum simulated depth

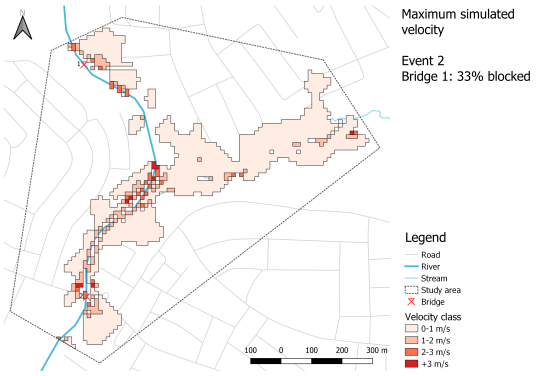

Figure H.27: Event 2 - bridge 1 33% blocked: Maximum simulated velocity

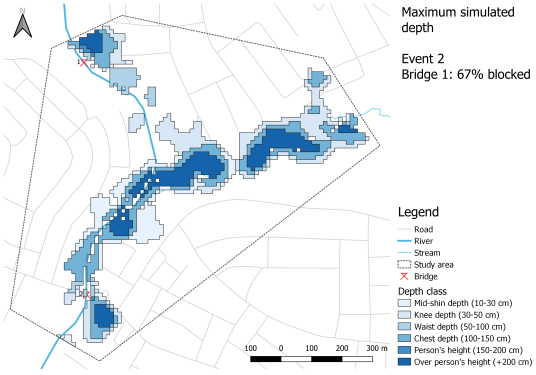

Figure H.28: Event 2 - bridge 1 67% blocked: Maximum simulated depth

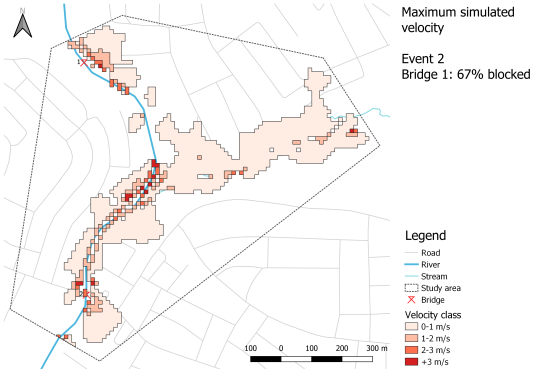

Figure H.29: Event 2 - bridge 1 67% blocked: Maximum simulated velocity

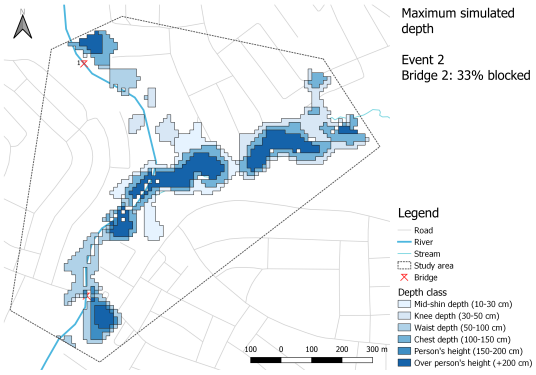

Figure H.30: Event 2 - bridge 2 33% blocked: Maximum simulated depth

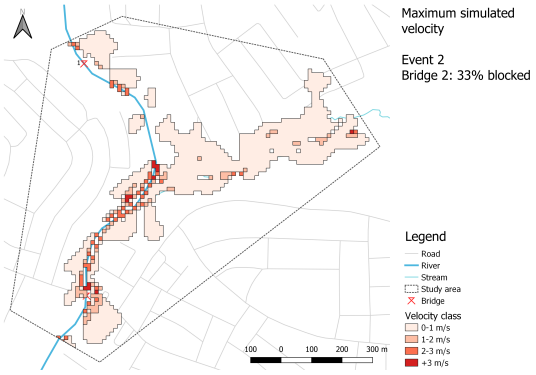

Figure H.31: Event 2 - bridge 2 33% blocked: Maximum simulated velocity

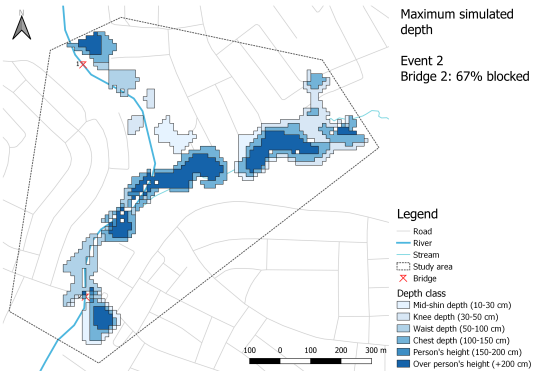

Figure H.32: Event 2 - bridge 2 67% blocked: Maximum simulated depth

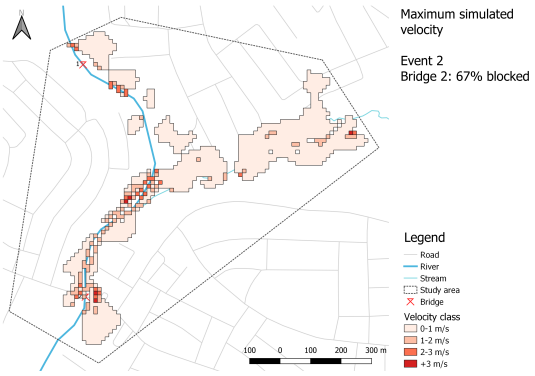

Figure H.33: Event 2 - bridge 2 67% blocked: Maximum simulated velocity

H.2.2. Distribution of depth and velocity classes per simulation

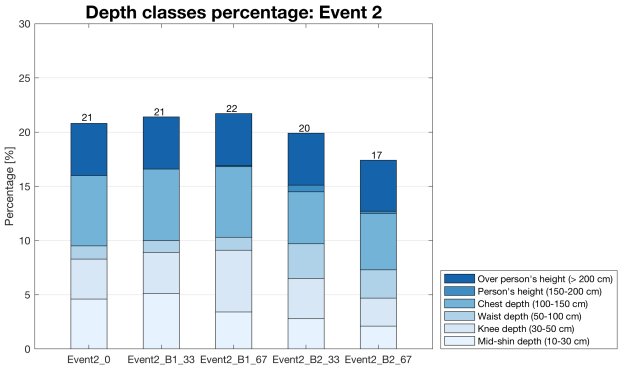

Figure H.34: Event 2 - Depth classes percentages

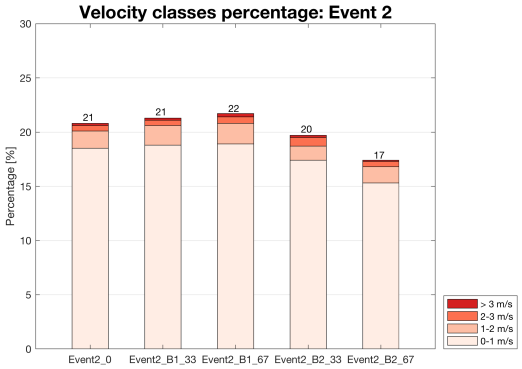

Figure H.35: Event 2 - Velocity classes percentages

H.2.3. Flow distribution over time

H.2.4. Maximum water surface profile

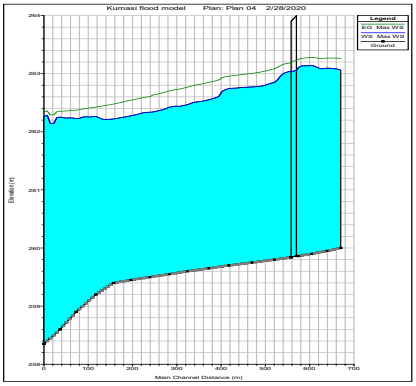

Figure H.37: Event 2 - Reach 1: Maximum WS and EG profile lines

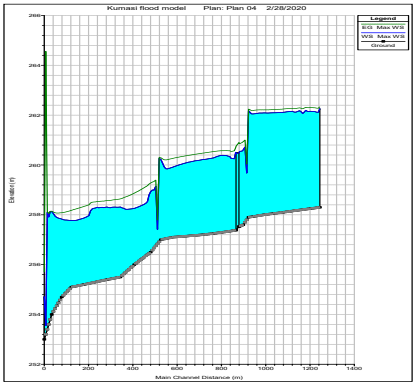

Figure H.38: Event 2 - Reach 1 lower: Maximum WS and EG profile lines

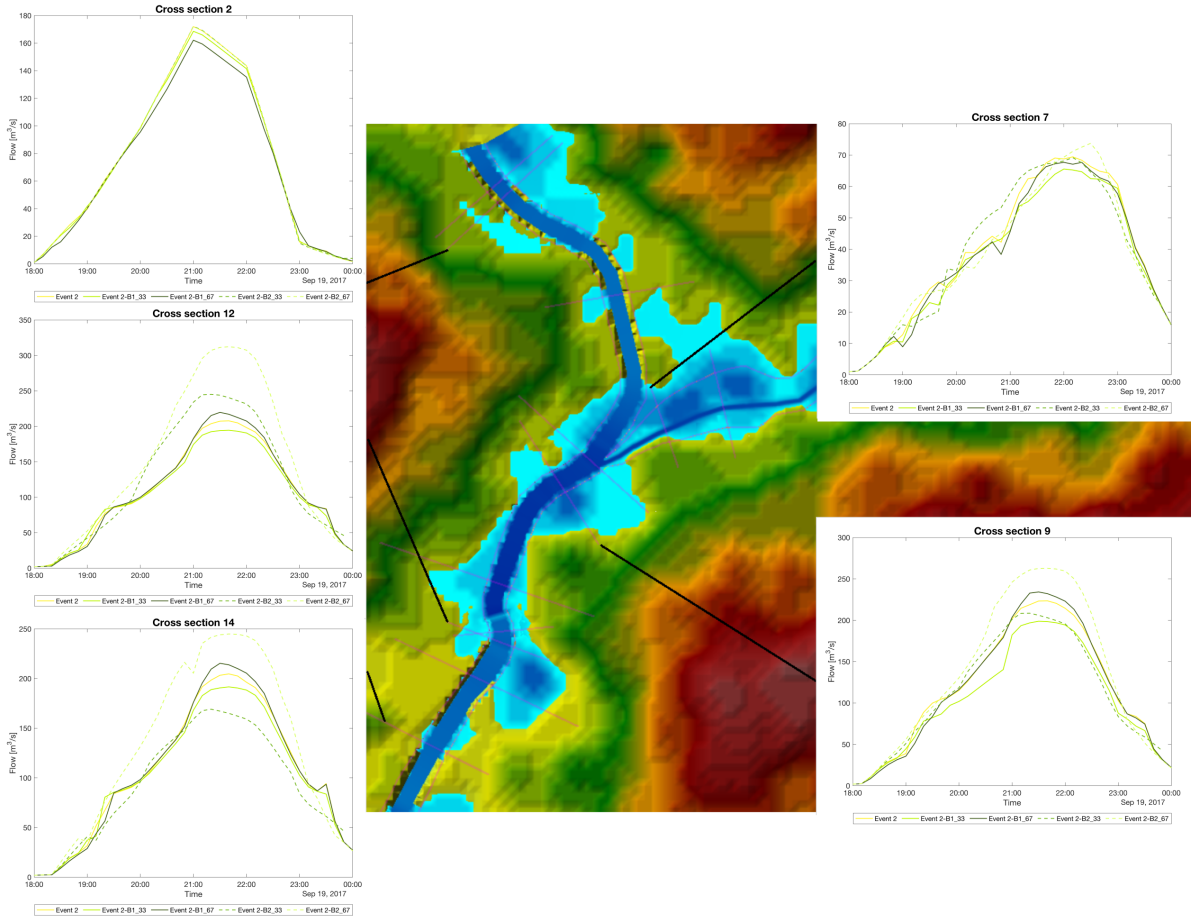

Figure H.36: Event 2: Flow time series at different cross-sections

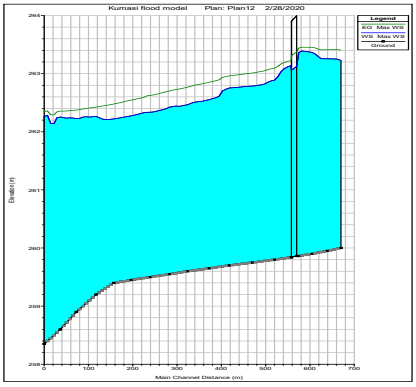

Figure H.39: Event 2 B1 33% - Reach 1: Maximum WS and EG profile lines

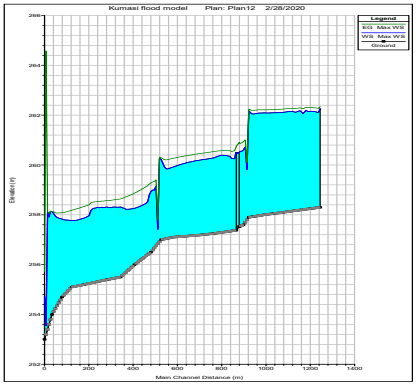

Figure H.40: Event 2 B1 33% - Reach 1 lower: Maximum WS and EG profile lines

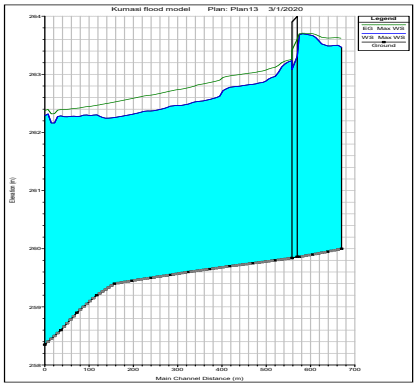

Figure H.41: Event 2 B1 67% - Reach 1: Maximum WS and EG profile lines

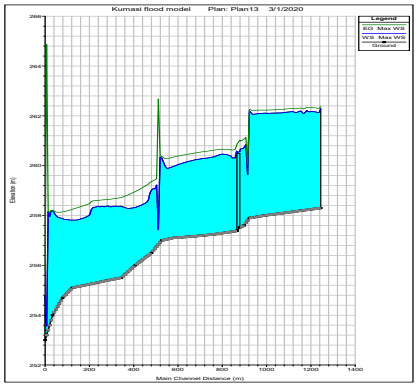

Figure H.42: Event 2 B1 67% - Reach 1 lower: Maximum WS and EG profile lines

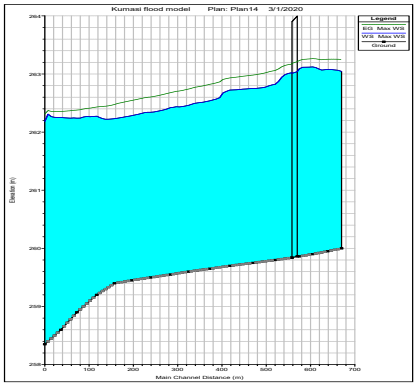

Figure H.43: Event 2 B2 33% - Reach 1: Maximum WS and EG profile lines

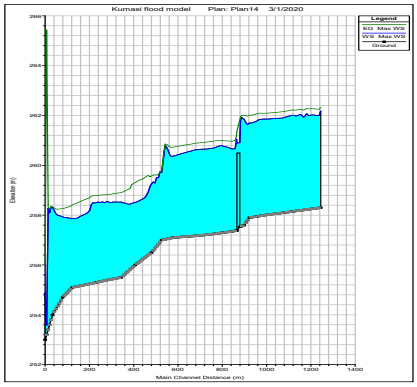

Figure H.44: Event 2 B2 33% - Reach 1 lower: Maximum WS and EG profile lines

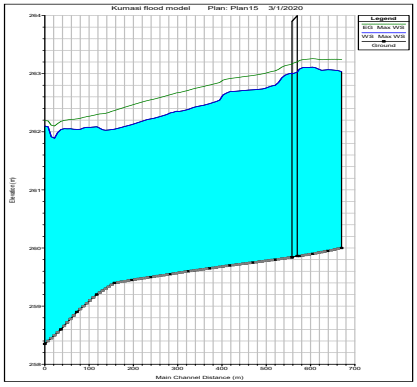

Figure H.45: Event 2 B2 67%- Reach 1: Maximum WS and EG profile lines

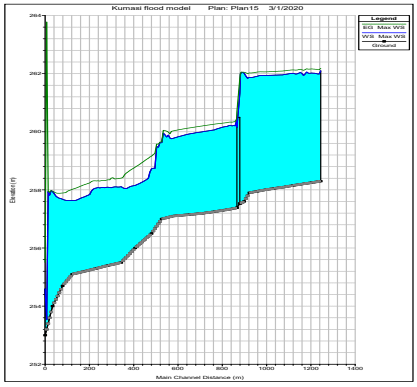

Figure H.46: Event 2 B2 67%- Reach 1 lower: Maximum WS and EG profile lines

H.3. Event 3

H.3.1. Maximum flood extent, depth and velocity

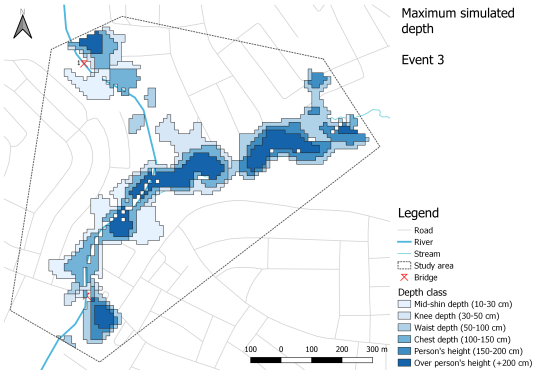

Figure H.47: Event 3: Maximum simulated depth

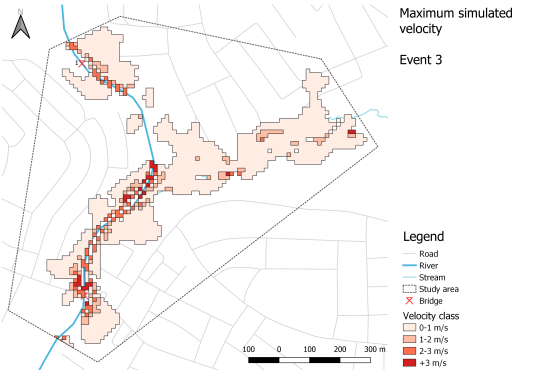

Figure H.48: Event 3: Maximum simulated velocity

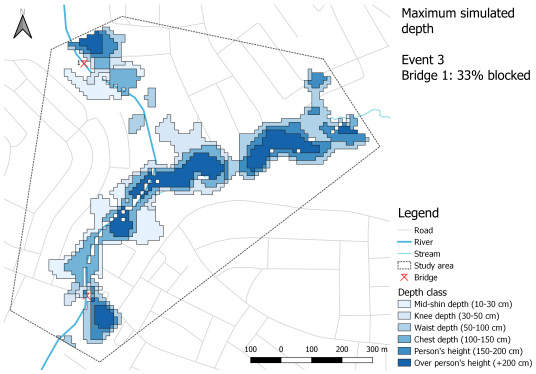

Figure H.49: Event 3 - bridge 1 33% blocked: Maximum simulated depth

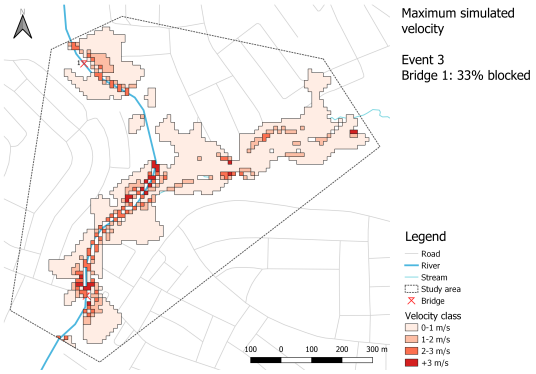

Figure H.50: Event 3 - bridge 1 33% blocked: Maximum simulated velocity

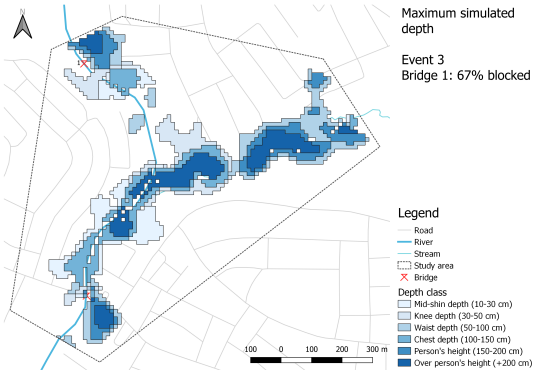

Figure H.51: Event 3 - bridge 1 67% blocked: Maximum simulated depth

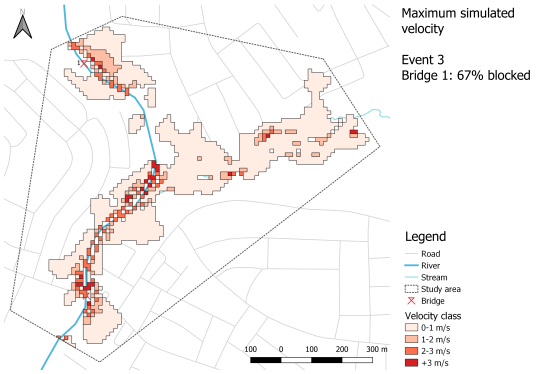

Figure H.52: Event 3 - bridge 1 67% blocked: Maximum simulated velocity

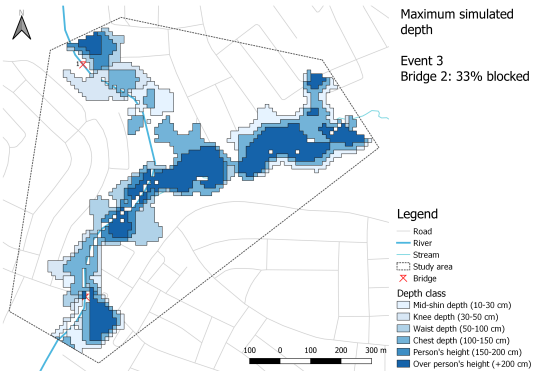

Figure H.53: Event 3 - bridge 2 33% blocked: Maximum simulated depth

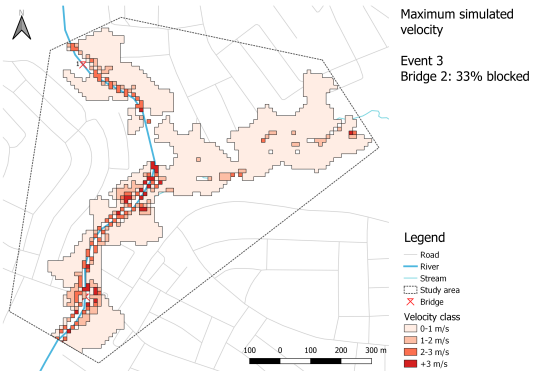

Figure H.54: Event 3 - bridge 2 33% blocked: Maximum simulated velocity

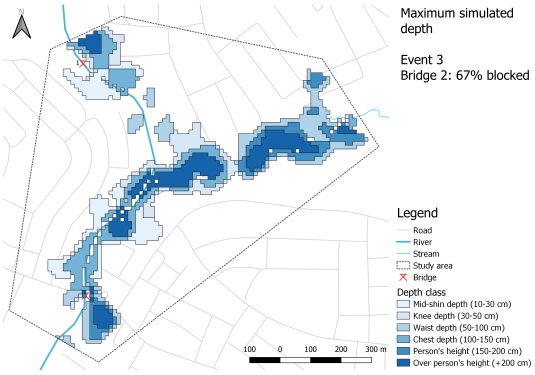

Figure H.55: Event 3 - bridge 2 67% blocked: Maximum simulated depth

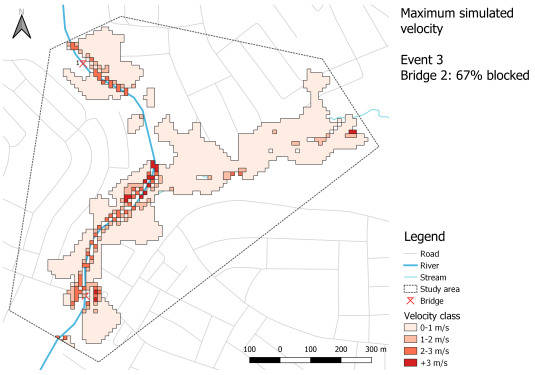

Figure H.56: Event 3 - bridge 2 67% blocked: Maximum simulated velocity

H.3.2. Distribution of depth and velocity classes per simulation

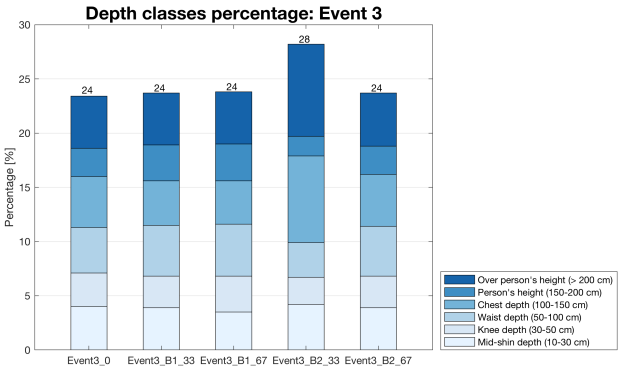

Figure H.57: Event 3 - Depth classes percentages

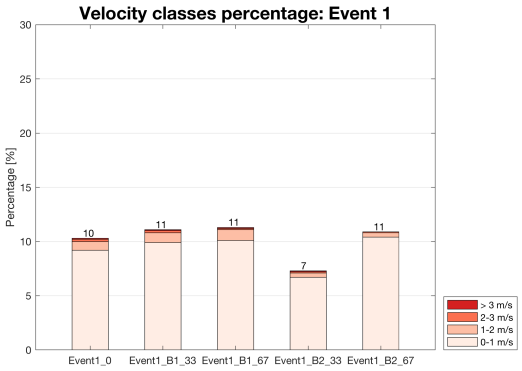

Figure H.58: Event 3 - Velocity classes percentages

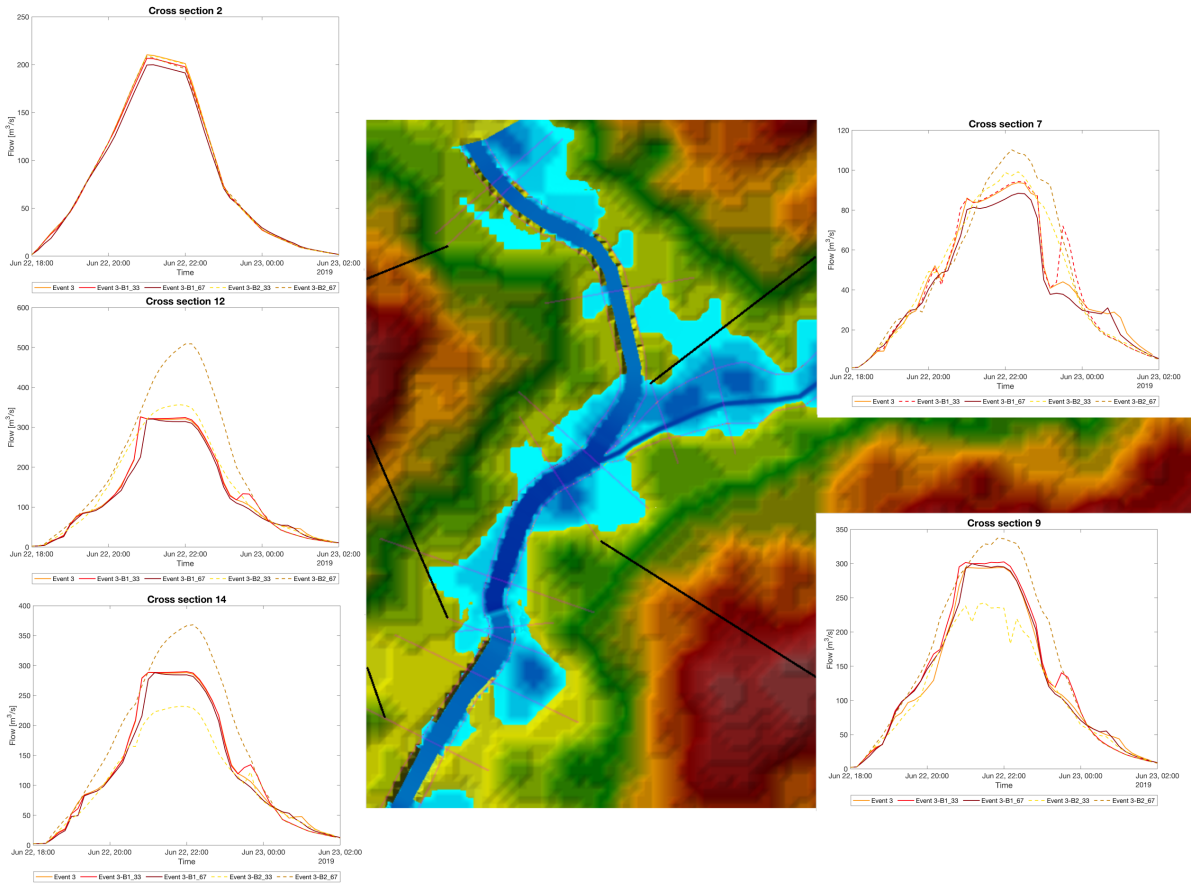

Figure H.59: Event 3: Flow time series at different cross-sections

H.3.3. Flow distribution over time

H.3.4. Maximum water surface profile

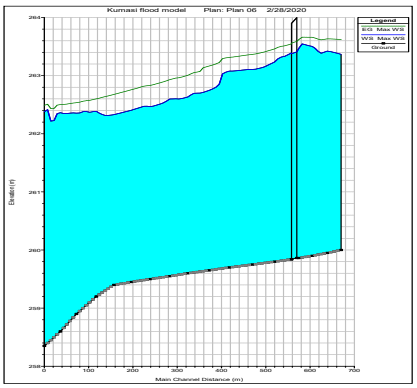

Figure H.60: Event 3 - Reach 1: Maximum WS and EG profile lines

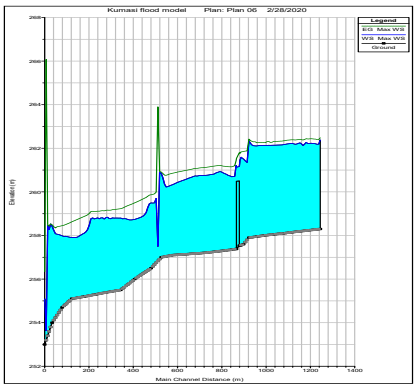

Figure H.61: Event 3 - Reach 1 lower: Maximum WS and EG profile lines

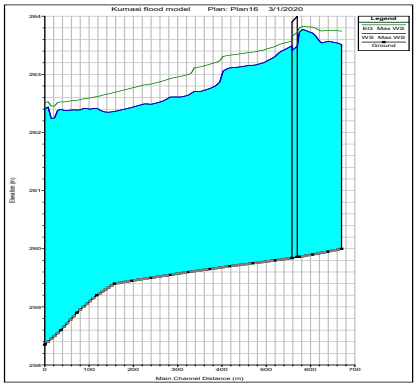

Figure H.62: Event 3 B1 33% - Reach 1: Maximum WS and EG profile lines

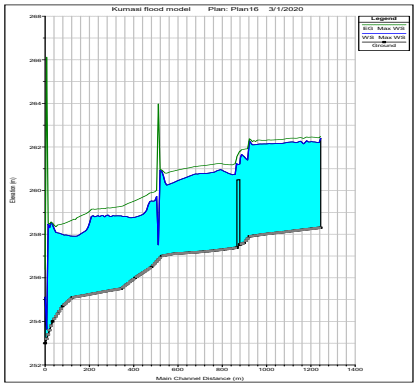

Figure H.63: Event 3 B1 33% - Reach 1 lower: Maximum WS and EG profile lines

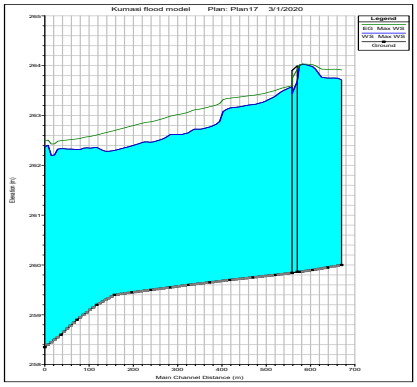

Figure H.64: Event 3 B1 67% - Reach 1: Maximum WS and EG profile lines

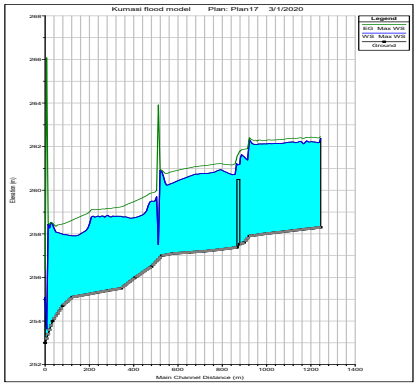

Figure H.65: Event 3 B1 67% - Reach 1 lower: Maximum WS and EG profile lines

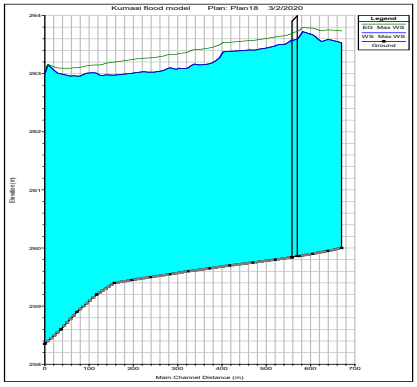

Figure H.66: Event 3 B2 33% - Reach 1: Maximum WS and EG profile lines

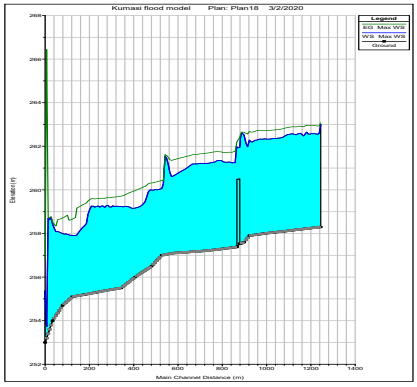

Figure H.67: Event 3 B2 33% - Reach 1 lower: Maximum WS and EG profile lines

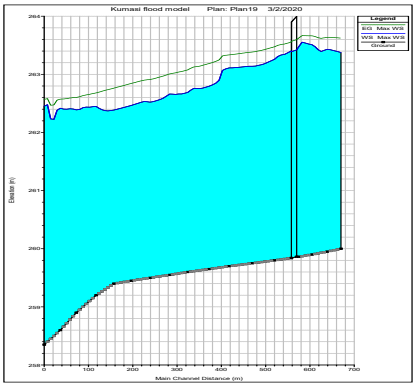

Figure H.68: Event 3 B2 67%- Reach 1: Maximum WS and EG profile lines

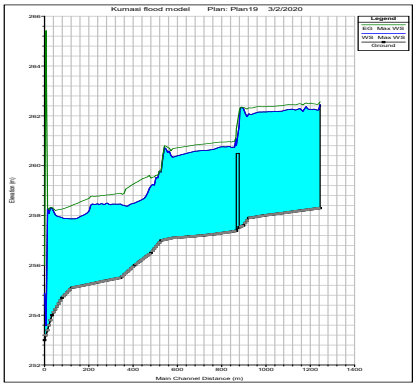

Figure H.69: Event 3 B2 67%- Reach 1 lower: Maximum WS and EG profile lines

H.4. Event 4

H.4.1. Maximum flood extent, depth and velocity

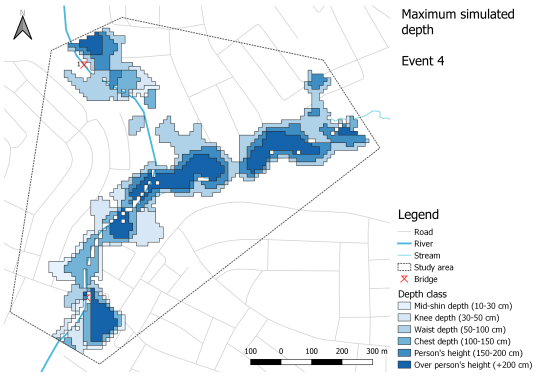

Figure H.70: Event 4: Maximum simulated depth

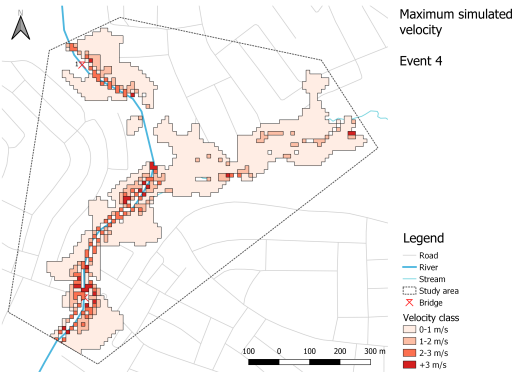

Figure H.71: Event 4: Maximum simulated velocity

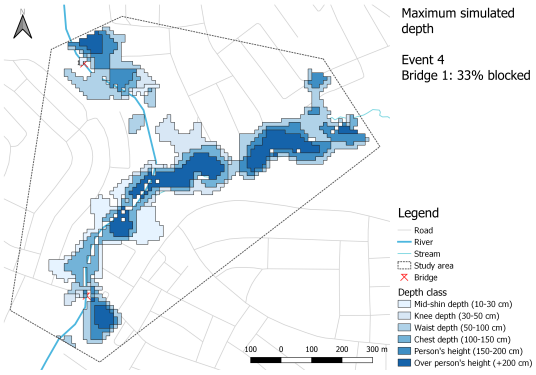

Figure H.72: Event 4 - bridge 1 33% blocked: Maximum simulated depth

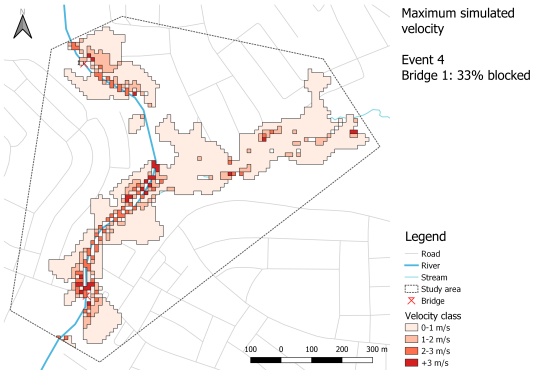

Figure H.73: Event 4 - bridge 1 33% blocked: Maximum simulated velocity

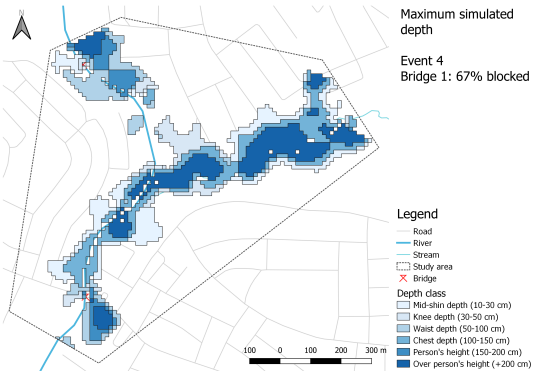

Figure H.74: Event 4 - bridge 1 67% blocked: Maximum simulated depth

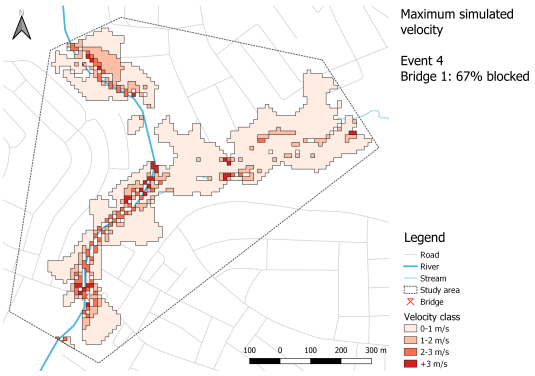

Figure H.75: Event 4 - bridge 1 67% blocked: Maximum simulated velocity

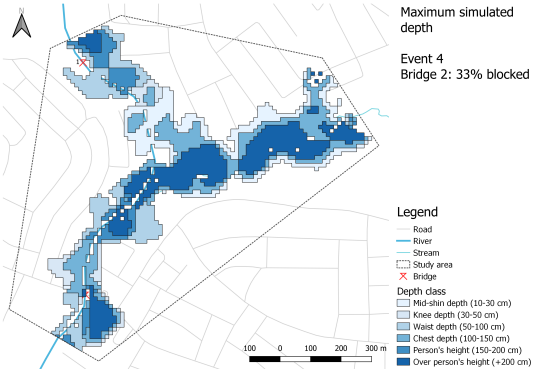

Figure H.76: Event 4 - bridge 2 33% blocked: Maximum simulated depth

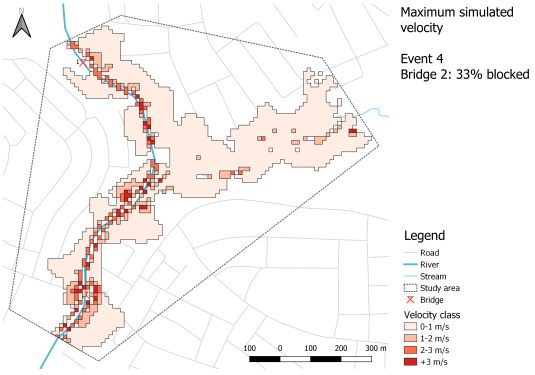

Figure H.77: Event 4 - bridge 2 33% blocked: Maximum simulated velocity

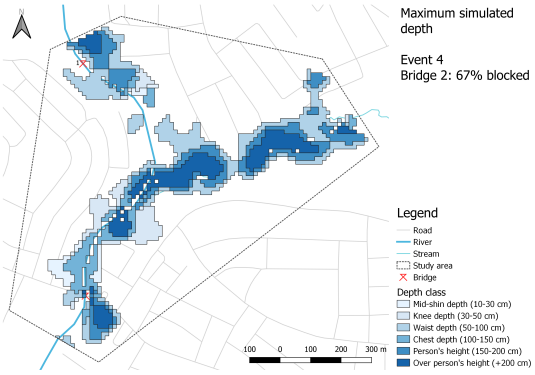

Figure H.78: Event 4 - bridge 2 67% blocked: Maximum simulated depth

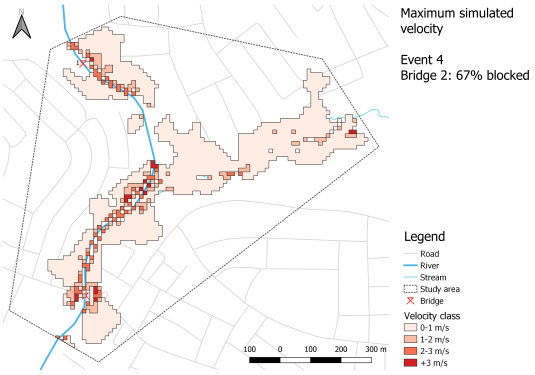

Figure H.79: Event 4 - bridge 2 67% blocked: Maximum simulated velocity

H.4.2. Distribution of depth and velocity classes per simulation

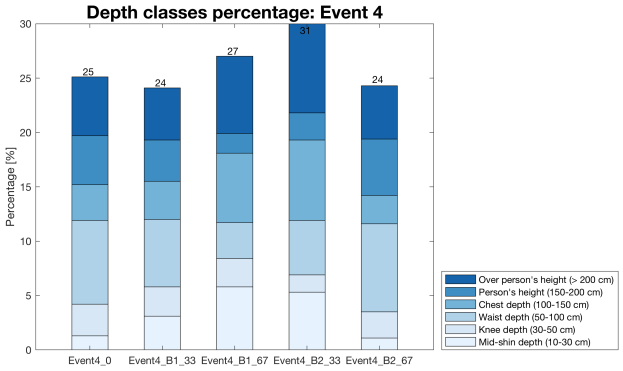

Figure H.80: Event 4 - Depth classes percentages

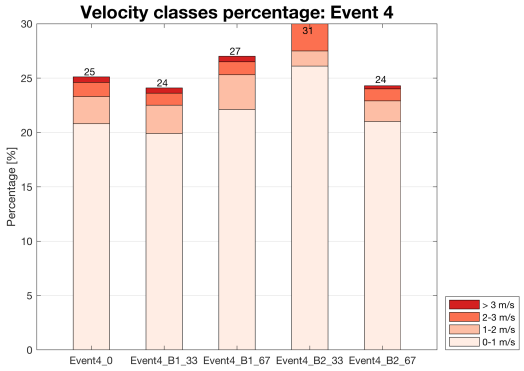

Figure H.81: Event 4 - Velocity classes percentages

H.4.3. Flow distribution over time

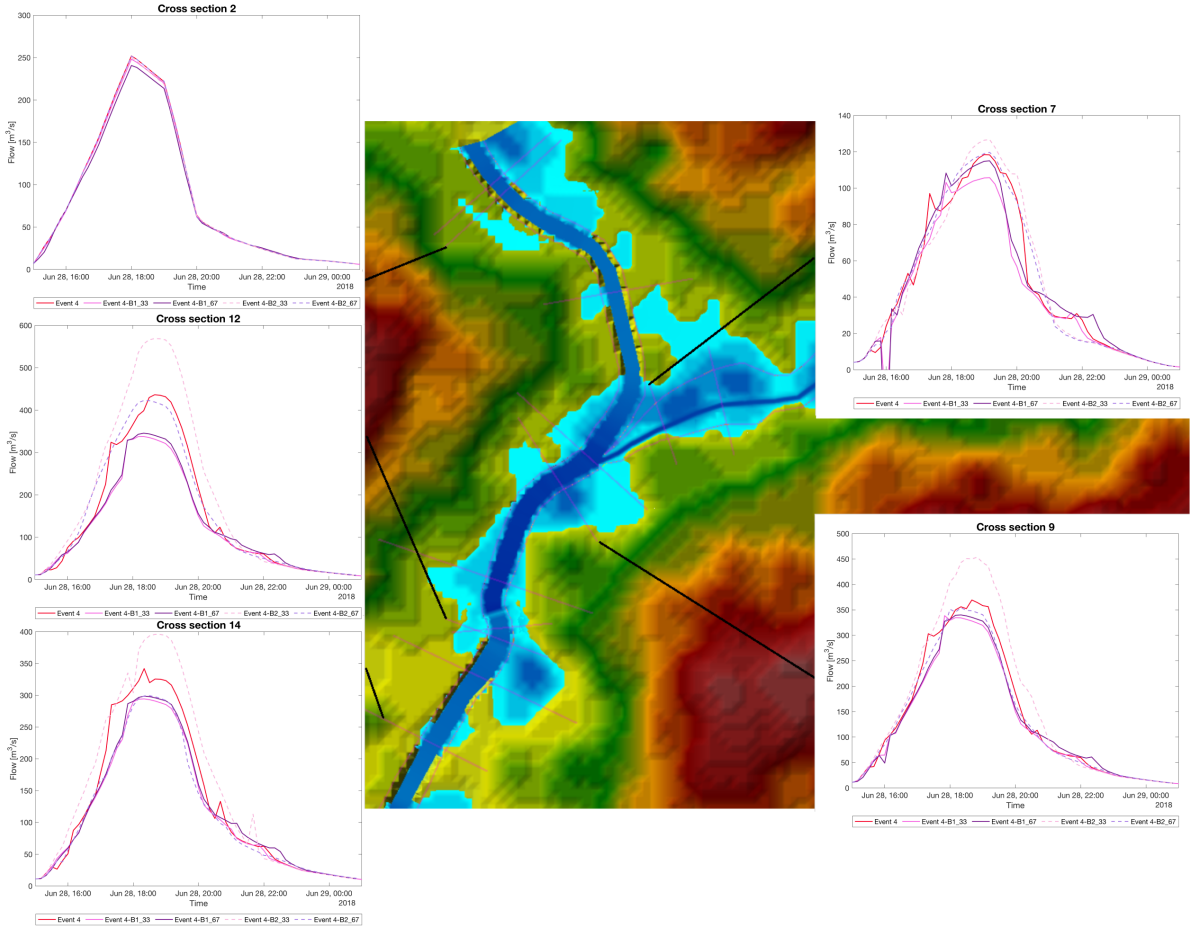

Figure H.82: Event 4: Flow time series at different cross-sections

H.4.4. Maximum water surface profile

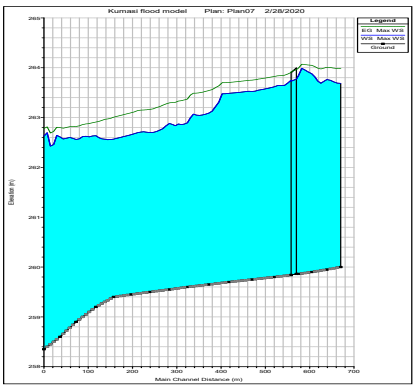

Figure H.83: Event 4 - Reach 1: Maximum WS and EG profile lines

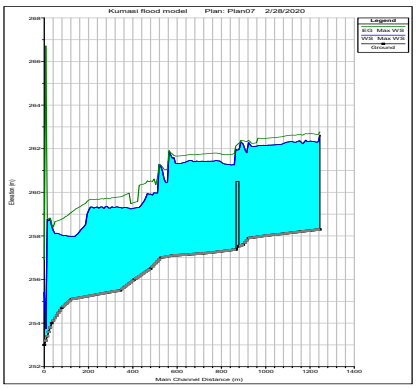

Figure H.84: Event 4 - Reach 1 lower: Maximum WS and EG profile lines

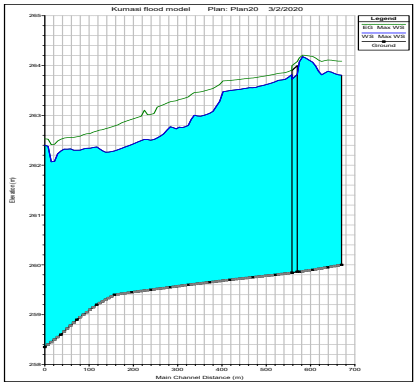

Figure H.85: Event 4 B1 33% - Reach 1: Maximum WS and EG profile lines

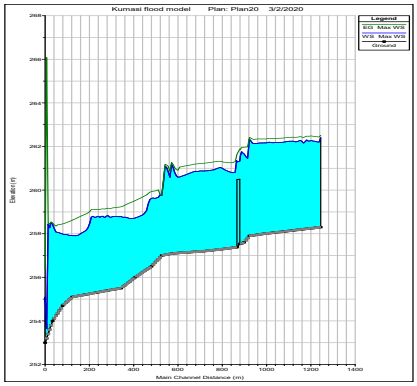

Figure H.86: Event 4 B1 33% - Reach 1 lower: Maximum WS and EG profile lines

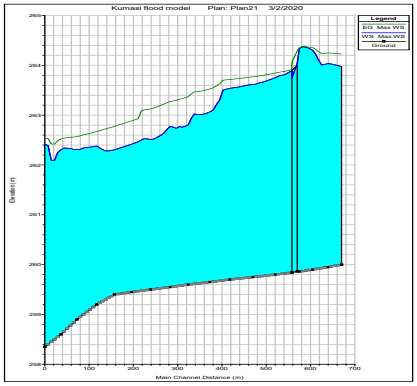

Figure H.87: Event 4 B1 67% - Reach 1: Maximum WS and EG profile lines

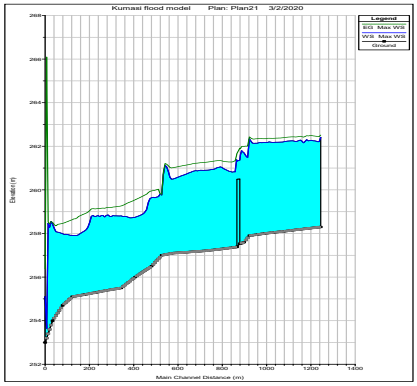

Figure H.88: Event 4 B1 67% - Reach 1 lower: Maximum WS and EG profile lines

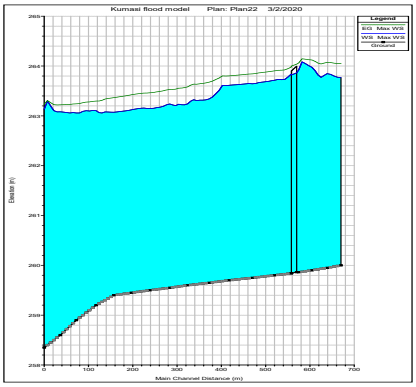

Figure H.89: Event 4 B2 33% - Reach 1: Maximum WS and EG profile lines

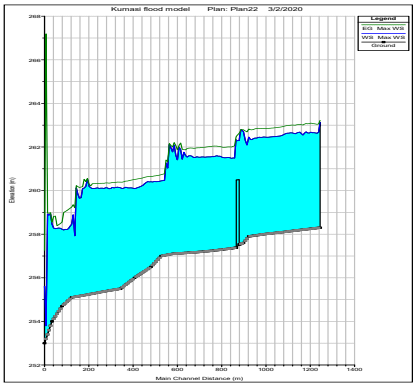

Figure H.90: Event 4 B2 33% - Reach 1 lower: Maximum WS and EG profile lines

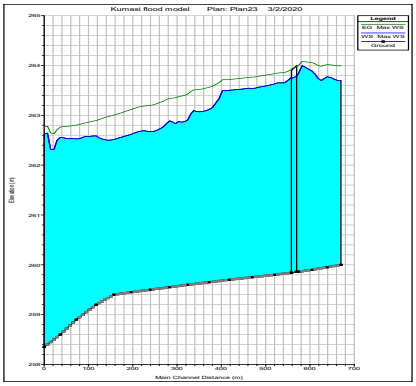

Figure H.91: Event 4 B2 67%- Reach 1: Maximum WS and EG profile lines

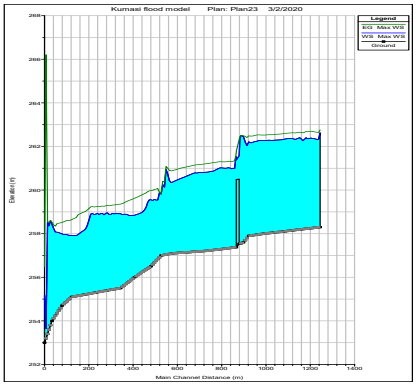

Figure H.92: Event 1 B2 67%- Reach 1 lower: Maximum WS and EG profile lines

Bibliography

[1] Alos palsar - radiometric terrain correction, 2019 Retreived on 11-12-2019. URL https://www.asf.alaska.edu/sar-information/alos-palsar-radiometric-terrain-correction/.

[2] Mcd12q1.006 modis land cover type yearly global 500m, 2019 Retrieved on 12-12-2019. URL https://developers.google.com/earth-engine/datasets/catalog/MODIS_006_MCD12Q1.

[3] Ghana districts, 2019 Retrieved on 24-09-2019. URL http://kma.ghanadistricts.gov.gh.

[4] Weather forecast kumasi, ghana, 2020 Retrieved on 03-01-2020. URL https://www.weather-atlas.com/en/ghana/kumasi-climate.

[5] D.K. Ahadzie and D.G. Proverbs. Flooding and post flooding response strategies in ghana. *WIT Transactions on Ecology and the Environment*, 133:281–291, 2010.

[6] D.K. Ahadzie and D.G. Proverbs. Emerging issues in the management of floods in ghana. *International Journal of Safety and Security Engineering*, Volume 1, Issue 2:182–292, 2011. doi: 10.2495/SAFE-V1-N2-182-192.

[7] C. Amoako. Emerging issues in urban flooding in african cities -the case of accra, ghana. Monash University, 11 2012.

[8] C. Amoako and E. Frimpong Boamah. The three-dimensional causes of flooding in accra, ghana. *International Journal of Urban Sustainable Development*, 7, 12 2014. doi: 10.1080/19463138.2014.984720.

[9] M. Asase, E. K. Yanful, M. Mensah, J. Stanford, and S. Amponsah. Comparison of municipal solid waste management systems in canada and ghana: A case study of the cities of london, ontario, and kumasi, ghana. *Waste Management*, 29(10):2779 – 2786, 2009. ISSN 0956-053X. doi: https://doi.org/10.1016/j.wasman.2009.06.019. URL http://www.sciencedirect.com/science/article/pii/S0956053X09002347.

[10] World Bank. *Rising through cities in Ghana: Ghana urbanization review overview report.* World Bank Washington, DC, 2015.

[11] N.H.H. Bashir. Plastic problem in africa. *Japanese Journal of Veterinary Research, 61 (supplement), S1-S11*, 02 2013. doi: 10.14943/jjvr.61.suppl.s1.

[12] A Betsholtz and B. Nordlof. Potentials and limitations of 1d, 2d and coupled 1d-2d flood modelling in hec-ras - a case study on höje river. Master's thesis, Lund University - Department of Building and Environmental Technology: Division of Water Resources Engineering, 2017.

[13] G.W. Brunner. Hec-ras river analysis system - hydraulic reference manual, version 5.0. Technical report, US Army Corps of Engineers, February 2016.

[14] G.W. Brunner. Hec-ras river analysis system - user's manual, version 5.0. Technical report, US Army Corps of Engineers, February 2016.

[15] G.W. Brunner. Hec-ras river analysis system - 2d modeling, user's manual version 5.0. Technical report, US Army Corps of Engineers, February 2016.

[16] G.W. Brunner. Common model stability problems when performing an unsteady flow analysis, 2020. URL https://www.nws.noaa.gov/oh/hrl/modelcalibration/6.%20%20Hydraulic%20Model%20Calibration/4.1%20L-11%20CommonModelStabilityProblemsInUnsteady%20FlowAnalysis.pdf.

[17] M. de Klerk C. Nolet, J. van Til. H2020 - twiga: Wp3 progress report. *FutureWater Report*, 2018.

[18] B.B. Campion and J.F. Venzke. Rainfall variability, floods and adaptations of the urban poor to flooding in kumasi, ghana. *Natural Hazards*, 65(3):1895–1911, 2 2013. ISSN 1573-0840. doi: 10.1007/s11069-012-0452-6. URL https://doi.org/10.1007/s11069-012-0452-6.

[19] S.S. Chung and C.S. Poon. Characterisation of municipal solid waste and its recyclable contents of guangzhou. *Waste Management & Research*, 19(6):473–485, 2001. doi: 10.1177/0734242X0101900603. URL https://doi.org/10.1177/0734242X0101900603. PMID: 12201677.

[20] P.B. Cobbinah, M.O. Erdiaw-Kwasie, and P. Amoateng. Africa's urbanisation: Implications for sustainable development. *Cities*, 47:62–72, 2015. ISSN 0264-2751. doi: https://doi.org/10.1016/j.cities.2015.03.013. URL http://www.sciencedirect.com/science/article/pii/S026427511500044X. Current Research on Cities (CRoC).

[21] G.M. Dawod, M.N. Mirza, K.A. Al-Ghamdi, and R.A. Elzahrany. Projected impacts of land use and road network changes on increasing flood hazards using a 4d gis: A case study in makkah metropolitan area, saudi arabia. *Arabian Journal of Geosciences*, 7(3):1139–1156, Mar 2014. ISSN 1866-7538. doi: 10.1007/s12517-013-0876-7. URL https://doi.org/10.1007/s12517-013-0876-7.

[22] Giuliano Di Baldassarre. Assessing the impact of different sources od topographic data on 1-d hydraulic modelling of floods. *Hydrology and Earth System Sciences*, 19(1):631–643, 2015.

[23] Google Earth Engine. Mcd12q1.006 modis land cover type yearly global 500m, 2019 Retrieved on 31-12-2019. URL https://developers.google.com/earth-engine/datasets/catalog/MODIS_006_MCD12Q1.

[24] D.S. Fernández and M.A. Lutz. Urban flood hazard zoning in tucumán province, argentina, using gis and multicriteria decision analysis. *Engineering Geology*, 111(1):90–98, 2010. ISSN 0013-7952. doi: https://doi.org/10.1016/j.enggeo.2009.12.006. URL http://www.sciencedirect.com/science/article/pii/S001379520900310X.

[25] C. Goodell. Bridge momentum: Understanding the weight component, 01 2018 Retrieved on 15-02-2020. URL https://www.kleinschmidtgroup.com/ras-post/bridge-momentum-understanding-the-weight-component/.

[26] N.K. Karley. Flooding and physical planning in urban areas in west africa: Situational analysis of accra, ghana. *Theoretical and Emperical Researches in Urban Management*, 13(4):25–41, 2009.

[27] P.I. Korah and P.B. Cobbinah. Juggling through ghanaian urbanisation: flood hazard mapping of kumasi. *GeoJournal*, 82(6):1195–1212, Dec 2017. ISSN 1572-9893. doi: 10.1007/s10708-016-9746-7. URL https://doi.org/10.1007/s10708-016-9746-7.

[28] N. Kortei and L. Quansah. Plastic waste management in ghana. *Daily Graphic*, 09 2016.

[29] D. Lea, K. Yeonsu, and A. Hyunuk. Case study of hec-ras 1d-2d coupling simulation: 2002 baeksan flood event in korea. *Water*, 11(10):2048, 2019.

[30] Litterati. How the litterati app works, 2020 Retrieved on 29-01-2020. URL www.litterati.org.

[31] I. McGraw-Hill Book Company. *Open Channel Hydraulics, Ven Te Chow, 1959: Open Channel Hydraulics*. Open Channel Hydraulics. Kogakusha, 1959. URL https://books.google.nl/books?id=N_tjDwAAQBAJ.

[32] Donald W. Meals and Steven A. Dressing. Surface water flow measurement for water quality monitoring projects. *Tech notes 3, National Nonpoint Source Monitoring Program*, pages 1–16, 2008.

[33] J.K. Owusu-Ansah. The influences of land use and sanitation infrastructure on flooding in kumasi, ghana. *GeoJournal*, 81(4):555–570, Aug 2016. ISSN 1572-9893. doi: 10.1007/s10708-015-9636-4. URL https://doi.org/10.1007/s10708-015-9636-4.

[34] Amoateng P., C.M. Finlayson, J. Howard, and B. Wilson. A multi-faceted analysis of annual flood incidences in kumasi, ghana. *International Journal of Disaster Risk Reduction*, 27:105 – 117, 2018. ISSN 2212-4209. doi: https://doi.org/10.1016/j.ijdrr.2017.09.044. URL http://www.sciencedirect.com/science/article/pii/S221242091630797X.

[35] H. Pazwash. *Urban Storm Water Management.* CRC Press, second edition, 2016.

[36] L. Petersson. Community mapping for flood modelling. Master's thesis, TU Delft, September 2019.

[37] United Nations Environment Programme. Marine litter: A global challenge. page 232, 2009.

[38] D. Roehr and E. Fassman-Beck. *Living Roofs in Integrated Urban Water Systems.* Taylor & Francis, 2015. ISBN 9781317537038. URL https://books.google.nl/books?id=kQvwBgAAQBAJ.

[39] Ghana Statistical Service. *National Analytical Report: 2010 Population and Housing Census.* 05 2013.

[40] TAHMO. Weather stations, 2020 Retrieved on 06-01-2020. URL https://tahmo.org/weather-stations/.

[41] J. Teng, A.J. Jakeman, J. Vaze, B.F.W. Croke, D. Dutta, and S. Kim. Flood inundation modelling: A review of methods, recent advances and uncertainty analysis. *Environmental Modelling and Software*, 90:201 – 216, 2017. ISSN 1364-8152. doi: https://doi.org/10.1016/j.envsoft.2017.01.006. URL http://www.sciencedirect.com/science/article/pii/S1364815216310040.

[42] R. Thompson, S. Swan, C. Moore, and F. vom Saal. Our plastic age. *Philosophical transactions of the Royal Society of London. Series B, Biological sciences*, 364:1973–6, 08 2009. doi: 10.1098/rstb.2009.0054.

[43] J.C. Thornton. 2d hec-ras model development in data poor areas of india - case study: Central krishna river basin. Master's thesis, Tennessee Technological University - Civil and Environmental Engineering, December 2016.

[44] Klement Tockner, Stuart E Bunn, Christopher Gordon, Robert J Naiman, Gerry P Quinn, and Jack A Stanford. Flood plains: Critically threatened ecosystems. *Aquatic ecosystems. Trends and Global Prospects*, 2008.

[45] TWIGA. Twiga transforming weather water data into value-added information services for sustainable growth in africa, 2019 Retrieved on 03-25-2019. URL http://twiga-h2020.eu/about/index.html.

[46] A.C. Twort, D.D. Ratnayaka, and M.J. Brandt. *Water Supply.* Elsevier Science, 2000. ISBN 9780080520803. URL https://books.google.nl/books?id=wjI_7A8ZMeIC.

[47] R. Vafa, R. Middendorp, and A. Schermerhorn. Final report minor international entrepeneurship and development - kwafi kumasi water and waste innovation. *TU Delft*, 2019.

[48] C. Wabnitz and W. Nichols. Editorial: Plastic pollution: An ocean emergency. *Marine Turtle News Letter*, 20, 01 2010.

[49] Y. Wang and X. Yang. Sensitivity analysis of the surface runoff coefficient of hipims in simulating flood processes in a large basin. *Water*, 10:253, 03 2018. doi: 10.3390/w10030253.

[50] Chris Zevenbergen, Adrian Cashman, Niki Evelpidou, Erik Pasche, Stephen Garvin, and Richard Ashley. *Urban flood management.* CRC Press, 2010.